AN OPTICALLY PUMPED MOLECULAR BROMINE LASER

THESIS

Jon W. Morrison, GM-13, AGMC

AFIT/GEO/ENP/90D-3

DEPARTMENT OF THE AIR FORCE
AIR UNIVERSITY
AIR FORCE INSTITUTE OF TECHNOLOGY

Wright-Patterson Air Force Base, Ohio

AFIT/GEO/ ENP/90D-3

AN OPTICALLY PUMPED MOLECULAR BROMINE LASER

THESIS

Jon W. Morrison, GM-13, AGMC

AFIT/GEO/ ENP/90D-3

Approved for public release; distribution unlimited

AFIT/GEO/ENP/90D-3

AN OPTICALLY PUMPED MOLECULAR BROMINE LASER

THESIS

Presented to the faculty of the School of Engineering

of the Air Force Institute of Technology

Air University

In Partial Fulfillment of the

Requirements for the Degree of

Master of Science in Electrical Engineering

Jon W. Morrison, B.S.
GM-13, AGMC

December 1990

Acknowledgments

I would like to acknowledge the Weapons Laboratory for sponsorship and financial support of this thesis work.

A great deal of appreciation is reserved for Capt Glenn P. Perram for serving as my thesis advisor and committee chairman. His guidance, insight, and patience were instrumental in this effort. Also, I wish to thank Dr. Ernest A. Dorko and Dr. Won B. Roh for serving on my thesis committee.

A word of thanks goes to M. Ray and J. Ray for fabrication of the glassware required in the experimental setup and to Dr. Mel Roquemore of Wright Research and Development Center (WRDC/POSF) for the loan of the Nd:YAG and dye laser system. This effort could not have been accomplished without their help.

I would like to thank my wife, Missy, for her love and support during this very hectic period of our lives. Missy's patience was tested several times while maintaining two households, but she managed quite well.

Finally, I would like to thank my two sons, Jacob and Jared, for helping me keep my priorities in order.

Jon W. Morrison

Table of Contents

List of Figures

List of Figures

List of Figures

List of Tables

Abstract

An optically pumped molecular bromine laser was studied to investigate the quenching kinetics of the $B^3\Pi(O_u^+)$ state of Br_2. This included characterization of the pressure dependence of the laser output power.

The approach was to excite molecular bromine in a sealed cell with a Nd:YAG pumped dye laser. Unresolved side fluorescence and amplified stimulated emission (ASE) spectra were recorded. ASE offered the advantage of a simpler optical system with no externally induced wavelength dependencies. Stimulated emission as a signal monitor offered greater resolution than side fluorescence spectra and facilitated spectroscopic assignment. The spectra obtained were attributed to the (14,0) band of the $^{79}Br^{81}Br$ isotope. The ASE output power peaked around Br_2 pressures from 8-12 Torr. A total removal rate, including all processes which remove population from the upper laser level, of 2.9×10^{-10} cm^3 $molecule^{-1}$ s^{-1} is proposed. This removal rate is consistent with the ASE output pressure dependence and the observed time delay between the dye pump beam and ASE pulses.

Inverted side fluorescence measurements were obtained. These spectra appear real and attributable to Br_2 due to agreement between observed and calculated differences of adjacent lines. However, these spectra could not be duplicated with a different pump source.

AN OPTICALLY PUMPED MOLECULAR BROMINE LASER

I. *Introduction*

A. *Background*

Visible chemical lasers are of great interest as potential directed energy weapons and as diagnostic tools (1:1). The diatomic interhalogens appear to be suitable candidates for visible lasing (2:191). The spectroscopy and kinetics of the interhalogens have been studied extensively (3; 4). While the demonstration of a visible chemical laser is difficult, the kinetics of visible chemical lasers can be approximated by an optically pumped laser (1:6). Optical pumping schemes have been used to demonstrate lasing of I_2, IF, and Br_2 (2:191).

Optical pumping facilitates the modeling of the laser medium. Using an appropriate pump laser to optically pump the gain medium at a specific wavelength, a portion of the ground state population is excited to a state of higher energy. If enough atoms are excited to create a population inversion, and to exceed losses due to collisions and radiative transitions, lasing will occur. The resulting stimulated emission spectra can be recorded and analyzed.(5:1)

B. *Problem*

The diatomic halogen molecules "have been found an ideal class of molecule for which the novel properties of lasers operating at visible wavelengths can be utilized"(4:177). Molecular bromine is one of the diatomic halogens which has been studied extensively (3; 6; 7; 8; 9;10).

Wodarczyk and Schlossberg observed lasing from molecular bromine in the visible and near infrared when optically pumped at 532 nm. The laser's output peak power as a function of Br_2 pressure was found to vary with changes to the pump energy. As the pump energy was lowered the peak output power shifted to lower Br_2 pressures. Fairly high gains were reported. The power output of the Br_2 was limited by the $B^3\Pi(O_u^+)$ state's large quenching cross section and collisional predissociation. (11:4476-4482)

Clyne *et al.* performed laser-excitation experiments of Br_2 to investigate the rates of energy transfer in the B state. Their studies were conducted using various collision partners. A quenching rate for Br_2 self-deactivation from the v' = 14 level was reported as $(4.2 \pm 1.3) \times 10^{-10}$ cm^3 $molecule^{-1}$ s^{-1}. Reported quenching rates for deactivation by other collision partners were significantly lower. (8:963-964, 971-977)

Perram and Davis performed studies of an optically pumped Br_2 laser. The laser was operated at Br_2 pressures up to 60 Torr. Power output was examined as a function of Br_2 pressure and was strongly peaked at Br_2 pressures of 10 to 15 Torr, very similar to the observations of Wodarczyk and Schlossberg. Modeling of the Br_2 laser kinetics yielded a removal rate, which included all population removal processes from the upper laser level, on the order of 2.5×10^{-10} cm^3 $molecule^{-1}$ s^{-1}. These results appear to be in disagreement

with the value reported by Clyne *et al.* In addition to the described work, the authors found Br_2 gain to be on the order of 0.11/cm and observed Amplified Spontaneous Emission (ASE) from the v' = 13, P(46) line of the Br_2.(12:2526-2533)

Van De Burgt and Heaven conducted an investigation of the electronic self-quenching of the B state of Br_2. Deactivation by $Br_2(X)$ and He over a pressure range of 0.002-5 Torr was examined. A quenching rate constant of $(4.2 \pm 0.5) \times 10^{-10}$ cm^3 $molecule^{-1}$ s^{-1} was reported. This is in close agreement with Clyne *et al.* A total removal rate, including the effects of the quenching rate and rotational, and vibrational energy transfer rates, was reported to be on the order of 1.4×10^{-9} cm^3 $molecule^{-1}$ s^{-1}. This is drastically different from the rate of 2.5×10^{-10} cm^3 $molecule^{-1}$ s^{-1} suggested by Perram and Davis. (13:407-416)

Thus, even though molecular bromine has been studied extensively, the kinetics of the upper laser level are not clear. The quenching rates reported by Clyne *et al.*(8) and Van De Burgt and Heaven (13) are not consistent with the laser output's pressure dependence measured by Perram and Davis (12:2531).

C. *Objective*

The primary objective of this effort was to investigate the quenching kinetics of the B state of Br_2 through a detailed characterization of an optically pumped molecular bromine laser. This included characterization of the pressure dependence of the laser.

The approach was to optically pump molecular bromine in a sealed cell. As the single pass gain for molecular bromine is high, on the order of 0.11/cm (12:2532), amplified spontaneous emission (ASE) was employed. Measurements of side fluorescence and stimulated emission spectra were recorded. Perram and Davis, in their study of an optically

pumped Br_2 laser, found stimulated emission as the signal monitor afforded much greater resolution than did side fluorescence as a signal monitor (12:2527). The Br_2 laser output consisted of a series of P-R doublets as observed in earlier experiments (11; 12). Assignment of the excitation spectral lines was accomplished using the constants of Barrow *et al.* (3). Power output was examined as a function of Br_2 pressure. Data was collected for Br_2 self-deactivation. The output power's dependence on the buffer gas pressure was anticipated by a simplified kinetic model

$$P = P_0 \exp(-k[M]t_D) \tag{1}$$

where P is the laser output power, P_0 is an initial condition constant, M is the buffer pressure, k is the collisional rate constant for all losses from the prepared (pumped) level, and t_D is the time delay between the pump pulse and the Br_2 laser pulses (5:41). This simplified model has also been used to study quenching of an optically pumped I_2 laser (5). The quenching rates extracted via the kinetic model were compared with previous experimental results and a mechanism for depopulation of the upper laser level was proposed.

D. *Presentation*

Chapter II contains theoretical background relevant to this thesis. This includes information on molecular energy levels and transitions, optically pumped diatomic lasers, amplified spontaneous emission, and a short history of molecular bromine studies.

Chapter III provides descriptions of the experiments performed including details of the experimental apparatus.

Chapter IV supplies results and discussion. This includes spectroscopy and pressure dependence studies.

Chapter V offers a summary and conclusions of this work and an outline of suggested future efforts.

II. *Theory*

A. *Molecular Energy Levels and Transitions*

The potential energy curves of a diatomic molecule are a function of the internuclear spacing of the atoms making up the molecule. The potential energy curve for an harmonic oscillator, a parabolic well, is divided into uniformly spaced vibrational energy levels. These vibrational energy levels are in turn subdivided into rotational energy levels as illustrated in Figure 1. Thus, the diatomic molecules possess electronic, vibrational, and rotational energy. These various energy levels give rise to rotational (far infrared to microwave), vibrational-rotational (mid infrared), and electronic (visible to ultraviolet) transitions. An important part of spectroscopy is to analyze these transitions and determine the vibrational and rotational energy levels involved.(15:551-553)

The molecule's energy levels are identified by vibrational and rotational quantum numbers, v and J. The electronic energy above ground state is T_e, the vibrational energy is denoted G_v and the rotational energy is termed F_J. The vibrational and rotational energy are given by equations 1 and 2 respectively:

$$G_v = w_e(v + 0.5) - w_e x_e(v + 0.5)^2 + w_e y_e(v + 0.5)^3 + \ldots \quad (2)$$

$$F_J = B_v J(J + 1) - D_v J^2(J + 1)^2 + H_v J^3(J + 1)^3 + \ldots \quad (3)$$

with

$$B_v = B_e + \alpha_e(v + 0.5) + \Gamma_e(v + 0.5)^2 + \ldots \quad (4)$$

$$D_v = D_e + \beta_e(v + 0.5) + \ldots \quad (5)$$

$$H_v = H_e + \ldots \quad (6)$$

where w_e, $w_e x_e$, $w_e y_e$, B_e, α_e, Γ_e, D_e, β_e, and H_e are molecular constants.(5:151-152) These constants, as derived by Barrow *et al.*(3) for Br_2, are contained in Table 1.

Equation 6 yields the molecular rovibronic transition energy v:

$$v = v_0 + (G_{v'} - G_{v''}) + (F_{J'} - F_{J''}) \quad (7)$$

"where v_0 (the band origin) is the transition energy between electronic states of the molecule with no rotational or vibrational energy" (5:12). Single primes are used to designate the upper energy level and double primes the lower energy level of the transition. Vibrational transitions are labelled by the upper and then lower vibrational quantum numbers as (v',v").(5:11-12)

TABLE 1

MOLECULAR CONSTANTS FOR Br_2
$X^1\Sigma_g^+$ and $B^3\Pi O_u^+$ STATES (3:440)

	$^{79}Br_2$ (cm^{-1})	$^{81}Br_2$ (cm^{-1})	$^{79,81}Br_2$ (cm^{-1})
T_∞	15823.47	15824.46	15822.96
T_e	15902.47	15902.47	15902.47
$^3\Pi O_u^+$ State $v \leq 8$			
w_e	167.6066	(165.5244)	(166.5688)
$w_e x_e$	1.63608	(1.5957)	(1.6159)
$10^3 w_e y_e$	-9.3687	(-9.0238)	(-9.1957)
$10^2 B_e$	5.9589	(5.8118)	(5.8853)
$10^4 \alpha_e$	4.89095	(4.7109)	(4.8007)
$10^6 \Gamma_e$	-6.6369		
r_e	2.6776Å	2.6776Å	2.6776Å
$10^8 D_e$ (Kratzer)	3.013	2.866	2.939
$^1\Sigma_g^+$ State $v \leq 10$			
w_e	325.3213	321.29 (321.2798)	(323.3069)
$w_e x_e$	1.07742	1.064 (1.0508)	(1.0641)
$10^3 w_e y_e$	-2.29798	(-2.2134)	(-2.2556)
$10^2 B_e$	8.2107	8.0088 (8.0080)	(8.1093)
$10^4 \alpha_e$	3.1873	3.19 (3.070)	(3.1285)
$10^6 \Gamma_e$	-1.045		
r_e	2.28107Å	2.28107Å	2.28107Å
$10^8 D_e$ (Kratzer)	2.092	1.990	2.041

Values in parentheses are calculated from isotope effects with
$^{79}\mu = 39.45915$, $^{81}\mu = 40.45815$, $^{79,81}\mu = 39.95240$

The possible transitions can be split into three branches, P, Q, and R. The assignment of the branch is determined by the change in the rotational quantum number J. The transition is assigned to the P branch if $\Delta J = -1$, to the Q branch if $\Delta J = 0$, and to the R branch if $\Delta J = +1$. The Q branch does not appear for most diatomic molecules. Rotational transitions are labeled by the lower-state J" values.(15:555-556) Figure 2 presents an energy level diagram. Note the P(2) and R(0) transitions of the (0,0) band and the P(3) and R(3) transitions of the (0,1) band are labelled as described previously.

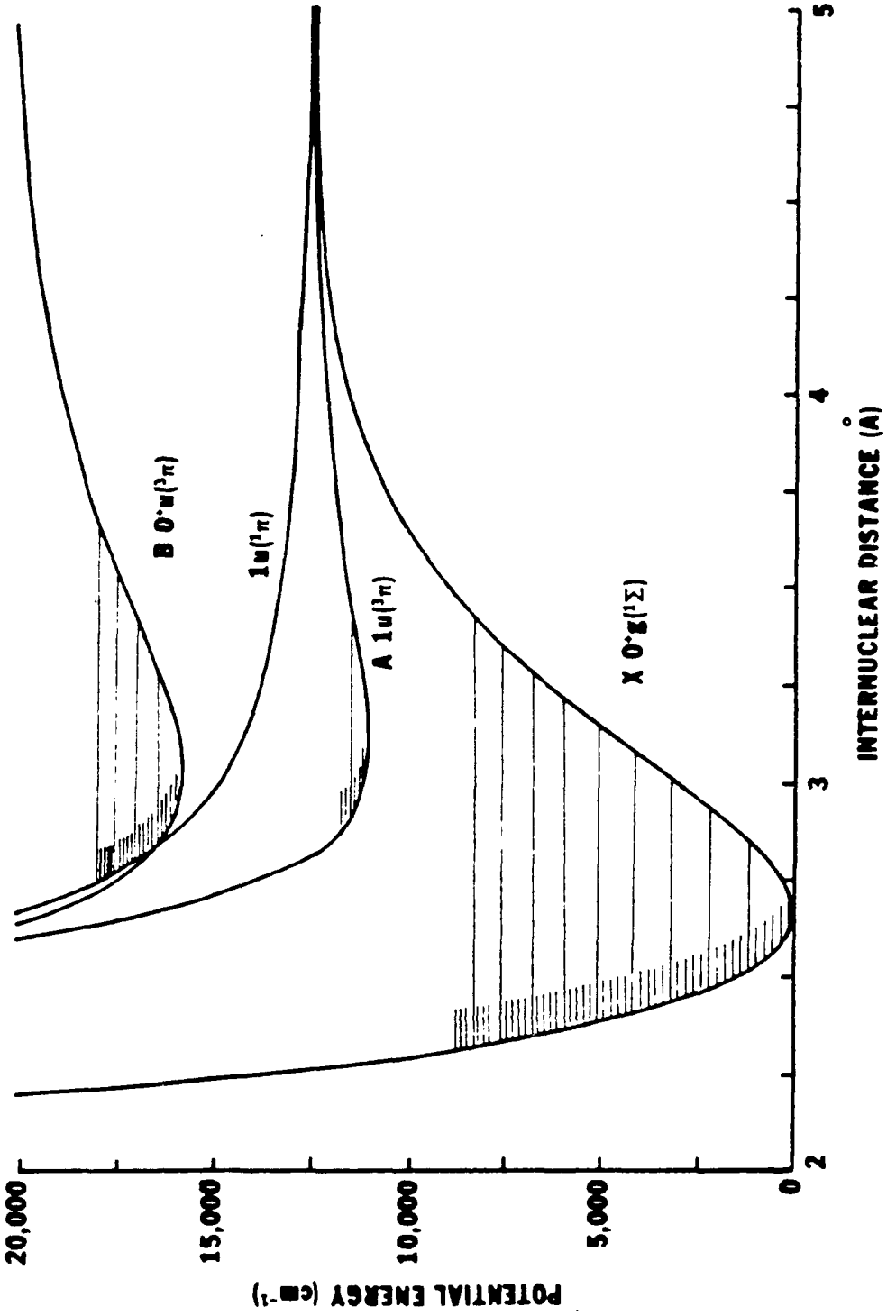

Figure 1. Molecular Potential Energy Curve (5:18)

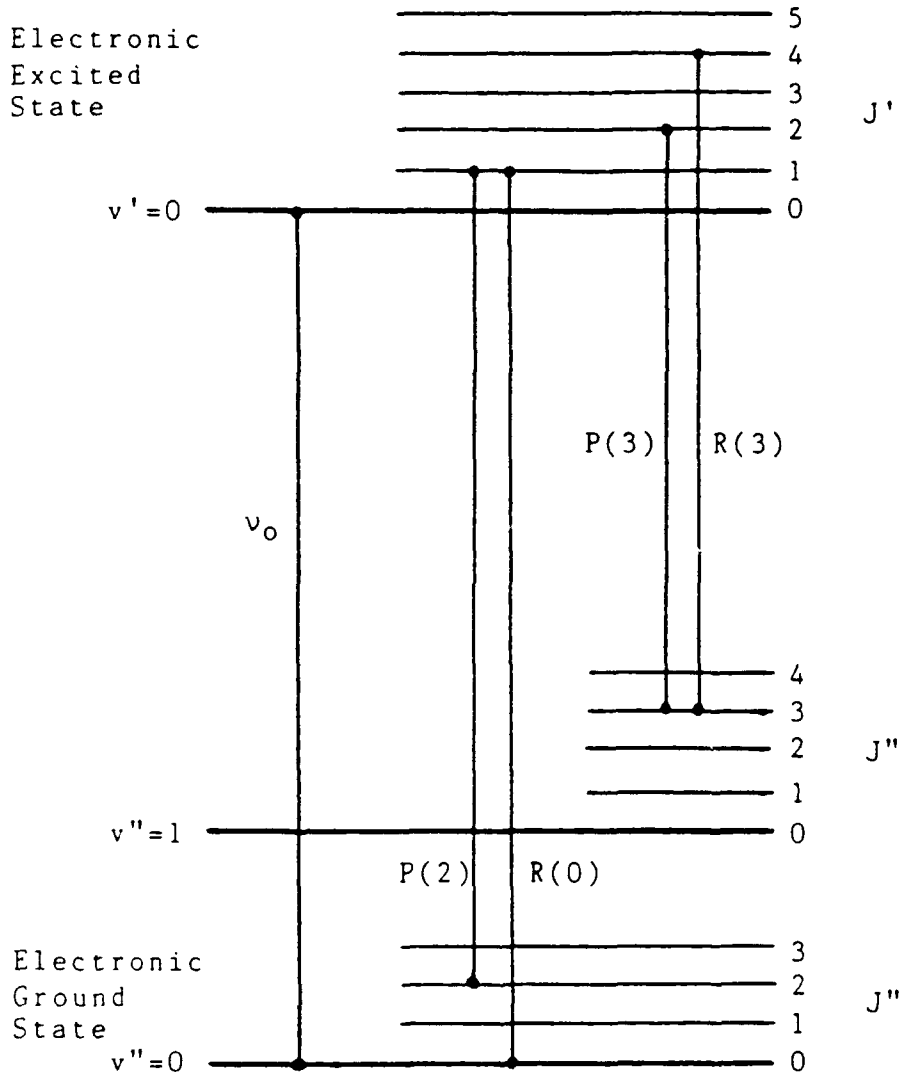

Figure 2. Energy Level Diagram (5:13)

B. *Optically Pumped Diatomic Lasers*

An optically pumped diatomic laser uses a pump source, usually a tunable dye laser, to excite molecules from the ground state to a higher energy level (16:385). Lasing occurs when a population inversion is created and losses due to collisions and radiative transitions are overcome (5:1). The diatomic halogen and interhalogen B-X systems are of great interest as optically pumped diatomic lasers due to their displaced potential energy curves. The internuclear spacing of the B (excited) state is shifted with respect to the X (ground) state.(5:5) In accordance with the Franck-Condon principle, which states that electronic processes (transitions) must take place along a vertical path (constant internuclear spacing), the most likely B-X transitions will terminate on high vibrational levels (v") of the X state. The potential energy curves of Br_2, Figure 3, show this shift of the B state relative to the X state which is typical of the halogens. As the vibrational levels initially have a Boltzmann distribution, the high v" levels are basically unpopulated in thermal equilibrium.(17:168-169). Thus, molecules excited from the X state to a specific rotational level of the B state will create a population inversion between the B state vibration level (v') and the unpopulated high v" level of the ground state. Once this inversion is created and losses due to collisions and radiative transitions are exceeded, lasing will occur as the molecule transitions from a B state (v', J') to an X state high (v",J").

An optically pumped diatomic laser may be modeled as a three level or a four level laser cycle (5:26). In a three level cycle, a molecule is pumped from the ground state to the excited state (v'). Once in the v' excited state, it transitions directly to a high v" level of the X state and lasing occurs. The molecule subsequently relaxes from the high v" level to the low-lying

vibrational levels of the ground state.(15:307) The relaxation to the low-lying vibrational levels is due to collisions and radiative transitions (5:29). Thus, in the three level diatomic laser, the stimulated emission occurs from the level excited by the pump (16:385). In the four level cycle, a molecule is again pumped from the ground state to an excited state (v'). However, once in the excited v' level, the molecule relaxes to a lower J' or even a lower v' level before transitioning, and lasing, to the high v" level of the ground state. The molecule then relaxes to the low-lying vibrational levels of the ground state as it did in the three level cycle.(15:307) Thus, in the four level diatomic laser, the pump energy is spread over several J' or even v' levels by relaxation and stimulated emission can result from each of these levels. As the pump energy is spread over several J' or v' levels, the population inversion is not as great and four level lasing is observed less frequently.(16:385) These optically pumped diatomic laser cycles are illustrated in Figure 4. Thus, the major difference between the three and four level cycles is that in the four level cycle the upper laser level and the pumped level are different (5:29).

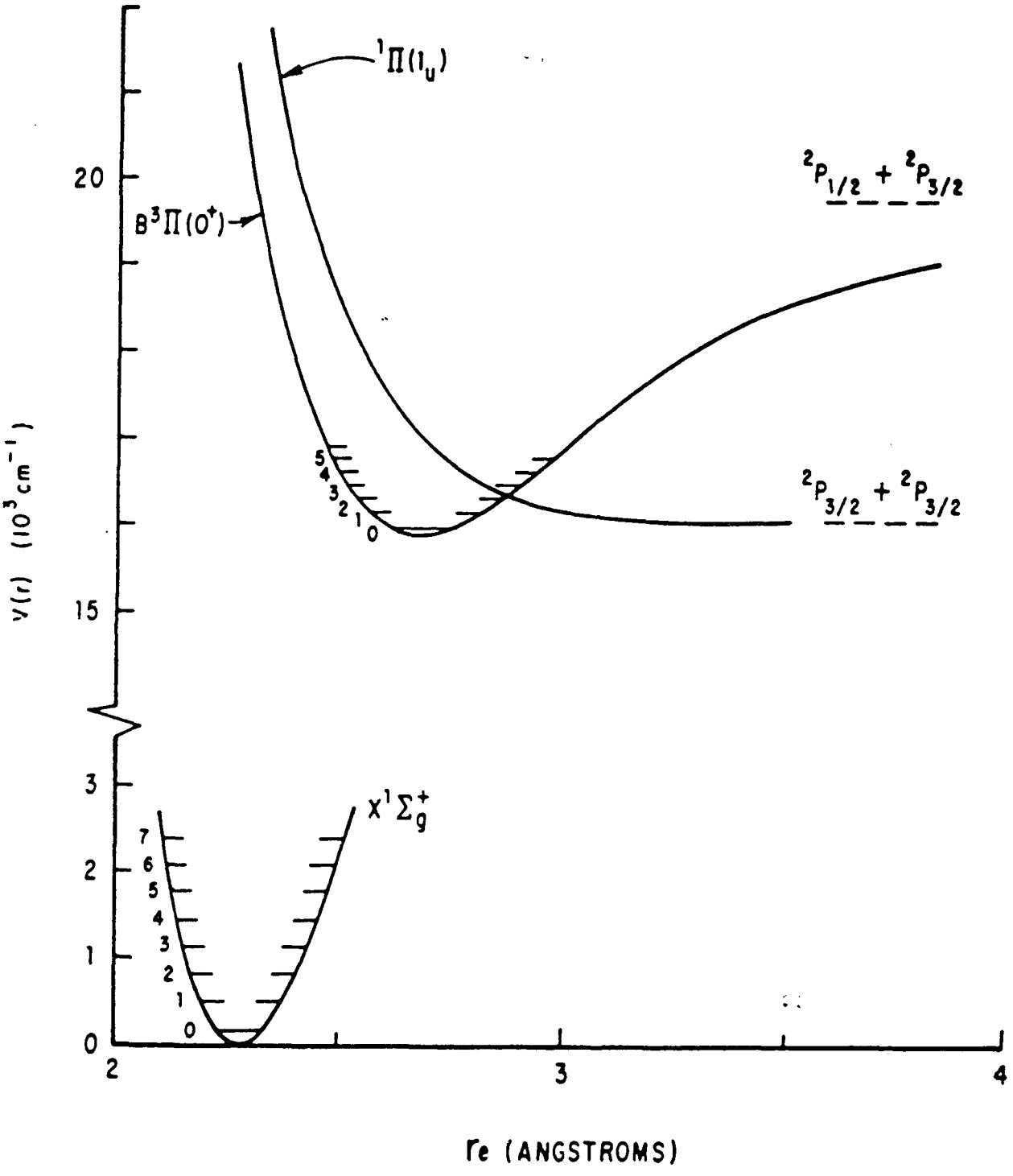

Figure 3. Potential Energy Curves for Br_2 (17:169)

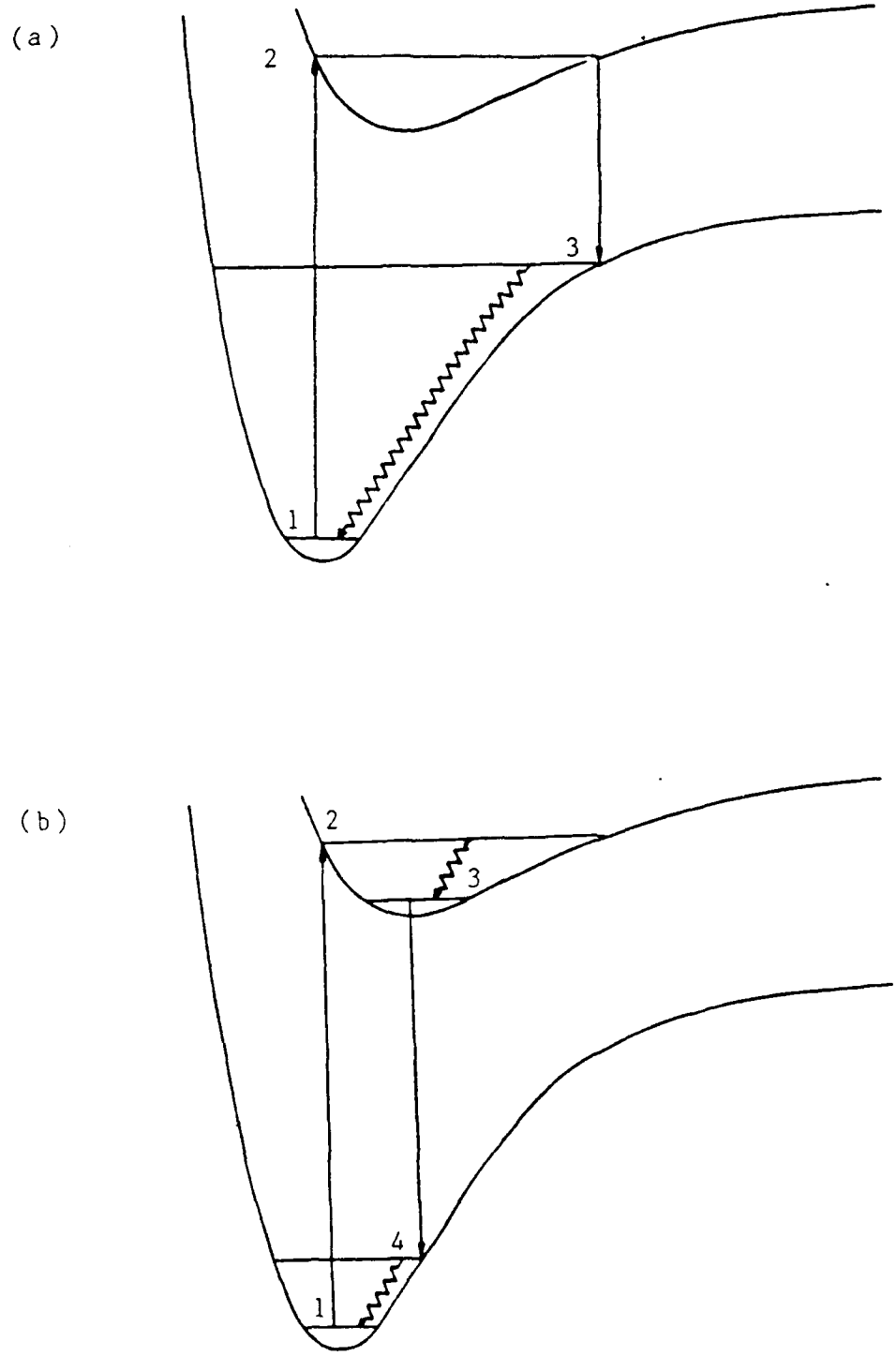

Figure 4. Optically Pumped Diatomic Laser Cycles
Three Level Cycle (a) and Four Level Cycle (b) (5:27)

C. *Amplified Spontaneous Emission*

A typical laser uses an optical cavity to promote oscillation, enhance gain, and reach lasing threshold. However, if the laser medium is of very high gain, mirrorless lasing can be achieved. In the latter case, Amplified Spontaneous Emission (ASE), the medium absorbs the pump energy and is allowed to radiate via spontaneous emission. The radiation due to spontaneous emission is incoherent and proceeds in all directions including along the medium's axis. Spontaneous emission is continuously added along the medium's axis and at the same time the power from previous sections of the medium is amplified exponentially by stimulated emission. The resultant emission can be very intense for certain media.(15:210) ASE has been observed for both I_2 and Br_2 (12:2532).

The output of a medium which supports mirrorless lasing or ASE will be controlled by the gain of the individual transitions. This can be very useful in examining the medium's spectroscopic and kinetic characteristics. The excited states of a molecule can be selectively populated via absorption of a tunable pump source and subsequently either the side fluorescence or stimulated emission may be monitored. Knowing that only transitions with relatively high Franck-Condon factors will be able to exceed threshold and support mirrorless lasing, or ASE, facilitates data analysis.(5:34)

A simplified model for the kinetic processes of pulsed optically pumped ASE of the I_2 B-X system was developed by Glessner. Glessner noted that "the populations of the various levels involved would be functions of vibration, rotation, position along the gain length, and time"(5:38). Glessner further noted several complications, such as the possibility of randomly initiated ASE and depletion due to ASE which is not in the proper solid angle,

which made difficult the development of a total model. However, Glessner was able to develop a simplified kinetic model which described the total loss from the upper energy state. (5:38-42) The following treatment for a simplified kinetic model of the Br_2 B-X system parallels Glessner's approach. The model incorporates the following assumptions:

1) The gain medium is an optically pumped three level system as shown in Figure 5a.

2) Both the pump and ASE pulses are considered instantaneous and copropagating.

3) Only the total energy per pulse is considered.

4) There is a time delay between the pump and ASE pulse as shown in Figure 5b. (5:39)

Collisional losses from the prepared (pumped) level are described as:

$$Br_2(B{:}v',J') + M \xrightarrow{k} Br_2 + M \tag{8}$$

where $Br_2(B{:}v',J')$ is the prepared (pumped) level, M is any collision partner, Br_2 is any state other than the prepared (pumped) state, and k is the collisional rate constant. From Equation 8 it follows that

$$d[Br_2(B{:}v',J')]/dt = -k[Br_2(B{:}v',J')][M] \tag{9}$$

Now, letting $N_2 = Br_2(B{:}v',J')$ yields

$$dN_2/dt = -kN_2[M] \tag{10}$$

Solving for N_2 as a function of time produces

$$N_2(t) = N_2(0)\exp(-tk[M]) \tag{11}$$

where $N_2(t)$ is the population density of the prepared (pumped) level at time t, $N_2(0)$ is the population density of the prepared (pumped) level at time zero, k is the collisional rate constant for all losses from the prepared (pumped) level, and [M] is the buffer concentration. N_2, the population density of the prepared (pumped) level, is shown as a function of time

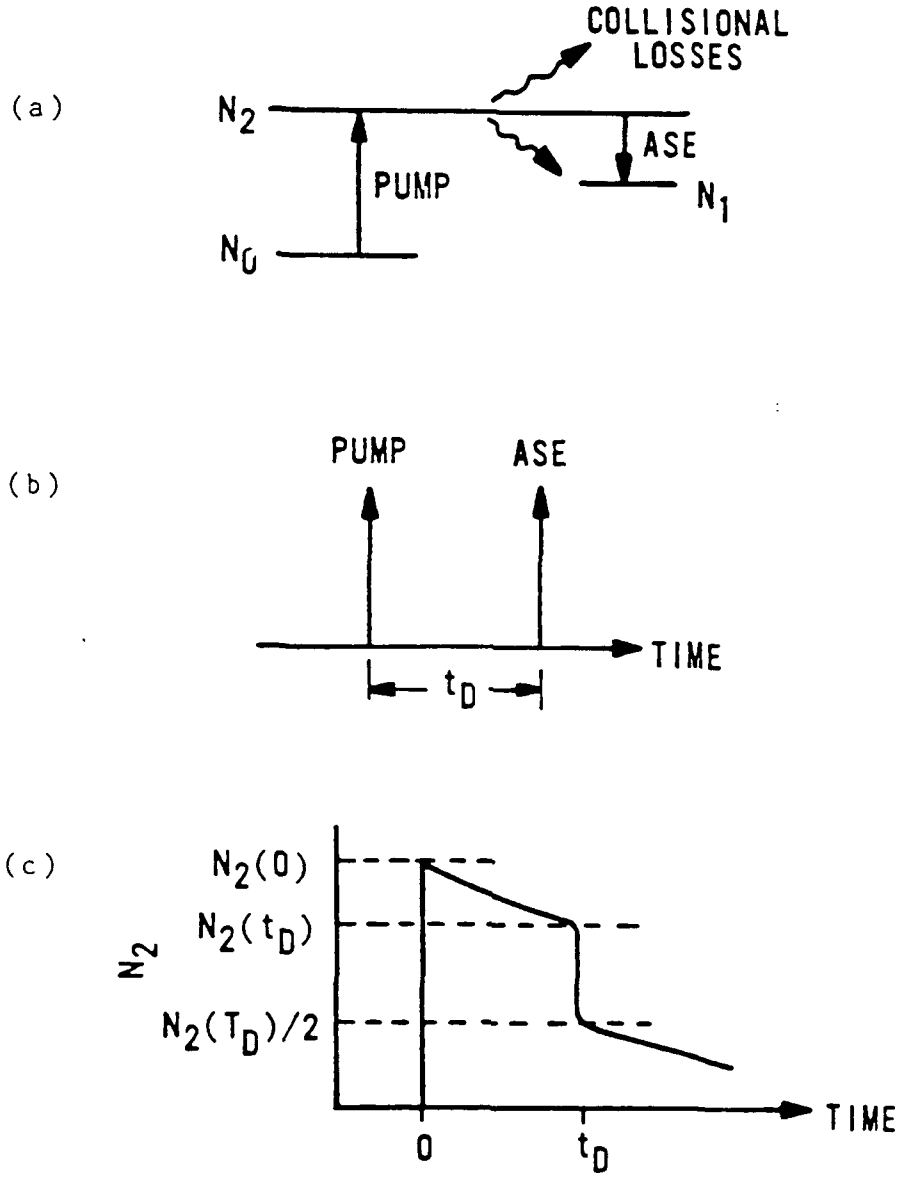

Figure 5. ASE Kinetic Model. Schematic energy level diagram (a), time history of transitions (b), and upper state population (c).(5:40)

in Figure 5c. Note that the population N_2 decays, due to collisions, from its peak value $N_2(0)$ to a lower value $N_2(t_D)$ at time t_D. Time t_D is the delay time between the pump pulse and the ASE pulse. Assuming the lasing transitions terminate on a single (v,J) level, which

is not necessarily true, mirrorless lasing or ASE ceases when the population of the prepared (pumped) level reaches a value of $N_2(t_D)/2$ as there is no longer a population inversion.(5:36-42) As the ASE output power is proportional to $N_2(t_D)$, Equation 11 leads to:

$$P = P_0 \exp(-k[M]t_D) \quad (1)$$

where P is the laser output power, P_0 is an initial condition constant dependent on the buffer concentration at time zero ($N_2(0)$), and t_D is the time delay between the pump pulse and the Br_2 laser pulses (5:41). This simplified model has been used to study quenching of an optically pumped I_2 laser (5). The quenching rates extracted via the kinetic model were compared with previous experimental results and a mechanism for depopulation of the upper laser level is proposed.

D. *Molecular Bromine Studies*

Considerable information is available for the electronic states of the diatomic halogen molecules (3; 4; 17). Molecular bromine is one of the diatomic halogens which has been studied extensively and has been successfully lased (11; 12).

Wodarczyk and Schlossberg observed lasing from molecular bromine in the visible and near infrared when optically pumped at 532 nm. They used a 21 cm long stainless steel laser cell with Pyrex Brewster windows to hold the room temperature Br_2. Br_2 pressures within the cell ranged from 0.7 to 40 Torr for the experiments. A 34 cm long optical cavity with dielectric coated end mirrors enclosed the laser cell. The end mirrors (two sets) were coated to facilitate lasing in either the visible or infrared. A frequency doubled Nd:YAG laser and intercavity etalon were used to generate a 532 nm 0.03 cm^{-1} wide pump signal. The laser

oscillated at several wavelengths, termed broadband lasing by Wodarczyk and Schlossberg, when the cavity consisted of only the laser cell and end mirrors. Insertion of a prism into the cavity allowed selection of individual wavelengths for observation. Spectroscopic assignments of the individual lines were based on the constants of Barrow *et al.* (3). The lasing output was found to consist of P and R doublets in all cases. The laser's output peak power as a function of Br_2 pressure was found to vary with changes to the pump energy. As the pump energy was lowered the peak output power shifted to lower Br_2 pressures. Fairly high gains, 0.05-0.40 cm^{-1} per pass, were reported due in part to the high pressures attainable with Br_2 at room temperature. The power output of the Br_2 was limited by the B state's large self-quenching cross section and collisional predissociation. (11:4476-4482)

Clyne *et al.* performed laser-excitation experiments of Br_2 to investigate the rates of energy (electronic, vibrational, and rotational) transfer in the B state. Their studies were conducted using various collision partners namely, Br_2, Ar, He, N_2, and Cl_2. The experiment involved populating selected ro-vibrational states of the bromine's excited B state. Both a cw dye laser operating in a single longitudinal mode and a 1 pm bandwidth pulsed dye laser were used as excitation sources.(8:961) The pulsed dye laser studies are most relevant to this thesis and therefore will be focused upon. For the pulsed dye laser studies, selected B state vibrational-rotational levels were populated. Fluorescent decay rates of various Br_2 pressures, up to 100 mTorr, were recorded by a photomultiplier and subsequently digitized for analysis. Electronic deactivation was assigned to collisional predissociation and therefore thought to be very efficient. A Stern-Volmer (SV) analysis of the fluorescent decay data was used to examine quenching rate constants for Br_2 self-deactivation and deactivation by

other partners. It was noted that the SV plots showed a strong dependence on J'. Reported quenching rates for Br_2 self-deactivation from the v' = 14 level ranged from (4.1-9.2) x 10^{-10} cm^3 $molecule^{-1}$ s^{-1} with the value reported as (4.2 $\pm$ 1.3) x 10^{-10} cm^3 $molecule^{-1}$ s^{-1}. Reported quenching rates for deactivation by Ar (1.7-4.5) x 10^{-10} cm^3 $molecule^{-1}$ s^{-1}, Cl_2 (3.9-6.0) x 10^{-10} cm^3 $molecule^{-1}$ s^{-1}, and He 2.3 x 10^{-10} cm^3 $molecule^{-1}$ s^{-1} were somewhat lower.(8:963-964; 971-977)

Perram and Davis performed studies of an optically pumped Br_2 laser. A dye laser (550-575 nm range) was used to pump the v' = 12-17 levels of the B state of Br_2. The Br_2 was sealed in a 60 cm long Brewster windowed Pyrex cell. The cell was contained in a laser cavity having dielectric coated mirrors with a 3 m radius of curvature. The laser was operated at Br2 pressures up to 60 Torr. Excitation spectra were recorded with side fluorescence and stimulated emission as a signal monitor. As Figure 6 shows, stimulated emission as the signal monitor afforded much greater resolution. Power output was examined as a function of Br_2 pressure (1.5-60 Torr) and was strongly peaked at Br_2 pressures of 10 to 15 Torr. This is very similar to the peak output versus Br_2 pressure observed by Wodarczyk and Schlossberg. Modeling of the Br_2 laser kinetics yielded a removal rate, including all processes which remove population from the upper laser level, on the order of 2.5 x 10^{-10} cm^3 $molecule^{-1}$ s^{-1}. Figure 7 shows Br_2 output power versus Br_2 pressure. Values measured by Perram and Davis as well as predicted curves using removal rates of 2.5 and 5.0 x 10^{-10} cm^3 $molecule^{-1}$ s^{-1} are shown in the figure. Note that the measured data more closely resembles the 2.5 x 10^{-10} cm^3 $molecule^{-1}$ s^{-1} predicted curve. These results appear to be in disagreement with the value of (4.2 $\pm$ 1.3) x 10^{-10} cm^3 $molecule^{-1}$ s^{-1} reported by Clyne *et*

al. Perram and Davis note the faster rates reported by Clyne *et al.* were obtained at Br_2 pressures several orders of magnitude lower. Therefore, the faster rates may contain R-T transfer contributions. At higher pressures, quenching effects will dominate over predissociation and R-T transfer contributions should be negligible and would lead to slower removal rates. In addition to the described work, the authors found Br_2 gain to be on the order of 0.11/cm and observed ASE from the v' = 13, P(46) line of Br_2. (12:2526-2533)

Van De Burgt and Heaven conducted an investigation of the electronic self-quenching of the B state of Br_2. A pulsed dye laser was used to excite molecules to specific rovibrational levels. Observations of real time fluorescence decay allowed the measurement of Br_2 B state lifetimes. Deactivation by $Br_2(X)$ and He over a pressure range of 0.002-5 Torr was examined. Stern Volmer (SV) plots and a computer model of spontaneous decay, quenching, and energy transfer were used in data analysis. SV plots for J' <15 and pressures <5 Torr exhibited significant curvature due to competition between spontaneous and collisional deactivation. For higher J' values the SV plots were linear. Effective Br_2 self-deactivation rates ranging from (4.0-11) x 10^{-10} cm^3 $molecule^{-1}$ s^{-1} were measured for pressures of 0-2 Torr. A quenching rate constant of (4.2 $\pm$ 0.5) x 10^{-10} cm^3 $molecule^{-1}$ $s.^{1}$ was reported. This is in close agreement with Clyne *et al.* Rotational energy transfer rates were reported to be (6 $\pm$ 2) x 10^{-10} cm^3 $molecule^{-1}$ s^{-1} and vibrational energy transfer rates were believed to be on the order of (2.5-3.5) x 10^{-10} cm^3 $molecule^{-1}$ s^{-1}. This yielded a total removal rate on the order of 1.4 x 10^{-9} cm^3 $molecule^{-1}$ s^{-1} which is drastically different from the rate of 2.5 x 10^{-10} cm^3 $molecule^{-1}$ s^{-1} suggested by Perram and Davis. Effective deactivation rates for

He as a collision partner at pressures of 0-5 Torr were measured to be less than 2×10^{-10} cm^3 $molecule^{-1}$ s^{-1}. (13:407-416)

Thus, even though molecular bromine has been studied extensively, the kinetics of the upper laser level are not clear. The quenching rates reported by Clyne *et al.*(8) and Van De Burgt and Heaven (13) are not consistent with the laser output's pressure dependence measured by Perram and Davis (12:2531).

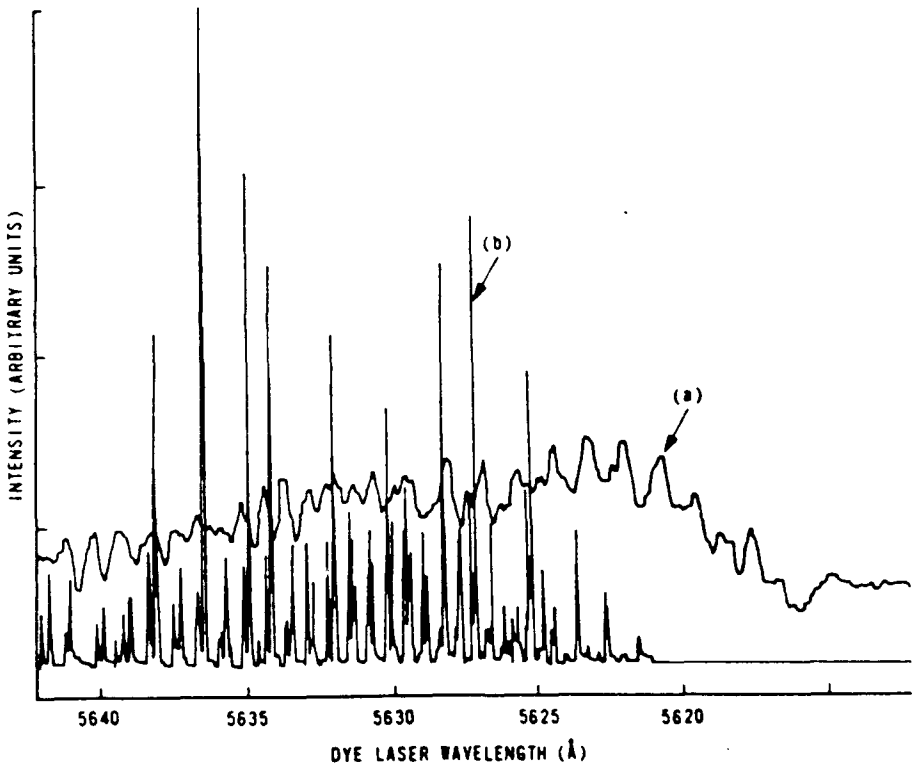

Figure 6. Excitation Spectra.
Spontaneous Side Fluorescence as a Signal Monitor (a)
and Stimulated Emission as a Signal Monitor (b).(12:2528)

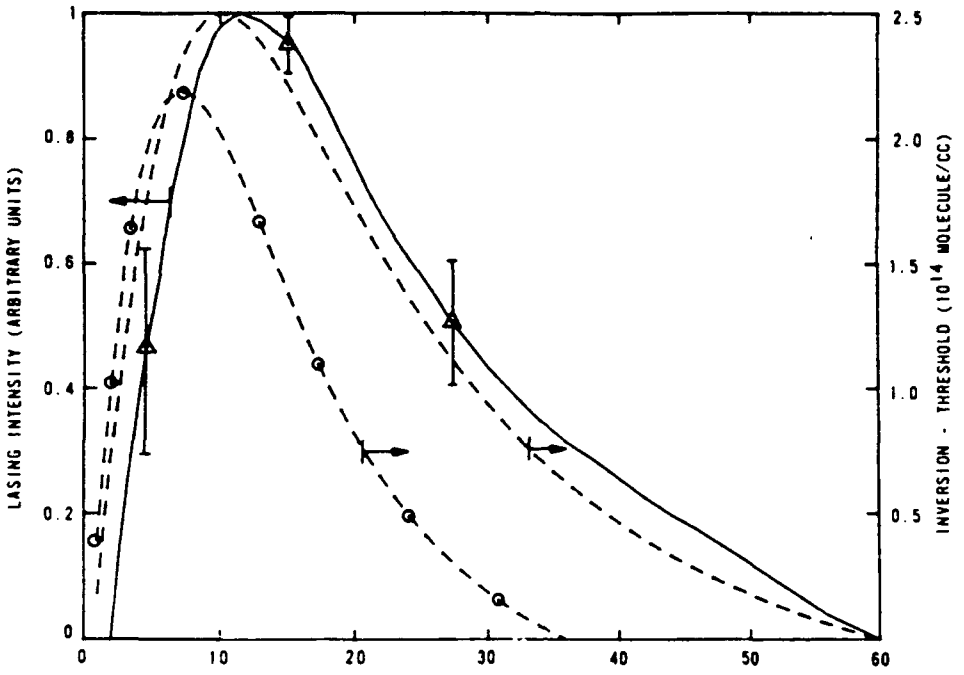

Figure 7. Br_2 Laser Output as a Function of Br_2 Pressure
Δ indicates measured values, --- indicates predicted curve with 2.5×10^{-10} cm^3 $molecule^{-1}$ s^{-1} rate, and -O- indicates predicted curve with 2.5×10^{-10} cm^3 $molecule^{-1}$ s^{-1} rate.(12:2531)

III. *Experimental*

A. *Pump Source*

Two pump sources were used during this effort. A Lambda Physik excimer and dye laser system served as the pump source for early side fluorescence measurements. However, the excimer laser developed a gas leak and became unusable. For the remaining side fluorescence and all stimulated emission measurements, a Quanta-Ray Nd:YAG pumped dye laser system was used to provide a tunable pump signal.

The Lambda Physik system consisted of a Model EMG 101 MSC Excimer Laser and a Model FL 3002 Dye Laser. The excimer laser used a XeCl active medium to produce a 308 nm pulse with a linewidth $10\ cm^{-1}$ to drive the dye laser. Coumarin 540A dye was used in the dye laser to provide a tunable output signal over the range of 522 to 600 nm. The Lambda Physik system provided approximately 17 ns pulses at a 20 Hz rate with $\leq$23 mJ/pulse. The dye laser's linewidth was not measured prior to system failure.

The Quanta-Ray Nd:YAG pumped dye laser system consisted of a Q-switched Nd:YAG laser (DCR-3), an harmonic generator (HG-2) containing KDP crystals, and a pulsed dye laser (PDL-2). The Q-switched Nd:YAG 1064 nm output was frequency doubled to 532 nm by the harmonic generator to drive the pulsed dye laser. The pulsed dye laser contained a motor controlled grating which allowed for output wavelength selection. Rhodamine 590 dye was used in the pulsed dye laser to provide pump wavelengths in the 550-575 nm range. The Nd:YAG pumped dye laser system provided 8 ns pulses at a 20 Hz rate with a bandwidth on the order of $0.3\ cm^{-1}$. The system's output ranged from 13 to 48 mJ/pulse, as measured

by a Quantronix 504 Energy Meter and 501 Energy Receiver, over the 550 to 575 nm range when operated at maximum power output. The bulk of experimental work was limited to pump wavelengths between 560 and 570 nm where the system's output was ≥35 mJ/pulse.

B. *Gain Cell and Gas Handling System*

The gain cell, shown in Figure 8, was constructed of glass with a 0.5 inch (12 mm) diameter. The gain cell was terminated on each end with removable one inch diameter glass windows at Brewster's angle. The removable windows were required to allow periodic cleaning. The length of the gain cell from input to exit Brewster windows was 130 cm. A gas handling system, also shown in Figure 8, was used to handle the Br_2. After placing the Br_2 in the handling system, the system was sealed. Gas pressures were monitored with an MKS Baratron PAR-100 Pressure Meter and 221AHS-A-100 100 Torr Pressure Transducer located near the laser o[illegible]. The Br_2 was subjected to repeated freeze-thaw-pumping cycles with liquid nitroge[illegible]. This allowed any impurities in the Br_2 to be effectively removed. Between e[illegible]perimental runs, the gain cell was evacuated to ≤0.01 Torr. A cold trap was used to capture any residual Br_2 from the gain cell and protect the Duo Seal Model 1376 Vacuum Pump during cell evacuation.

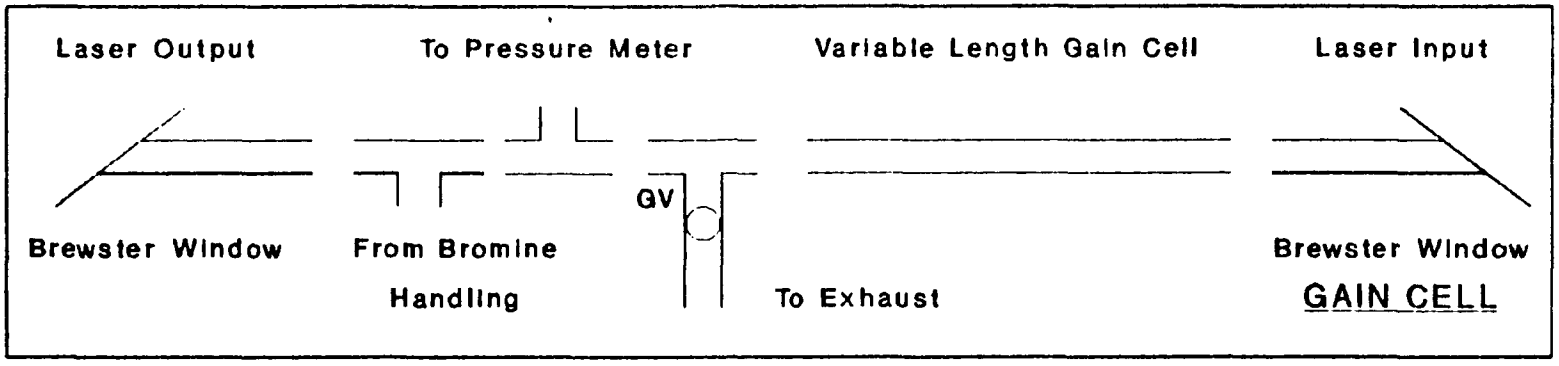

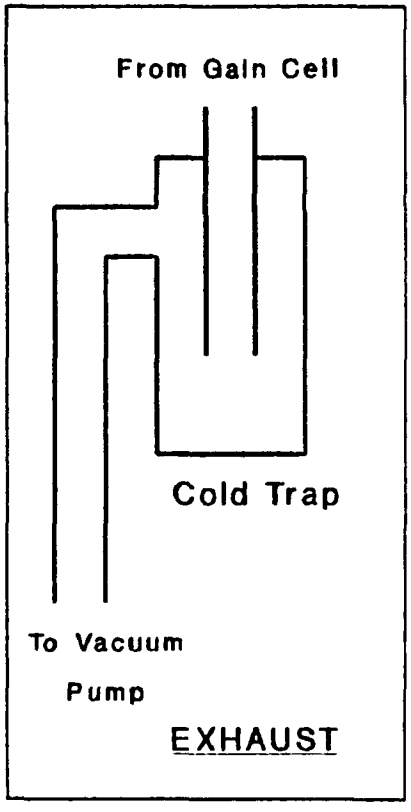

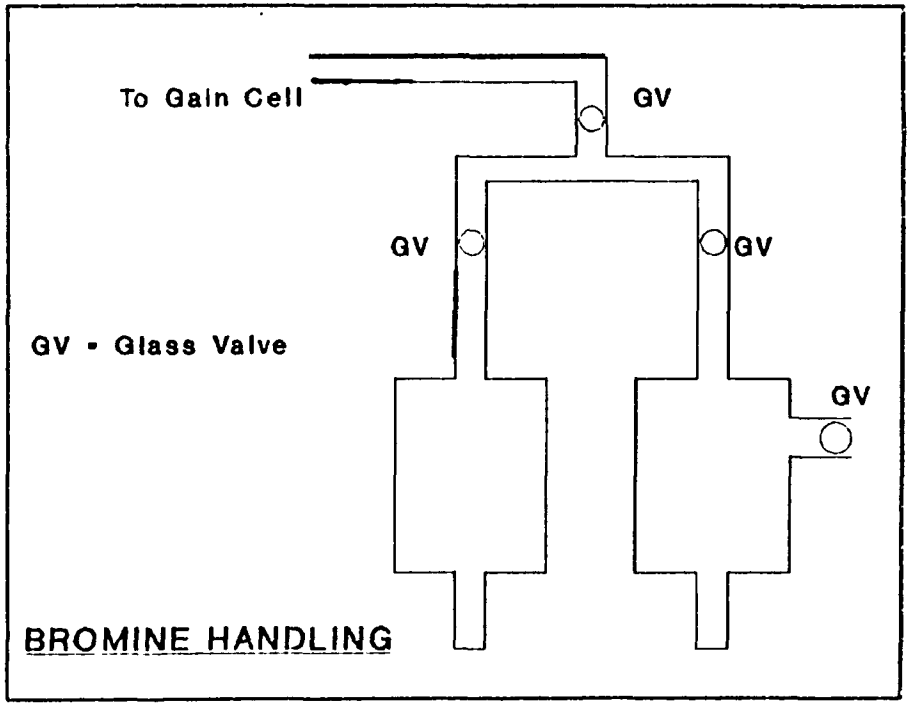

Figure 8. Gain Cell and Gas Handling System

C. *Data Acquisition*

As described earlier, both side fluorescence (perpendicular to the excitation beam) and stimulated emission were used as signal monitors during data acquisition. In order to block the dye pump beam from the detector, 630 nm long-pass filters were employed. A photomultiplier (RCA Type 7326), boxcar integrator (PARC Model 162), and strip chart were used to record the stimulated emission intensity and unresolved side fluorescence as a function of pump wavelength at specific gas pressures. The boxcar integrator averaged the 20 Hz signal and provided a voltage proportional to the input signal's intensity. A Tektronix Model 7834 Oscilloscope was used to monitor the photomultiplier signal and boxcar integrator's gate. The Oscilloscope was also used to measure the time delay between the dye laser pump pulse and Br_2 ASE pulse during stimulated emission experiments. To measure this time delay, it was necessary to remove the 630 nm long pass filter closest to the photomultiplier to allow a portion of the dye pump beam to be detected. A typical measurement configuration is shown in Figure 9.

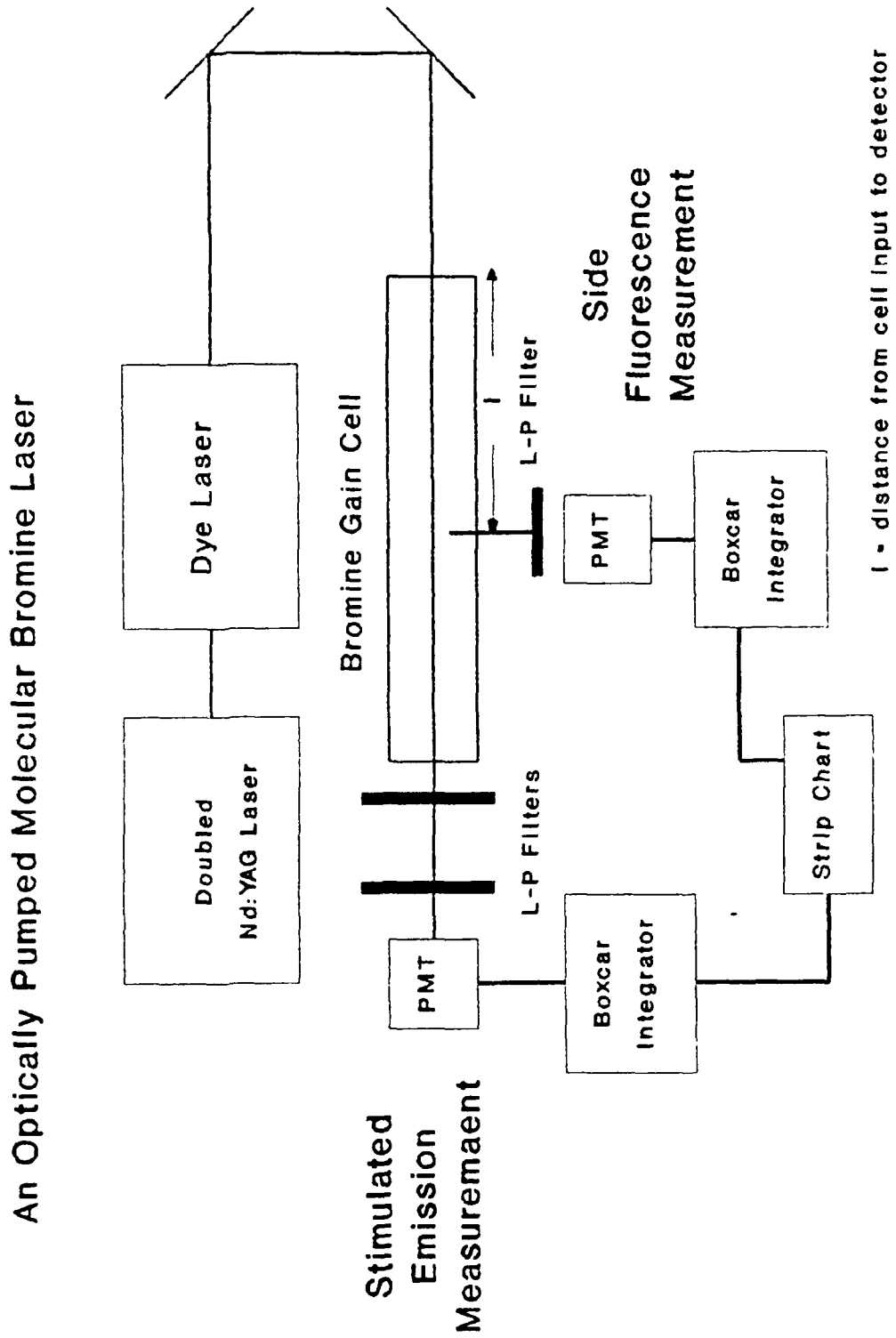

Figure 9. Experimental Setup

IV. *Results and Discussion*

A. *Spectroscopic Assignments*

Spectra were obtained using both side fluorescence and stimulated emission as signal monitors. A typical side fluorescence spectra depicting the majority of the (14,0) band is shown in Figure 10. This spectra along with additional side fluorescence spectra found in Appendix A were obtained using the Quanta-Ray Nd:YAG pumped dye laser system as the pump source. Using the constants of Barrow *et al.*(3), it can be determined that the bandhead is at 562.0 nm. The side fluorescence spectra obtained lack the resolution necessary to perform detailed assignments. The lack of resolution is due to the presence of the three bromine isotopes ($^{79}Br^{79}Br$, $^{79}Br^{81}Br$, and $^{81}Br^{81}Br$) and the relatively wide bandwidth (0.3 cm^{-1}) of the dye laser.

Figure 11 shows a typical excitation spectra of the (14,0) band using stimulated emission as the signal monitor. The characteristic P-R doublet structure of the halogen molecules is apparent. The ASE output signal being monitored fluctuated between shots and even "turned off" at times implying that it was being run just over the threshold level. As the bromine isotopes $^{79}Br^{79}Br$ and $^{81}Br^{81}Br$ each have relative populations of approximately one half the $^{79}Br^{81}Br$ isotope population, they were not sufficiently excited to achieve the threshold level. Therefore, the spectra in Figure 11 was assigned to the $^{79}Br^{81}Br$ isotope of bromine. The increased resolution provided by the use of stimulated emission as the signal

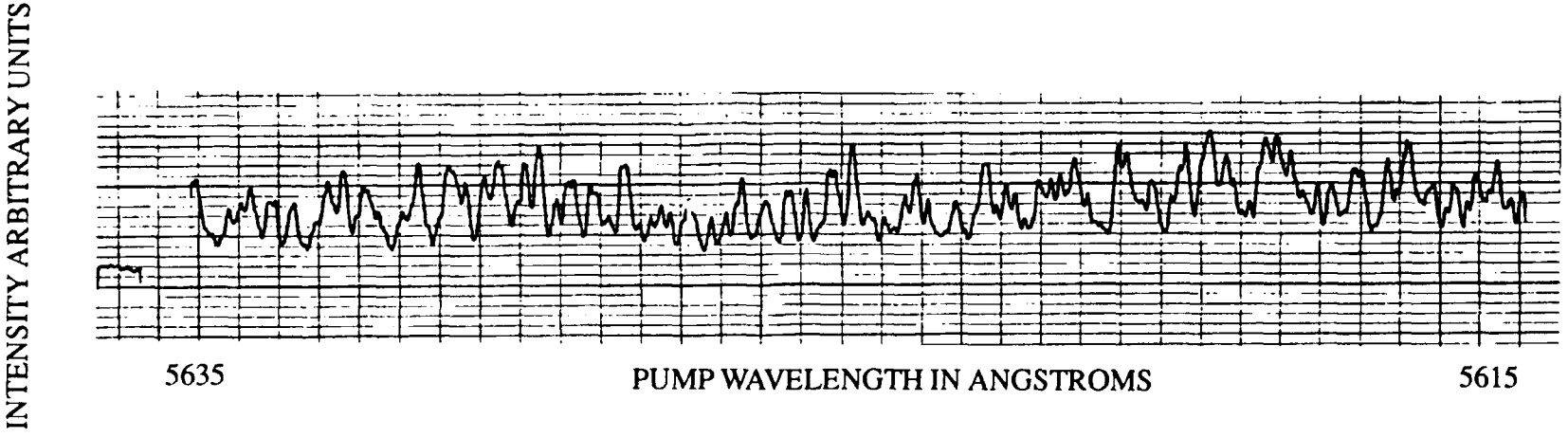

Figure 10. Side Fluorescence Spectra

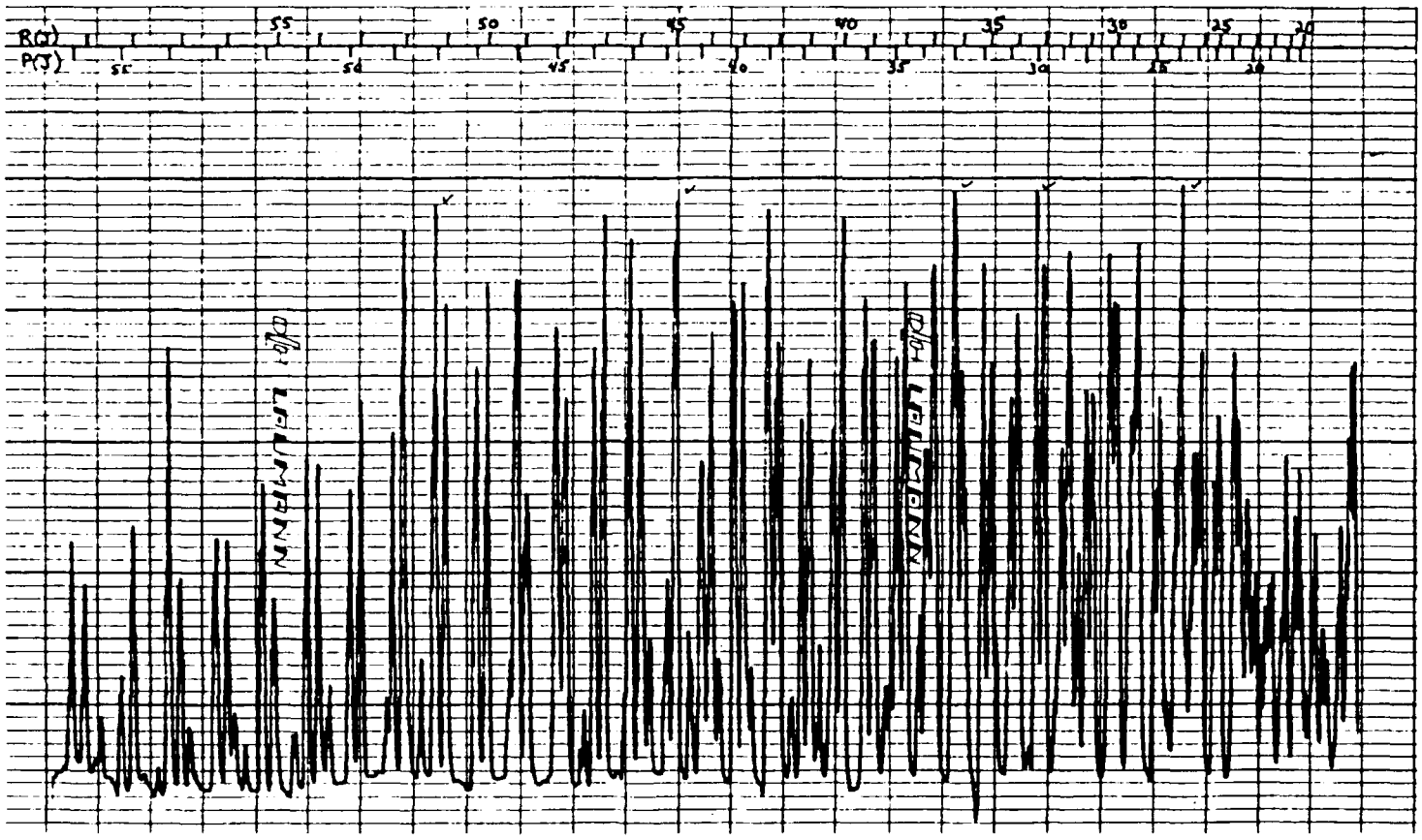

Figure 11. Stimulated Emission Spectra

monitor facilitated further spectroscopic assignment. Examination of the second differences between adjacent doublets allowed rotational assignments to be made. Figure 12 shows a comparison of the measured differences $\Delta F(J)=P(J)-P(J+1)$ with the differences obtained using the constants of Barrow *et al.*(3) for the (14,0) band. The observed and calculated differences are in good agreement.

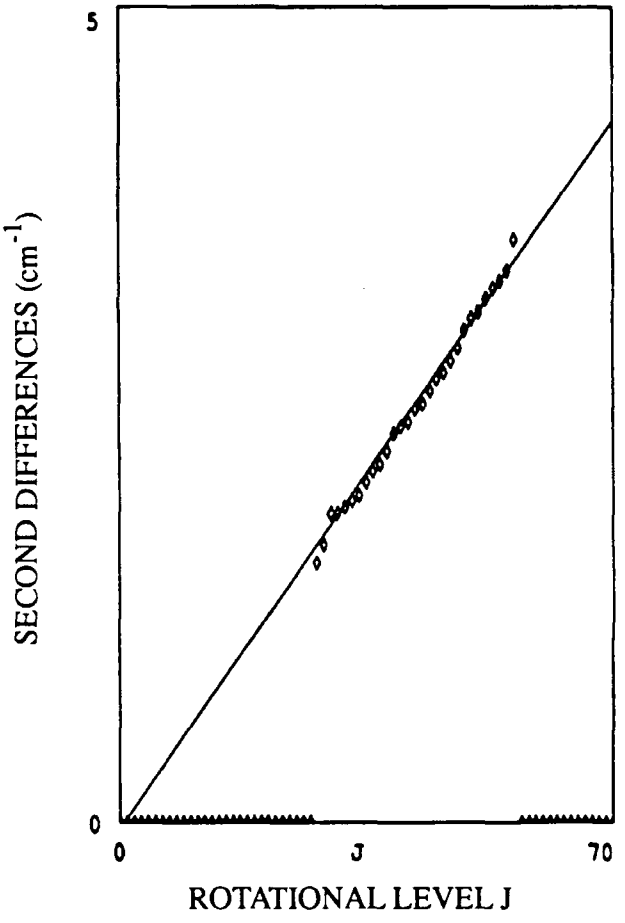

Figure 12. Second Differences A comparison of the measured differences $\Delta F(J)=P(J)-P(J+1)$ with the differences obtained using the constants of Barrow *et al.*(3) for the (14,0) band.

B. *Side Fluorescence Spectra*

Side Fluorescence data was examined to observe the effect that changes to the pump power, the bromine vapor pressure, and location of the detection device with respect to the gain cell input have on the magnitude and characteristics of the side fluorescence spectra. As the pump beam proceeds down the length of the gain cell, more and more of the input intensity is absorbed resulting in a dropoff of the detected side fluorescence output intensity. The detected side fluorescence can be described by:

$$I_{out} = I_{in} \exp(\Delta N \, \sigma_{SE} \, l) \tag{12}$$

where I_{in} is the intensity of the pump signal, σ_{SE} is the stimulated emission cross section, and l is the distance from the input of the cell (gain medium) to the location of the detector (15:176). ΔN can be approximated as:

$$\Delta N \approx N_2 - N_1 \approx -N1 \approx -P/(k\,T) \tag{13}$$

where N_2 is the population of the excited energy state (assumed zero initially), N_1 is the population of the unexcited energy state, P is the pressure of the gain medium (bromine), k is Boltzmann's constant, and T is the ambient temperature. Thus, equation (12) can be recast as:

$$I_{out} = I_{in} \exp[-(P\sigma_{SE} \, l)/(k\,T)] \tag{14}$$

where $-(P\sigma_{SE}\, l)/(k\,T)$ describes the absorption of the media. Equation (14) states the measured side fluorescence intensity varies linearly with respect to changes of the input pump intensity (Iin) and exponentially with changes to the gain medium (bromine) pressure (P) or changes to the detector distance from the gain cell input (l). The relationships

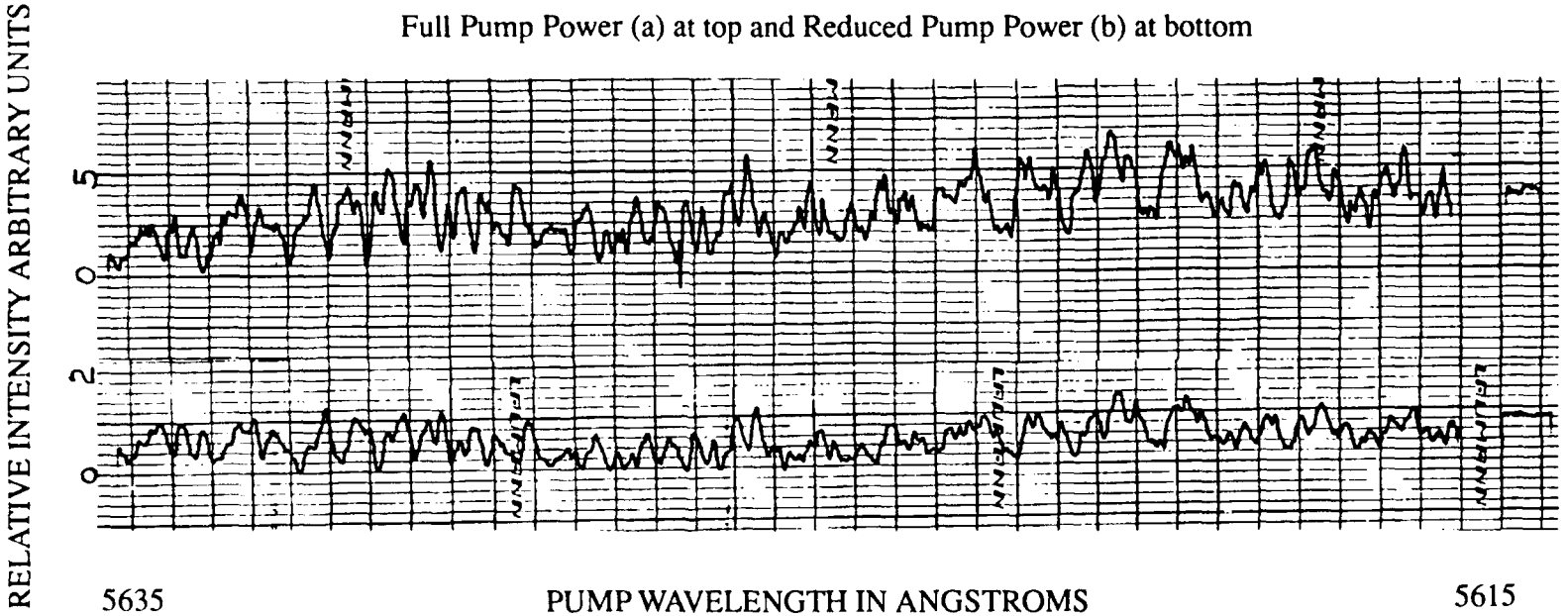

Figure 13. Side Fluorescence as a Function of Input Pump Intensity: Full (a) and Reduced (b) Power

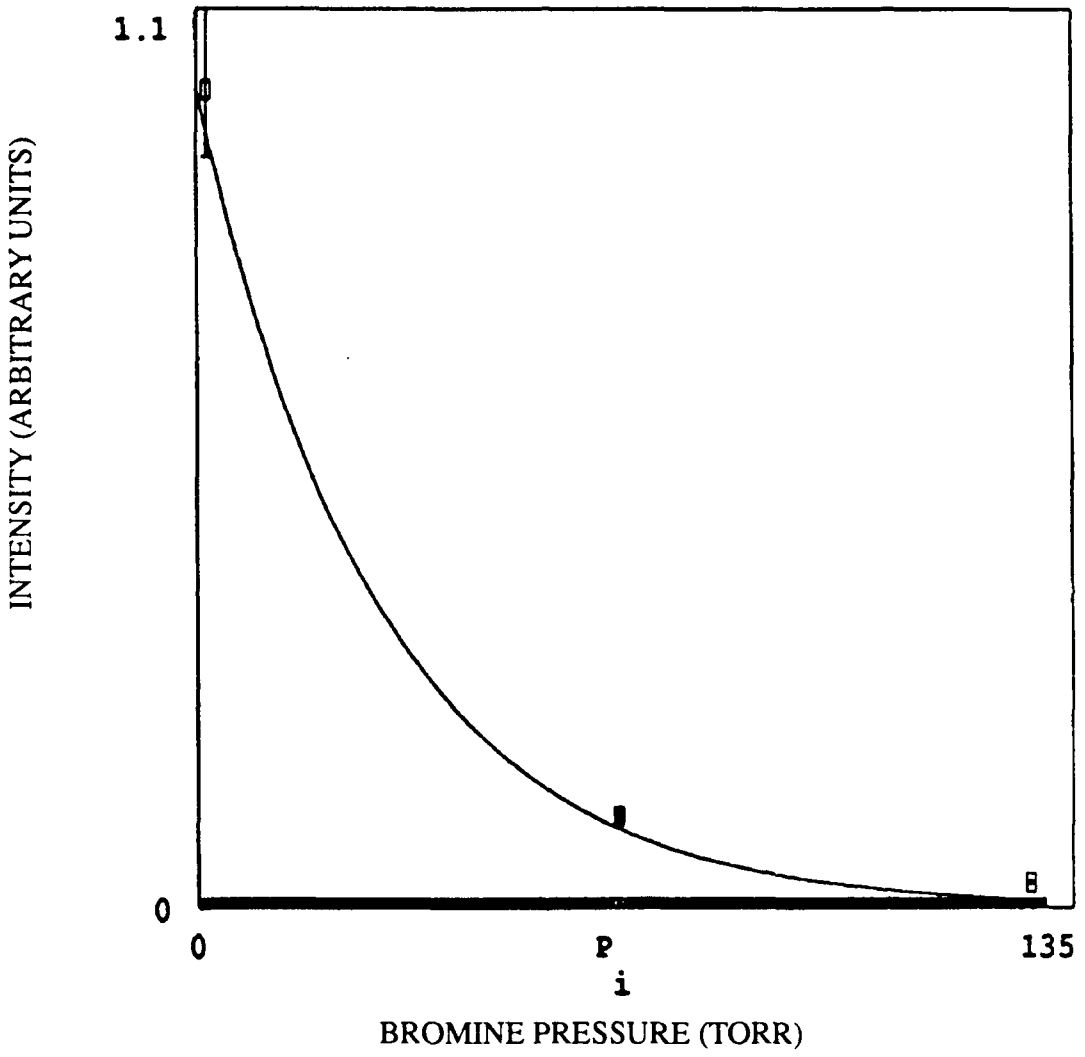

Figure 14. Side Fluorescence as a Function of Bromine Pressure
Detector located 25 cm from Cell Input

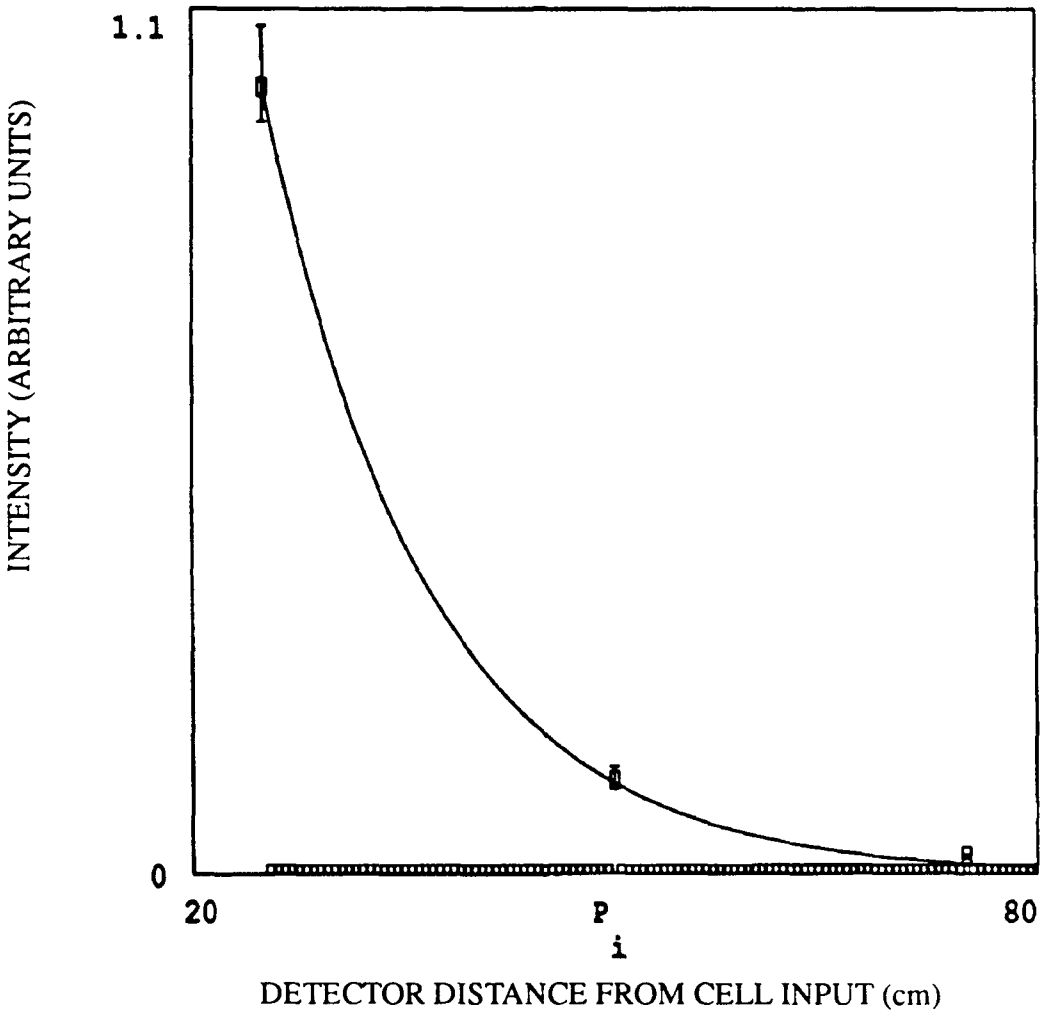

Figure 15. Side Fluorescence as a Function of Detector Location
Bromine Pressure is 128 Torr

anticipated by Equation (14) are confirmed by Figures 13, 14, and 15 which depict side fluorescence as a function of input intensity, bromine pressure, and detector location respectively.

C. *Power Output vs Br_2 Pressure*

Mirrorless lasing or ASE was observed over a wide range of bromine pressures (4-40 Torr). Stimulated emission was used as a signal monitor to determine the peak signal occurred around 8-12 Torr. This behavior is similar to the output peak near 10 Torr observed by Wodarczk and Schlossberg (11:4480) and the peaked output around 10-15 Torr noted by Perram and Davis (12:2530). The relative strength of the Br_2 mirrorless lasing was determined by two different methods The first method consisted of scanning the dye laser over the (14,0) band and averaging the magnitude of the five strongest Br_2 lines observed while holding the Br_2 pressure constant. This process was then repeated for various Br_2 pressures similar to the work of Perram and Davis.(12:2530) Figure 16 shows the resulting Br_2 ASE power as a function of Br_2 pressure achieved via this method. It should be noted that the data is fairly erratic as denoted by the error bars. This is due to the fact the mirrorless lasing was occurring very near threshold which resulted in an output beam that varied in intensity from shot to shot. The solid curves of Figure 16 will be explained later. Actual spectra obtained via this method are contained in Appendix B.

In an effort to average out some of the erratic nature of the data a second method of determining the relative strength of the Br_2 mirrorless lasing was employed. This method involved tuning the dye laser to a fixed pump wavelength, adjusting the Br_2 pressure to a

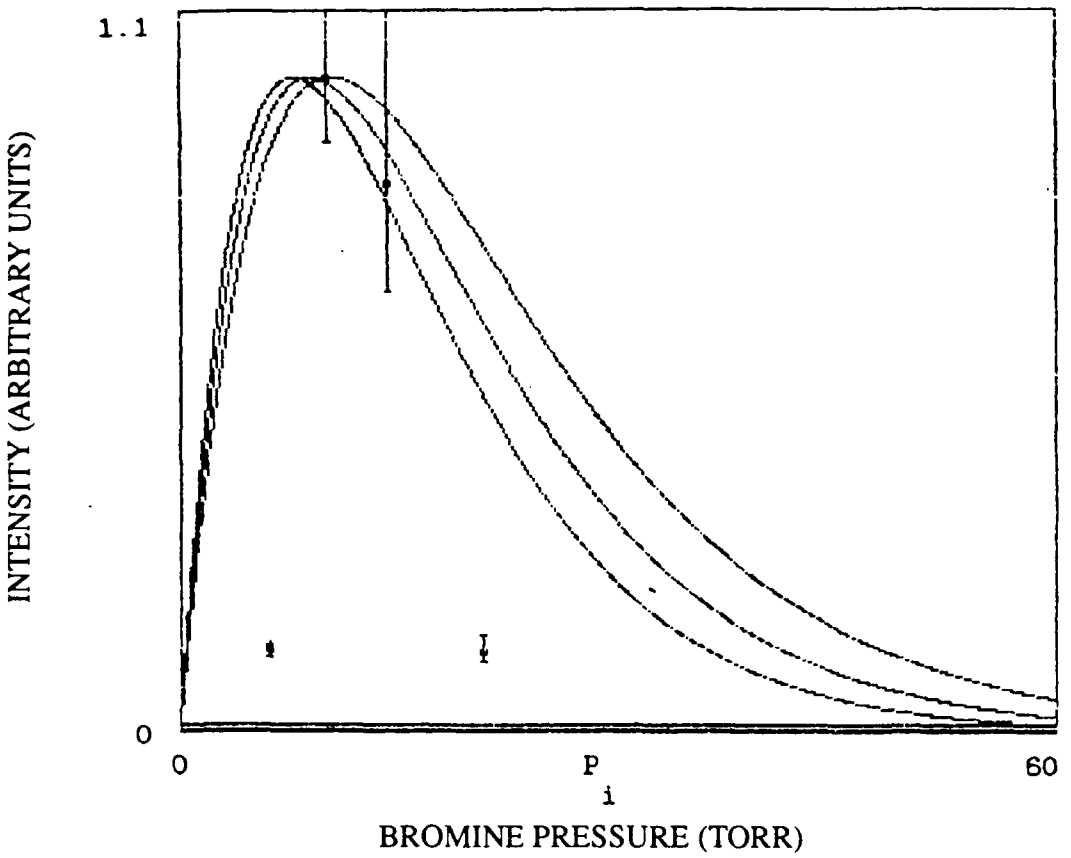

Figure 16. ASE Output vs Br_2 Pressure Via Dye Laser Scan
The solid curves represent a total removal rate of
2.5×10^{-10} cm^3 $molecule^{-1}$ s^{-1} with a time delay (t_D) of
12 (a), 14 (b), and 16 (c) nanoseconds.

stable value, and then averaging the ASE output for approximately 4 minutes. The Br_2 pressure was then adjusted to a new stable value and the process was repeated. The longer averaging period reduced the erratic nature of the data. This procedure was employed at various pump wavelengths representing a wide range of rotational levels in the (14,0) band. Figure 17 shows a typical data set employing this collection method. The solid curves in

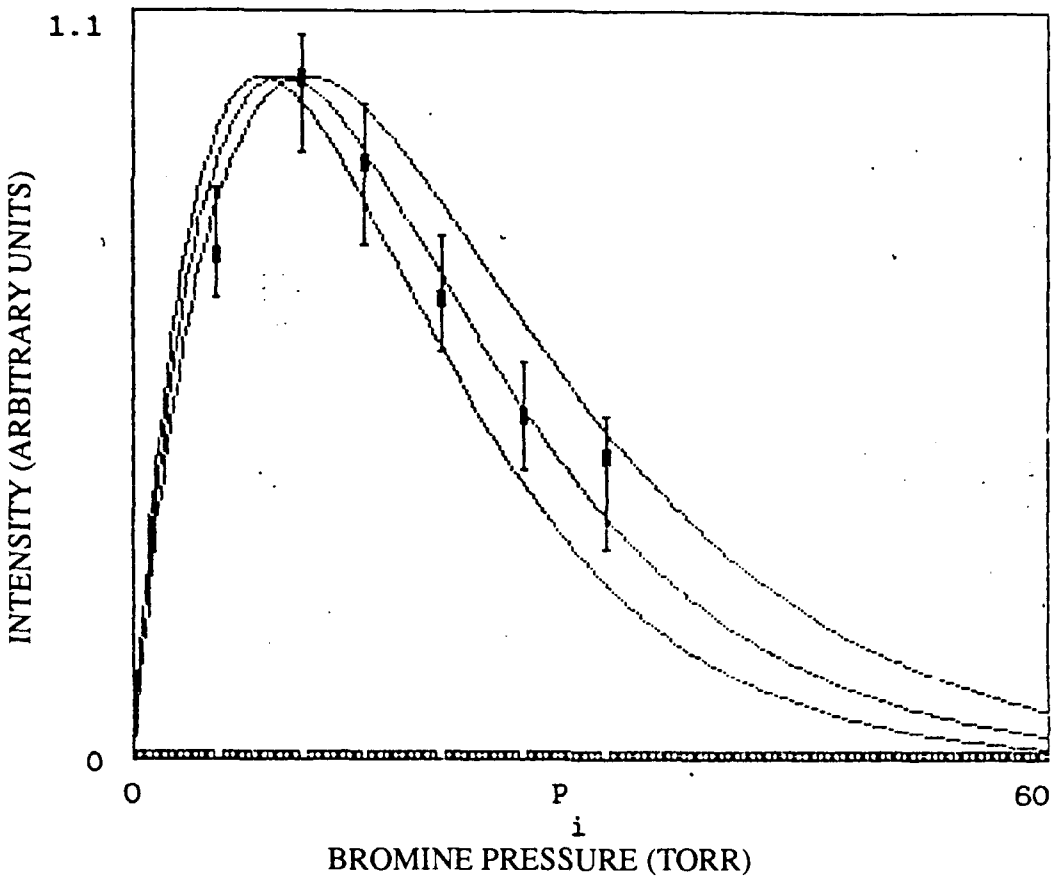

Figure 17. ASE Output vs Br_2 Pressure at Fixed Pump Wavelength
Pump Wavelength = 564.164 nm Corresponding to the P(46) Br_2 Line.
The solid curves represent a total removal rate of
2.3×10^{-10} cm^3 $molecule^{-1}$ s^{-1} with a time delay (t_D) of
12 (a), 14 (b), and 16 (c) nanoseconds.

Figure 17 will be described shortly. Additional data sets and actual raw data plots are contained in Appendix C.

This ASE output power as a function of Br_2 pressure data can be used to obtain a total removal rate for depopulation of the upper lasing level, if we recall the simplified model to

study quenching described earlier:

$$P = P_0 \exp(-k[M]t_D) \quad (1)$$

Dividing by P_0 and taking the natural log leads to:

$$\ln(P/P_0) = -k[M]t_D \quad (15)$$

from which the total removal rate k can be extracted. The time delay between the dye laser pump pulse and the Br_2 ASE pulse, measured between the peak of the two pulses, was 14 $\pm$ 2 nanoseconds. The solid curves in Figures 16 and 17 represent total removal rates of 2.5 x 10^{-10} cm^3 $molecule^{-1}$ s^{-1} and 2.3 x 10^{-10} cm^3 $molecule^{-1}$ s^{-1} respectively with time delays (t_D) of 12 (a), 14 (b) , and 16 (c) nanoseconds. Figure 18 a displays the same data as Figure 17. However, the solid curves of Figure 18 represent a time delay of 14 nanoseconds with total removal rates of 2.3 x 10^{-10} cm^3 $molecule^{-1}$ s^{-1} (a), 5 x 10^{-10} cm^3 $molecule^{-1}$ s^{-1} (b), and 1.4 x 10^{-9} cm^3 $molecule^{-1}$ s^{-1} (c). Figure 18b plots ln (P/P_0) vs bromine pressure. The solid line of Figure 18b depicts a line with slope -kt_D and shows that with a time delay (t_D) of 14 nanoseconds, a total removal rate (k) of 2.3 x 10^{-10} cm^3 $molecule^{-1}$ s^{-1} provides a good fit to the observed data. The agreement between the actual data and the predicted values is much better with the slower removal rate of 2.3 x 10-10 cm^3 $molecule^{-1}$ s^{-1}. This agreement with the slower removal rate is typical of the data sets collected. Total removal rates of 2.3 x 10^{-10} cm^3 $molecule^{-1}$ s^{-1} to 5.0 x 10^{-10} cm^3 $molecule^{-1}$ s^{-1} with a time delay of 14 nanoseconds are shown to be in good agreement with the data in Appendix C. Thus, a total removal rate, including all processes which remove population from the upper laser level, of 2.9 x 10^{-10} cm^3 $molecule^{-1}$ s^{-1} is proposed. This value is the average of all data sets collected.

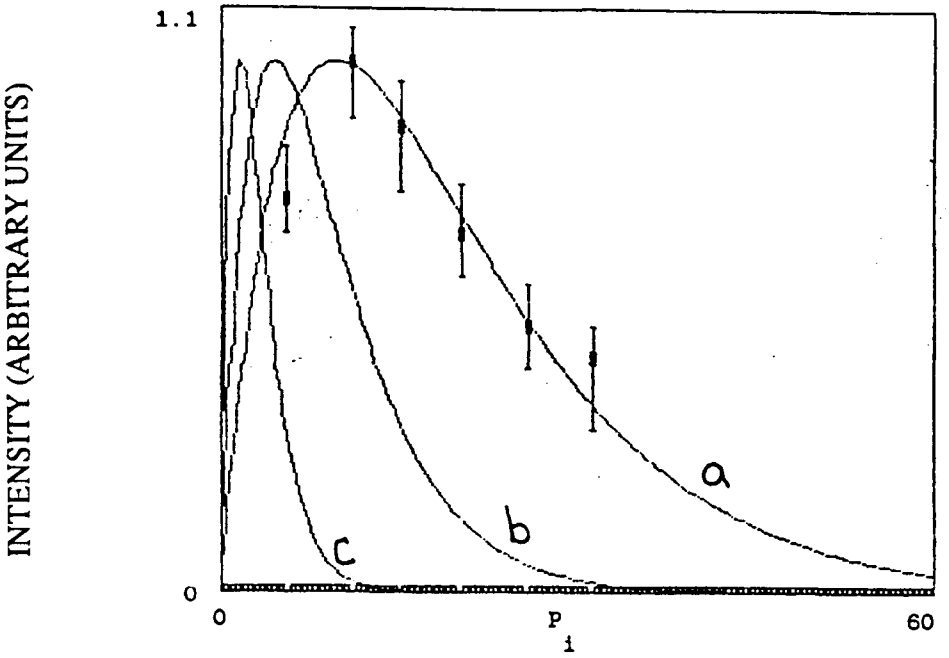

Figure 18a. The solid curves represent a time delay (t_D) of 14 nanoseconds with total removal rates of 2.3×10^{-10} cm^3 $molecule^{-1}$ s^{-1} (a), 5×10^{-10} cm^3 $molecule^{-1}$ s^{-1} (b), and 1.4×10^{-9} cm^3 $molecule^{-1}$ s^{-1} (c).

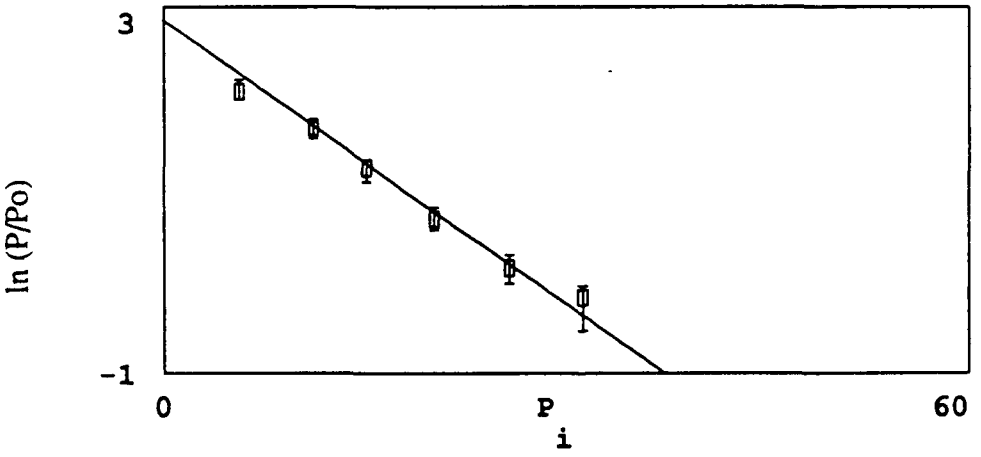

Figure 18b. $\ln(P/P_0)$ vs bromine pressure. The solid line represents a slope of $-kt_D$ with t_D = 14 ns and $k = 2.3 \times 10^{-10}$ cm^3 $molecule^{-1}$ s^{-1}.

Figure 18. ASE Output vs Br_2 Pressure with Different Removal Rates

The proposed total removal rate of 2.9 x 10^{-10} cm^3 $molecule^{-1}$ s^{-1} is in close agreement with the value of 2.5 x 10^{-10} cm^3 $molecule^{-1}$ s^{-1} suggested by Perram and Davis (12:2531), but disagrees with the quenching rate constant of (4.2 $\pm$ 1.3) x 10^{-10} cm^3 $molecule^{-1}$ s^{-1} reported by Clyne *et al.* (8:961) and the total removal rate on the order of 1.4 x 10^{-9} cm^3 $molecule^{-1}$ s^{-1} reported by Van De Burgt and Heaven (13:415). It should be noted that the Clyne *et al.* work was conducted at pressures less than 100 mTorr (8:972) and the Van De Burgt and Heaven data was taken at pressures less than 5 Torr (13:408). Meanwhile, the present work concentrated on pressures above 5 Torr similar to the efforts of Perram and Davis (12:2531). At these higher pressures quenching should be the main factor depleting the upper laser level and the effects of energy transfer should be negligible which should yield a slower removal rate. Also, the slower removal rates seem to be in closer agreement with the laser's observed performance. Using the simple relationship:

$$P = N k T \tag{16}$$

where P is pressure, N is the number of molecules/cm3, k is Boltzmann's constant, and T is the temperature yields approximately 3.2 x 10^{17} molecules/cm^3 at a pressure of 10 Torr, near the laser's peak output. At 10 Torr, a removal rate of 1.4 x 10^{-9} cm^3 $molecule^{-1}$ s^{-1} would depopulate the upper lasing level in 2.2 nanoseconds. This does not agree with the observed time delay between the dye pump pulse and ASE pulse of 12-16 nanoseconds. However, the slower removal rate of 2.9 x 10^{-10} cm^3 $molecule^{-1}$ s^{-1} depopulates the 10 Torr upper lasing level in 10.8 nanoseconds which is much closer to the observed time delay.

D. *Inverted Side Fluorescence*

Early side fluorescence measurements using the Lambda Physik Excimer and Dye Lasers as the dye pump source resulted in some very unusual spectra. During these measurements, a pressure meter was unavailable. Qualitatively, three sets of spectra were obtained: one set at extremely high bromine pressure (enough to totally absorb the dye pump beam) shown in Figure 19, one set at a moderately high bromine pressure (enough to totally absorb the dye pump beam at certain wavelengths and partially absorb it at other wavelengths) displayed in Figure 20, and one set at relatively low bromine pressure (the dye pump beam was only partially absorbed at all wavelengths observed) depicted in Figure 21. Examination of the three scans reveals some very unusual features. The spectra at extremely high and moderately high pressures appear to be inverted. Nulls rather than peaks occur at strong bromine absorption lines. Secondly, all three spectra seem to lack the characteristic P-R doublet structure expected of the halogen molecules. Examination of the second differences between adjacent deep nulls in Figures 19 and 20 and strong peaks in Figure 21 allowed rotational assignments to be made. Figure 22 shows a comparison of the measured differences $\Delta F(J)=P(J)-P(J+1)$ with the differences obtained using the constants of Barrow *et al.*(3) for the (14,0) band for the extremely high pressure (a), moderately high pressure (b), and relatively low pressure (c) cases. The observed and calculated differences show a fair agreement. This agreement leads to the belief that the spectral features are indeed real and attributable to Br_2. It is believed the inverted nature of the spectra at higher pressures is due to the weakness of the pump beam, and the lack of P-R doublet structure is due to the duration and linewidth of the pump beam. It is suggested that the pump beam signal is weak

enough that, at the higher pressures, the entire pump beam has been absorbed at the strong Br_2 lines before reaching the detector location. Thus, at these strong absorption lines, no incident beam exists and the detected signal is weaker than the side fluorescence at adjacent wavelengths and therefore appears as a null or inverted peak. Although this behavior could not be precisely modeled, a model showing the relative intensity of the beam at the detector has been developed. This model, detailed in Appendix D, calculates the bromine absorption coefficient and uses it to plot $I_{out}/I_{in} = \exp(-\alpha l)$ as a function of dye pump beam wavelength. A sample plot at a Br_2 pressure of 128 Torr and a detector location (l) of 25 cm is contained in Figure 23. Although this plot does not precisely match the actual spectra observed, it does show the nulling of the beam intensity in a periodic fashion due to strong bromine absorption lines.

During the experimentation, the Lambda Physik Excimer Laser developed a gas leak necessitating a change of pump sources to the Quanta-Ray Nd:YAG pumped dye laser system described earlier. After changing to the Quanta-Ray system, the inverted side fluorescence spectra could not be duplicated.

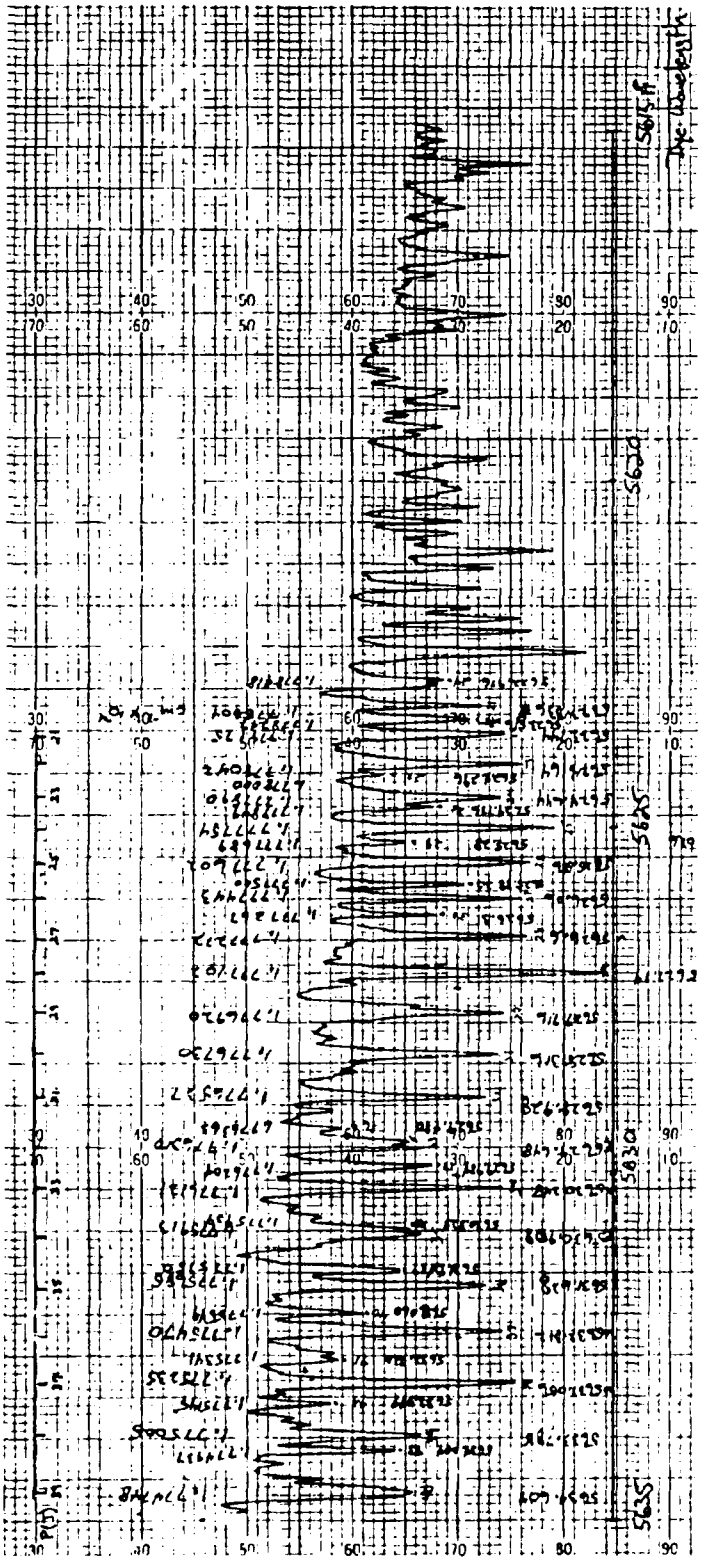

Figure 19. Inverted Side Fluorescence at Extremely High Pressure

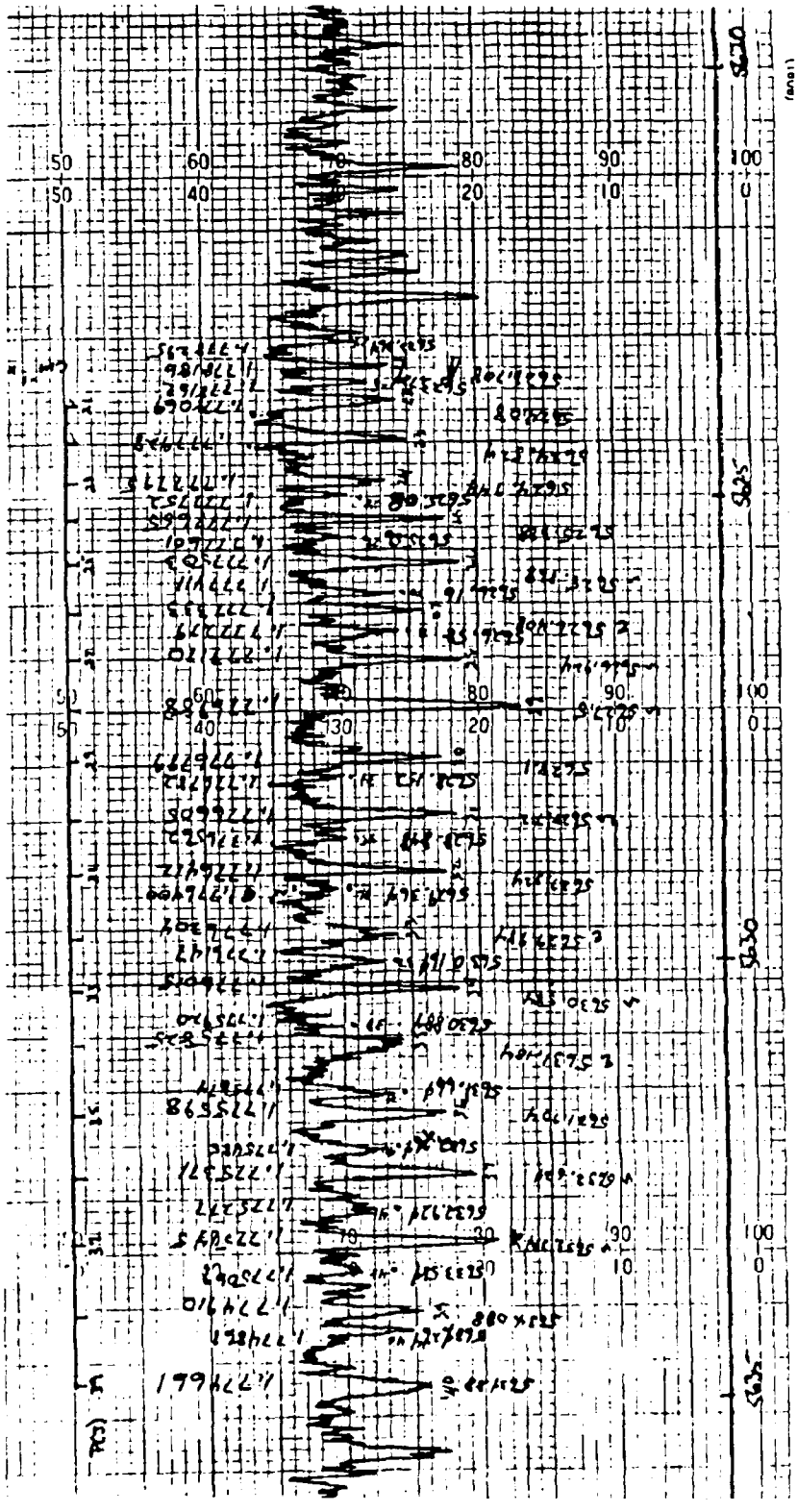

Figure 20. Inverted Side Fluorescence at Moderately High Pressure

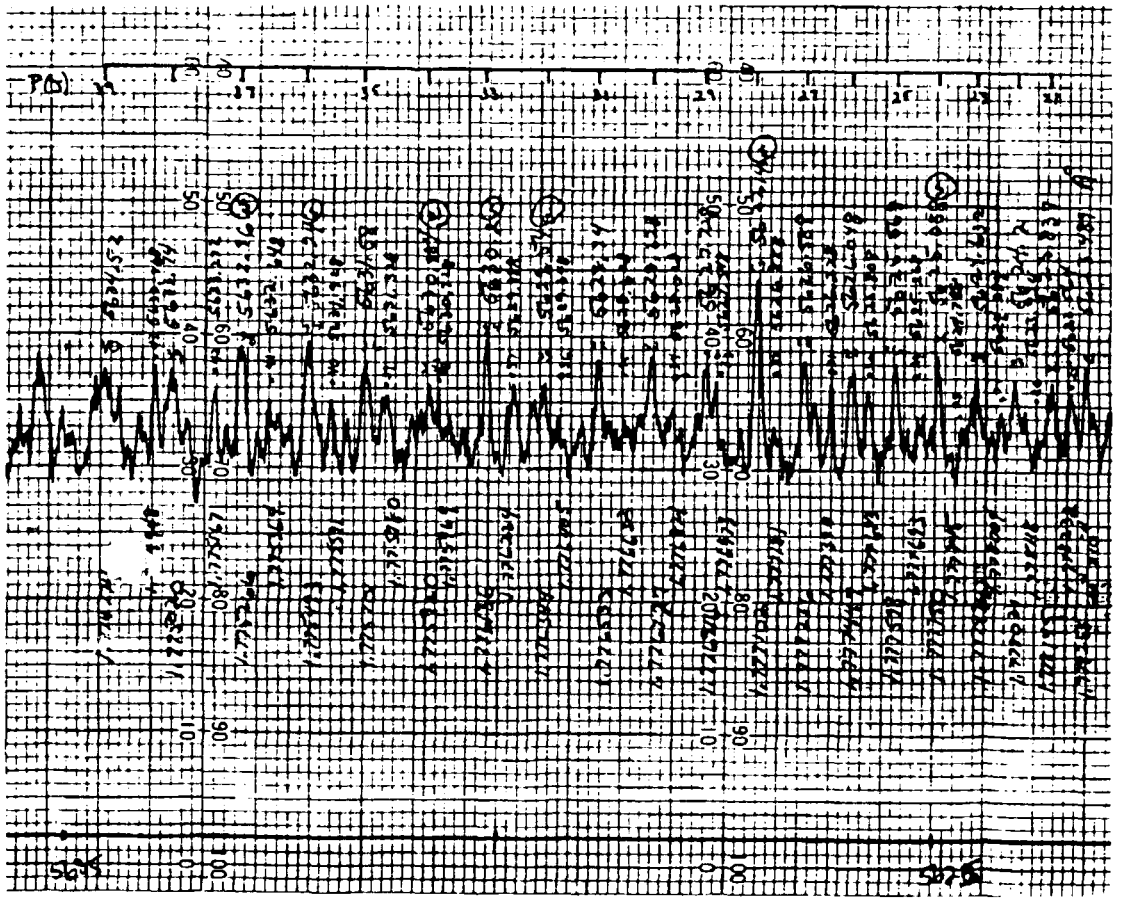

Figure 21. Inverted Side Fluorescence at Relatively Low Pressure

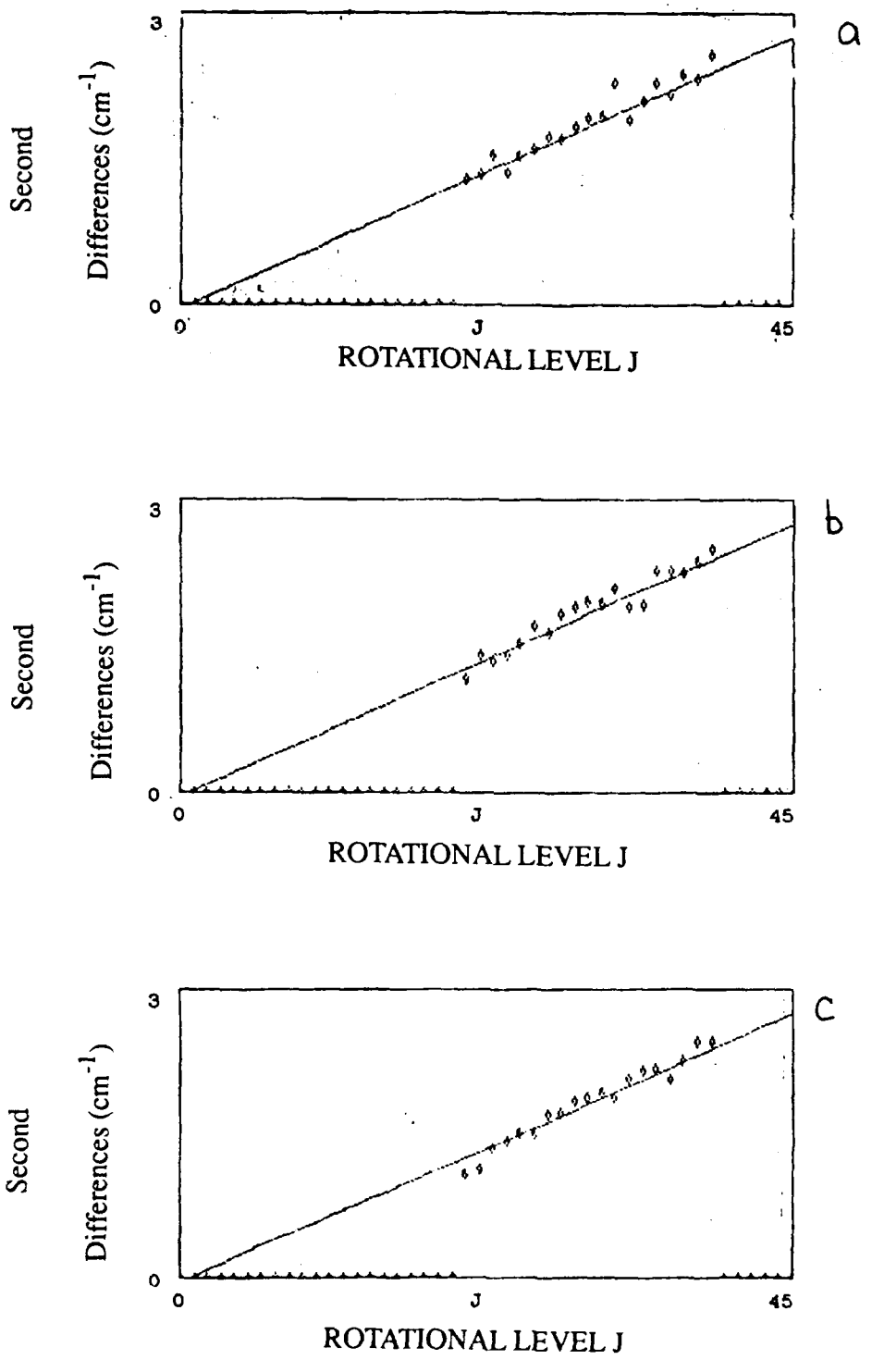

Figure 22. Second Differences for Inverted Spectra extremely high pressure (a), moderately high pressure (b), and relatively low pressure (c) cases.

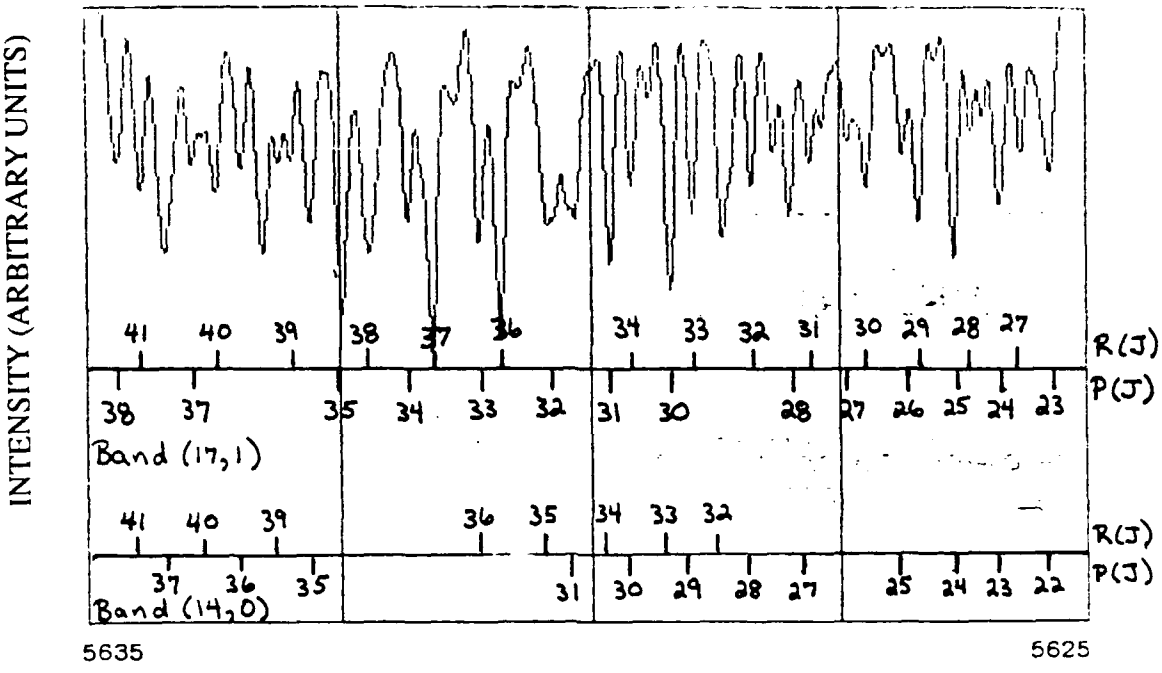

Figure 23. Theoretical Beam Intensity
Br_2 Pressure is 128 Torr, Detector Located 25 cm from Cell Input

V. *Conclusion*

A. *Summary and Conclusions*

The primary objective of this effort was to investigate the quenching kinetics of the B state of Br_2 through a detailed characterization of an optically pumped molecular bromine laser. This included characterization of the pressure dependence of the laser.

The approach was to optically pump molecular bromine in a sealed cell. As the single pass gain for molecular bromine is on the order of 0.11/cm (12:2532), amplified spontaneous emission (ASE) was employed. ASE offered the advantage of a simpler optical system with no externally induced wavelength dependencies. Measurements of unresolved side fluorescence and stimulated emission spectra were recorded. Stimulated emission as a signal monitor offered greater resolution than side fluorescence spectra and facilitated spectroscopic assignment. The spectra obtained were attributed to the (14,0) band of the $^{79}Br^{81}Br$ isotope. The data showed the ASE output to be dependent on the Br_2 pressure in the gain cell. The ASE output peaked around Br_2 pressures from 8-12 Torr. This behavior is similar to the output peak near 10 Torr observed by Wodarczk and Schlossberg (11:4480) and the peaked output around 10-15 Torr noted by Perram and Davis (12:2530). The data was also used to extract and propose a total removal rate, including all processes which remove population from the upper laser level, of 2.9×10^{-10} cm^3 $molecule^{-1}$ s^{-1}. This removal rate is in close agreement with the value of 2.5×10^{-10} cm^3 $molecule^{-1}$ s^{-1} suggested by Perram and Davis (12:2531), but disagrees with the quenching rate constant of $(4.2 \pm 1.3) \times 10^{-10}$ cm^3 $molecule^{-1}$ s^{-1} reported by Clyne *et al.* (8:961) and the total removal rate on the order of 1.4×10^{-9} cm^3 $molecule^{-1}$ s^{-1} reported by Van De Burgt and Heaven (13:415). The slower

removal rates proposed by the current work and suggested by Perram and Davis seem to more closely describe the observed performance of the optically pumped molecular bromine laser. The slower rates are more consistent with the ASE output pressure dependence and the observed time delay between the dye pump beam and ASE pulses.

An interesting, but not fully understood, set of inverted side fluorescence measurements were obtained during the early portions of the work. These spectra appear real and attributable to Br_2 due to a fair agreement between observed and calculated differences of adjacent lines. It is believed the inverted nature of the spectra at higher pressures is due to the weakness of the pump beam, and the lack of P-R doublet structure may be due to the duration and linewidth of the pump beam. It is suggested that the pump beam signal is weak enough that, at the higher pressures, the entire pump beam has been absorbed at the strong Br_2 lines before reaching the detector location. Thus, at these strong absorption lines, no incident beam exists and the detected signal is weaker than the side fluorescence at adjacent wavelengths and therefore appears as a null or inverted peak. Although these spectra do indeed appear attributable to Br_2, they could not be duplicated in later measurements made with a different pump source.

B. *Future Work*

Reported total removal rates for the upper laser level range from the 2.5×10^{-10} cm^3 $molecule^{-1}$ s^{-1} suggested by Perram and Davis (12:2531) to the 1.4×10^{-9} cm^3 $molecule^{-1}$ s^{-1} reported by Van De Burgt and Heaven (13:415). Further studies are required to resolve these differences. It is suggested that additional measurements be taken via method two which involved using stimulated emission as a signal monitor, tuning the dye laser to a fixed

pump wavelength, adjusting the Br_2 pressure to a stable value, and then averaging the ASE output for approximately 4 minutes. The Br_2 pressure was then adjusted to a new stable value and the process was repeated. This method allows a longer averaging period and reduces the erratic nature of the data. Measurements should be made at many Br_2 pressures from 1 to 60 Torr and at various pump wavelengths to gain a better understanding of the laser output's pressure dependence. Another interesting study would be to examine the upper laser level removal rate with collision partners other than Br_2.

Finally, the inverted side fluorescence spectra should be revisited. This could be done in two ways: The first would be to use the Lambda Physik system, once it is operational, as the pump source and attempt to duplicate the inverted spectra. The second would be to put more effort into development of a theoretical model of the spectra. These inverted spectra are of interest as the null to background ratio appears to provide greater resolution than does a typical side spectra.

Appendix A

Side Fluorescence Data

Figures 24 and 25 display the side fluorescence magnitude's exponential dependence on bromine pressure and detector location respectively. Figures 26 through 34 depict raw side fluorescence data.

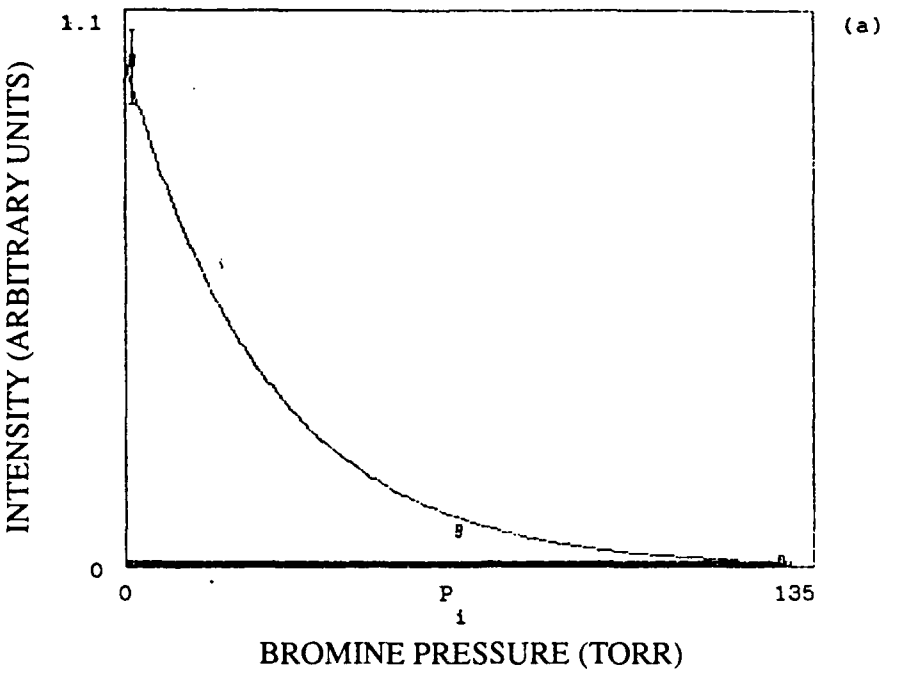

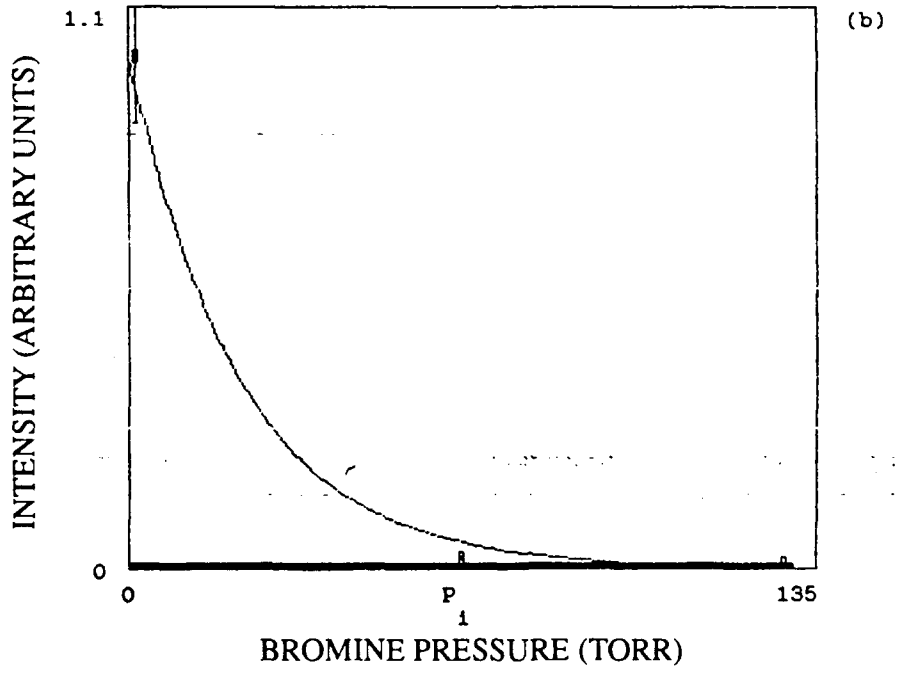

Figure 24. Side Fluorescence as a Function of Bromine Pressure
Detector Location is 50 cm (a) and 75 cm (b) from Cell Input

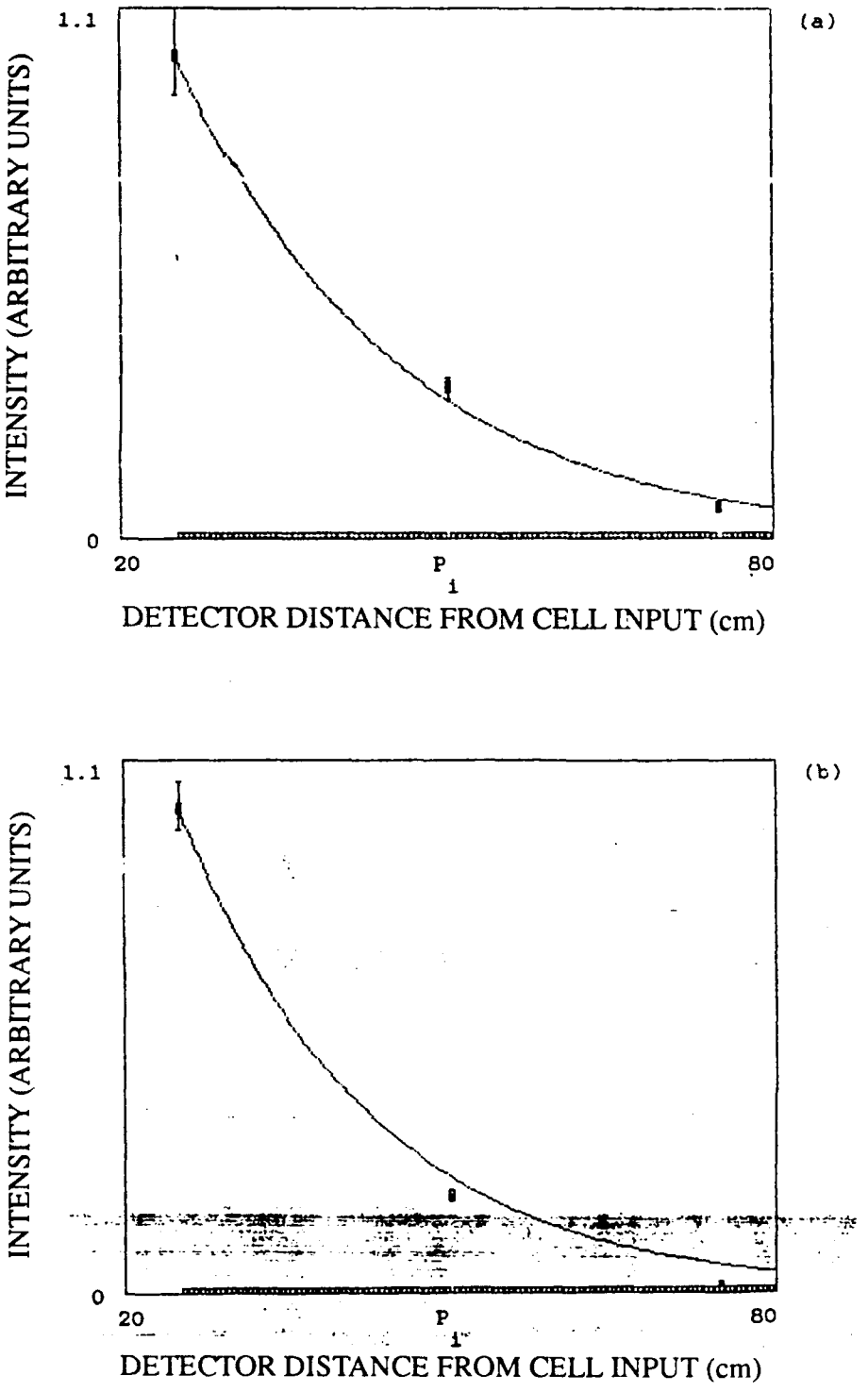

Figure 25. Side Fluorescence as a Function of Detector Location
Br2 Pressure is 14 $\pm$ 0.5 Torr (a) and 63.5 $\pm$ 1.5 Torr (b)

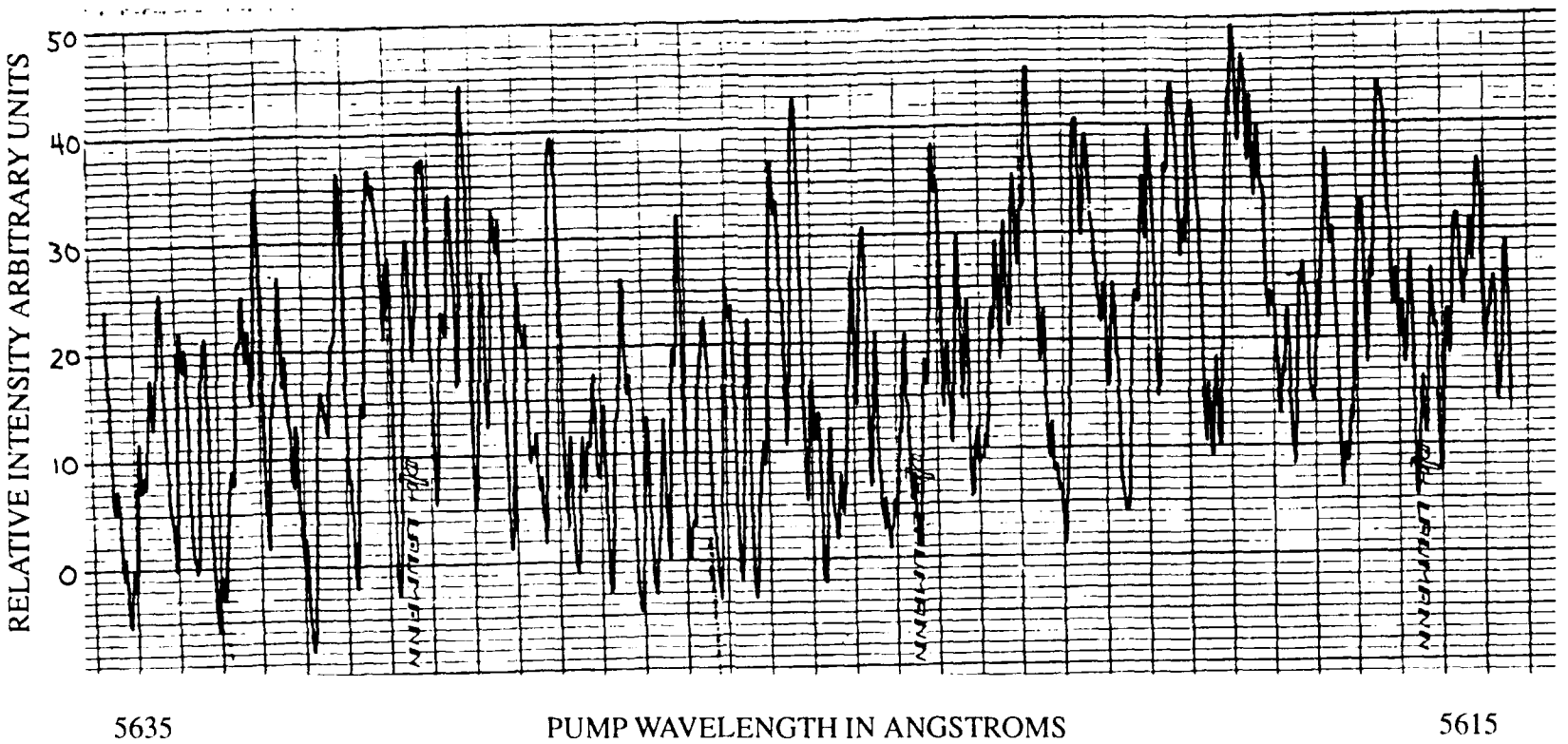

Figure 26. Side Fluorescence: Detector at 25cm, Br_2 Pressure 128 Torr

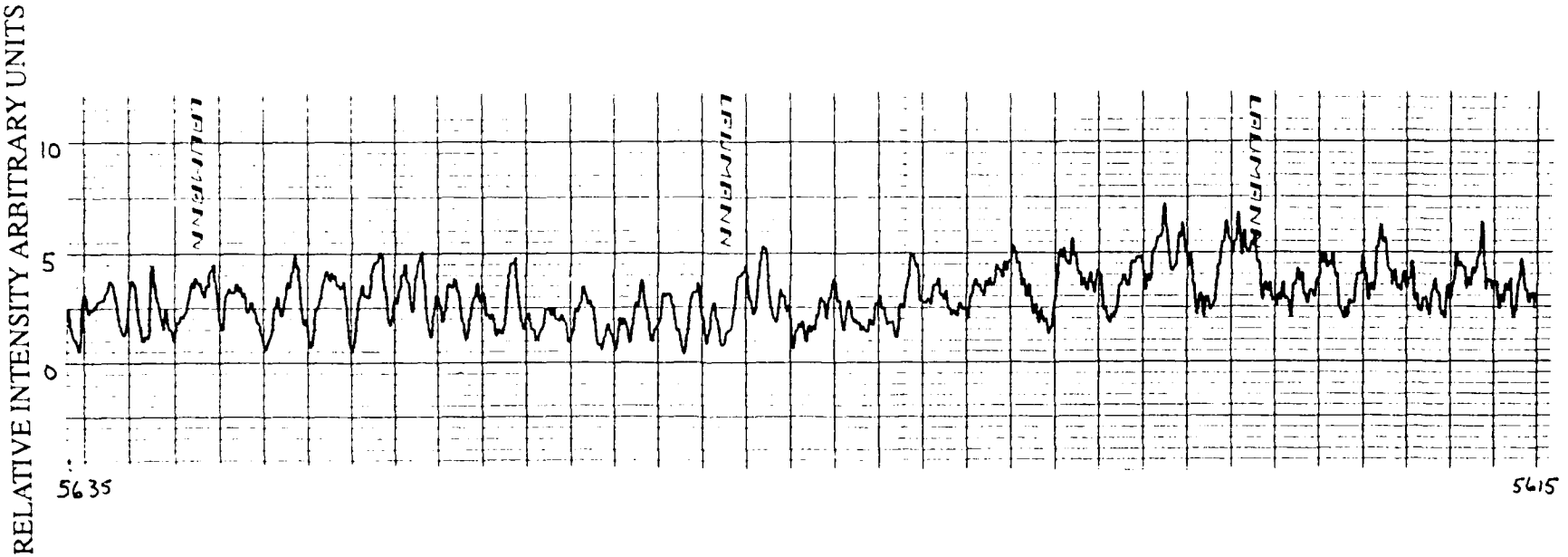

Figure 27. Side Fluorescence:
Detector at 50 cm, Br_2 Pressure 128 Torr

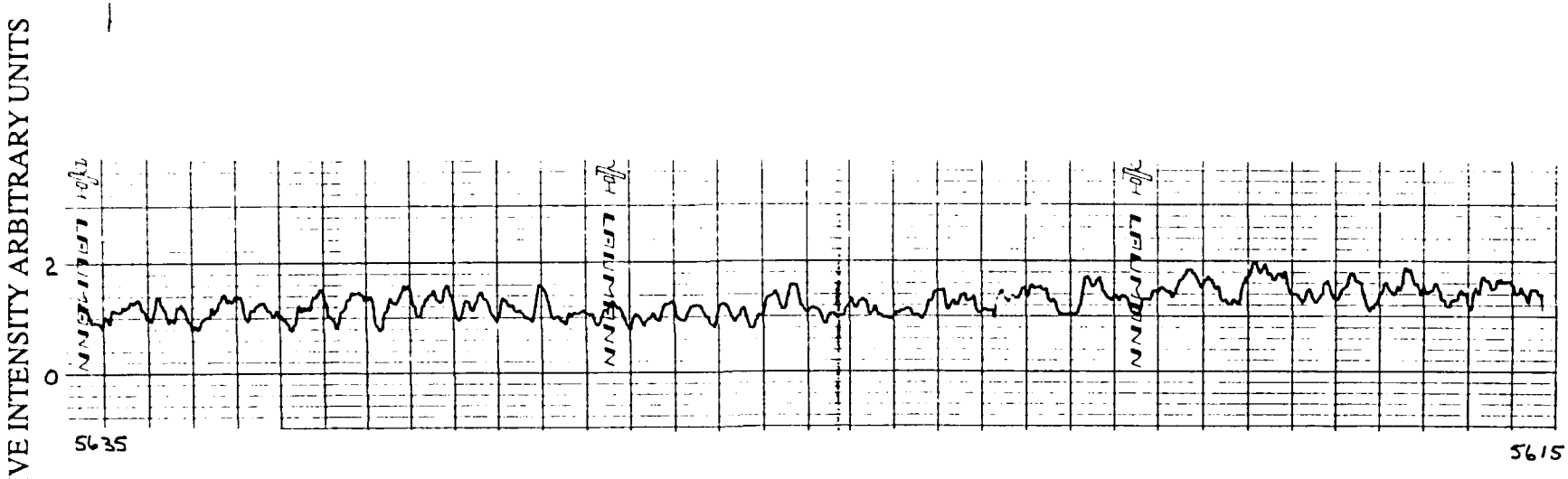

Figure 28. Side Fluorescence:
Detector at 75 cm, Br_2 Pressure 128 Torr

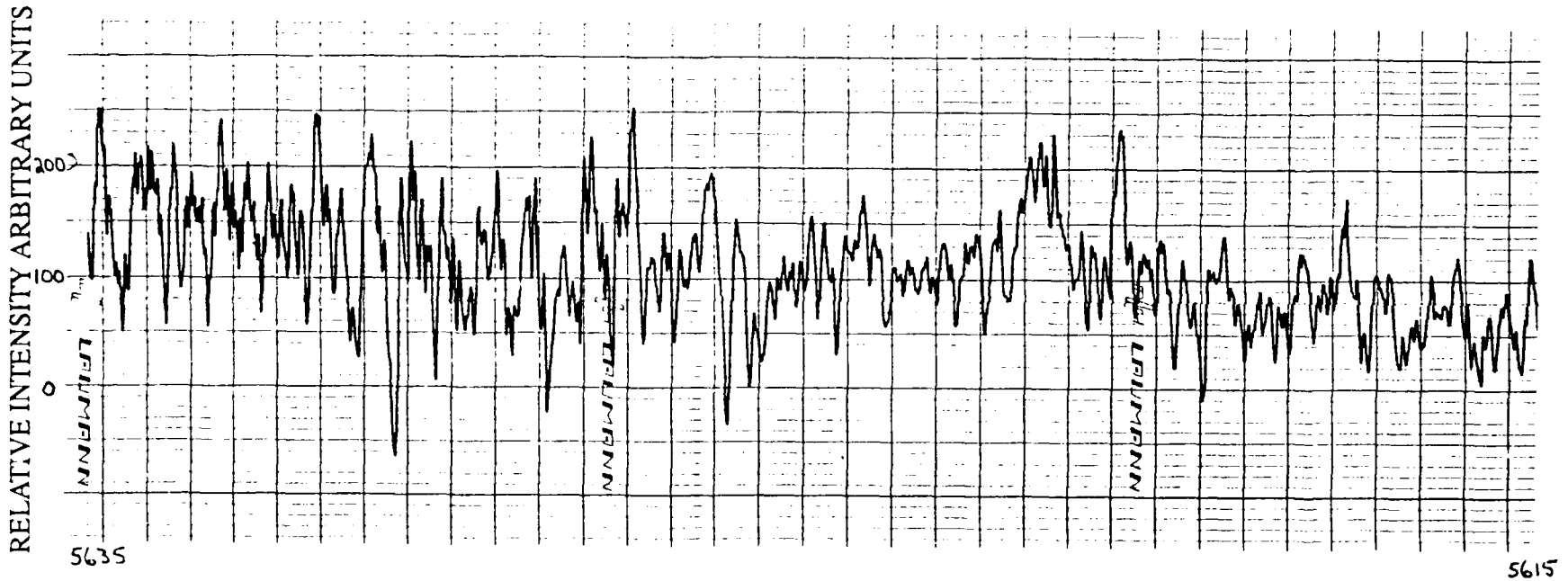

Figure 29. Side Fluorescence:
Detector at 25 cm, Br_2 Pressure 65 Torr

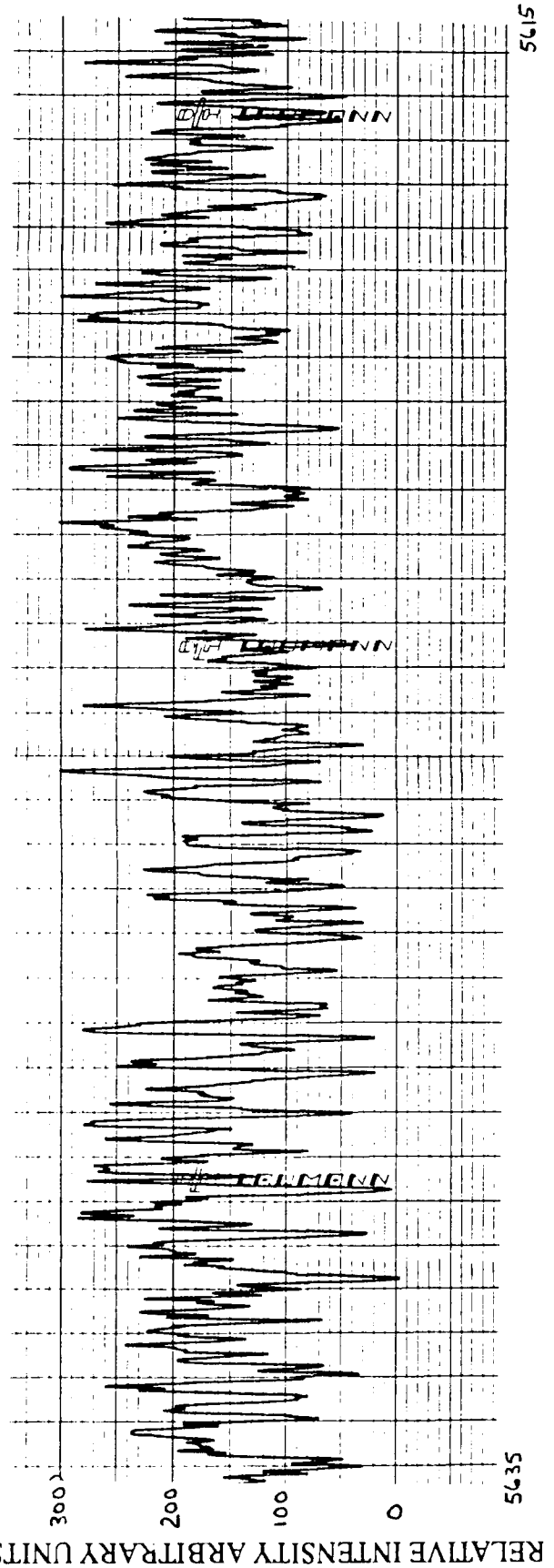

Figure 30. Side Fluorescence:
Detector at 50 cm, Br2 Pressure 62 Torr

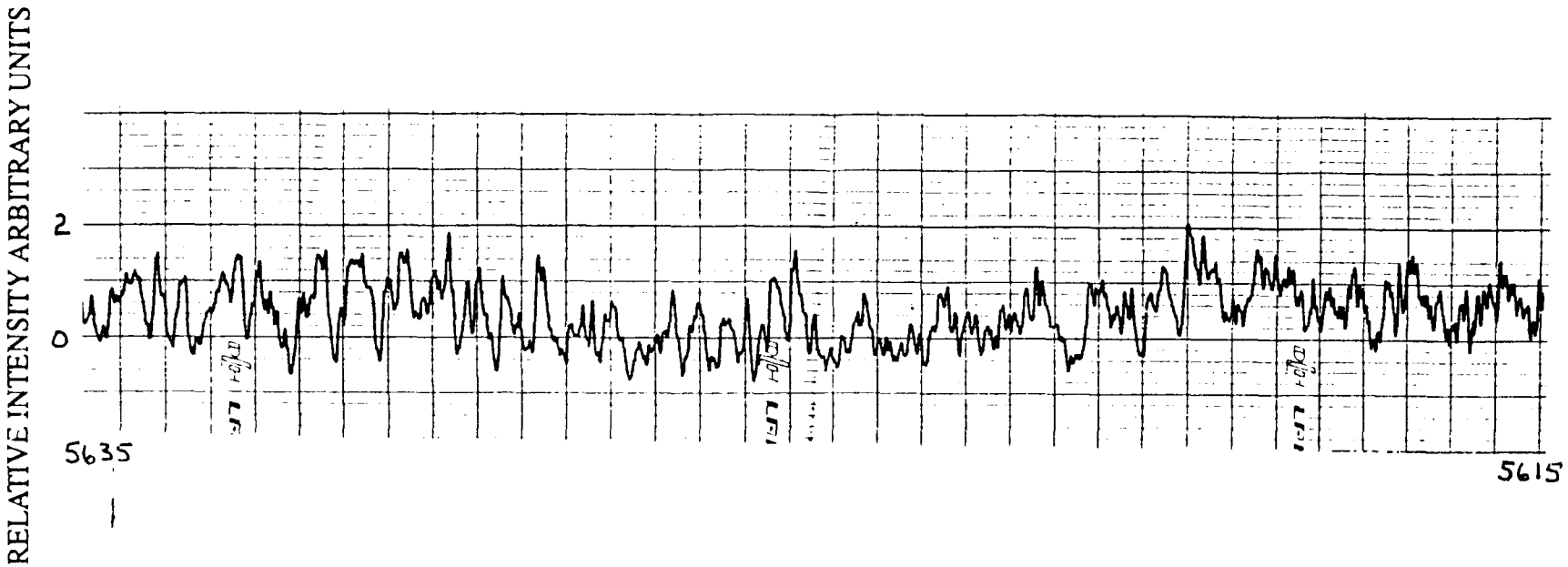

Figure 31. Side Fluorescence:
Detector at 75 cm, Br_2 Pressure 63 Torr

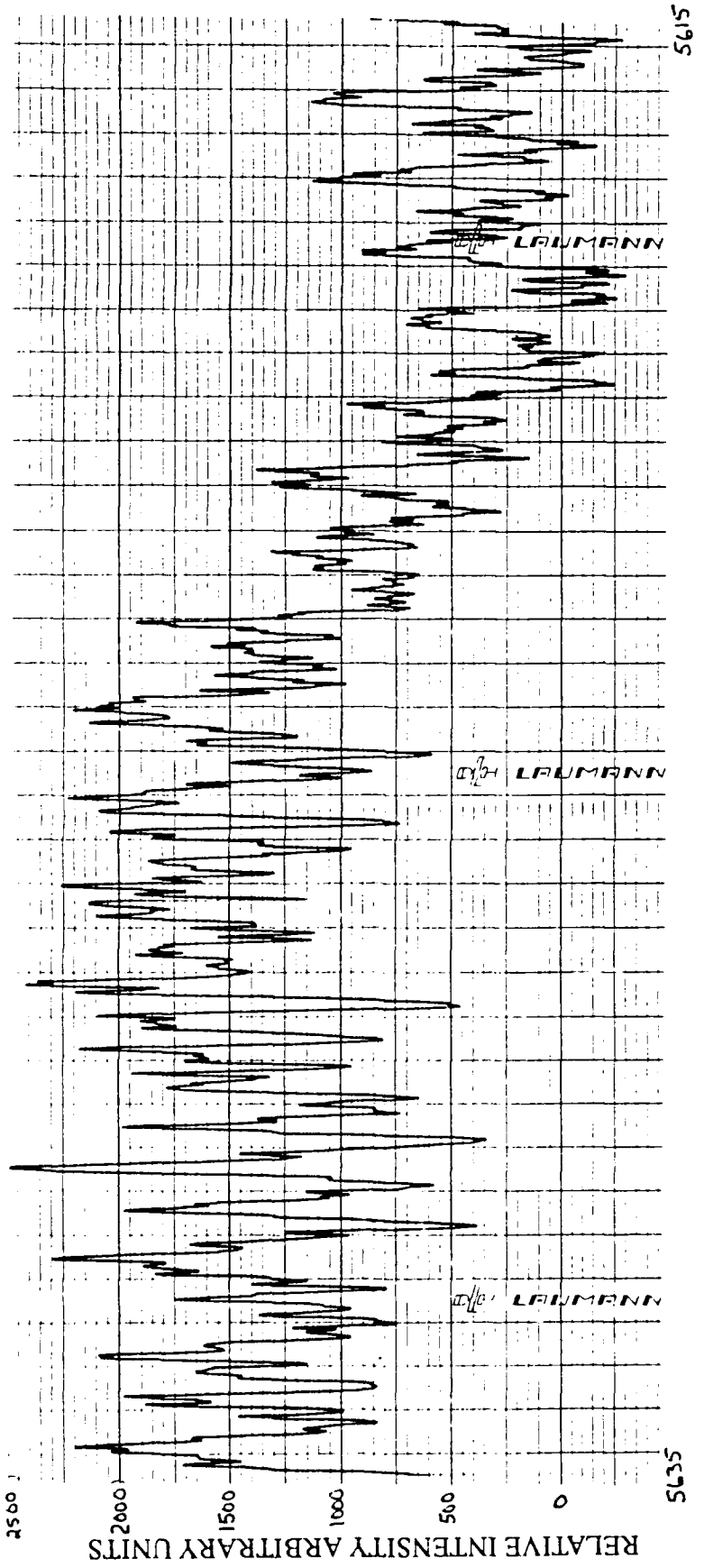

Figure 32. Side Fluorescence:
Detector at 25 cm, Br_2 Pressure 14 Torr

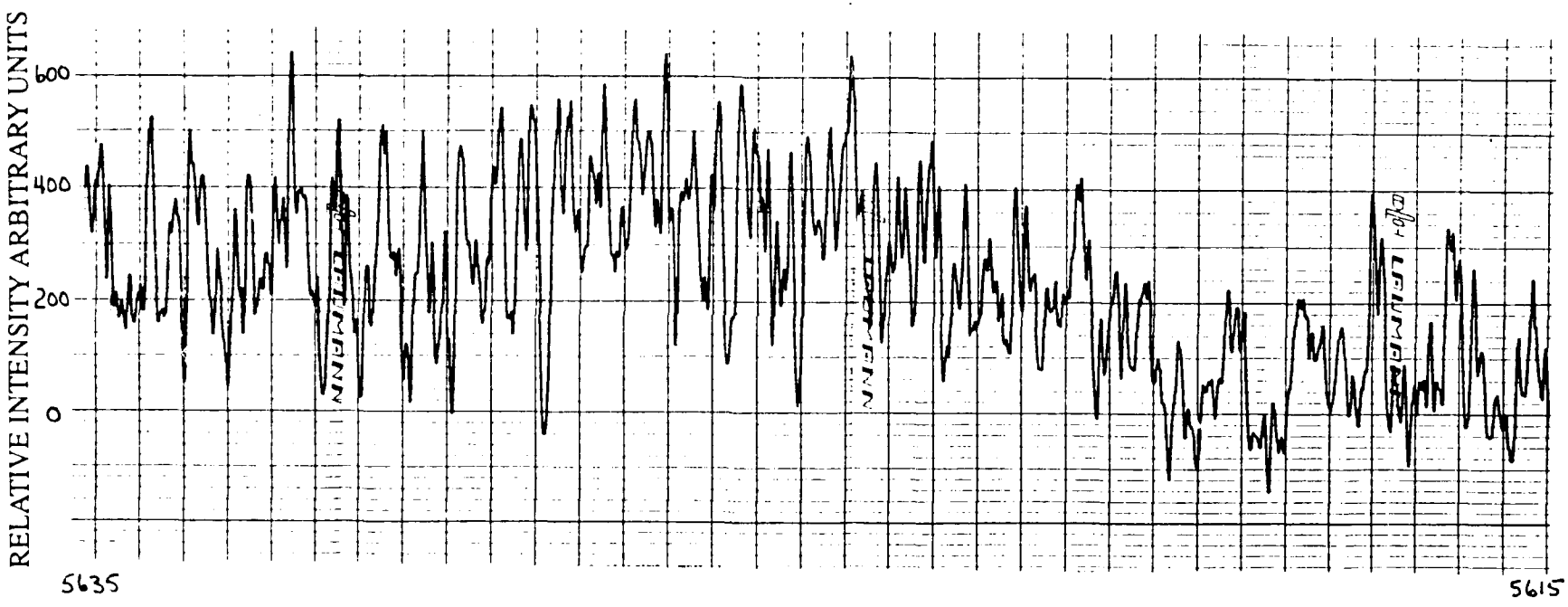

Figure 33. Side Fluorescence:
Detector at 50 cm, Br_2 Pressure 14.5 Torr

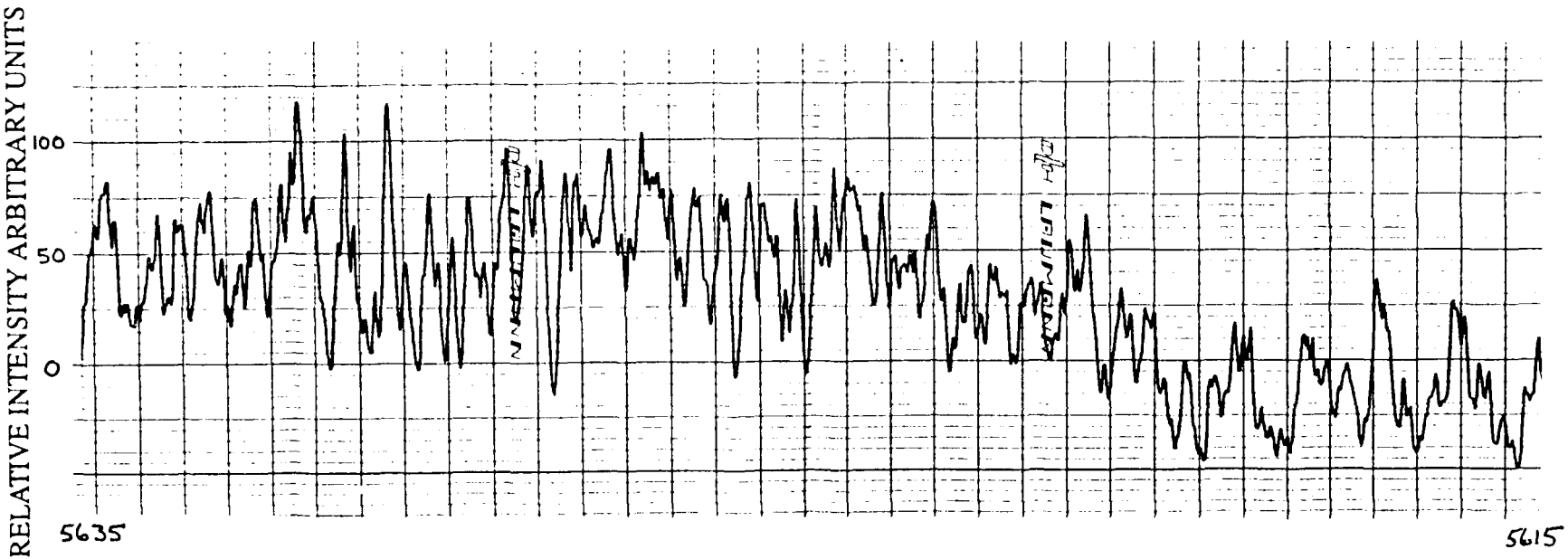

Figure 34. Side Fluorescence:
Detector at 75 cm, Br_2 Pressure 13.5 Torr

Appendix B

Stimulated Emission Spectra

Figures 35 through 38 display spectra obtained using stimulated emission as a signal monitor. This raw data was used to construct Figure 16.

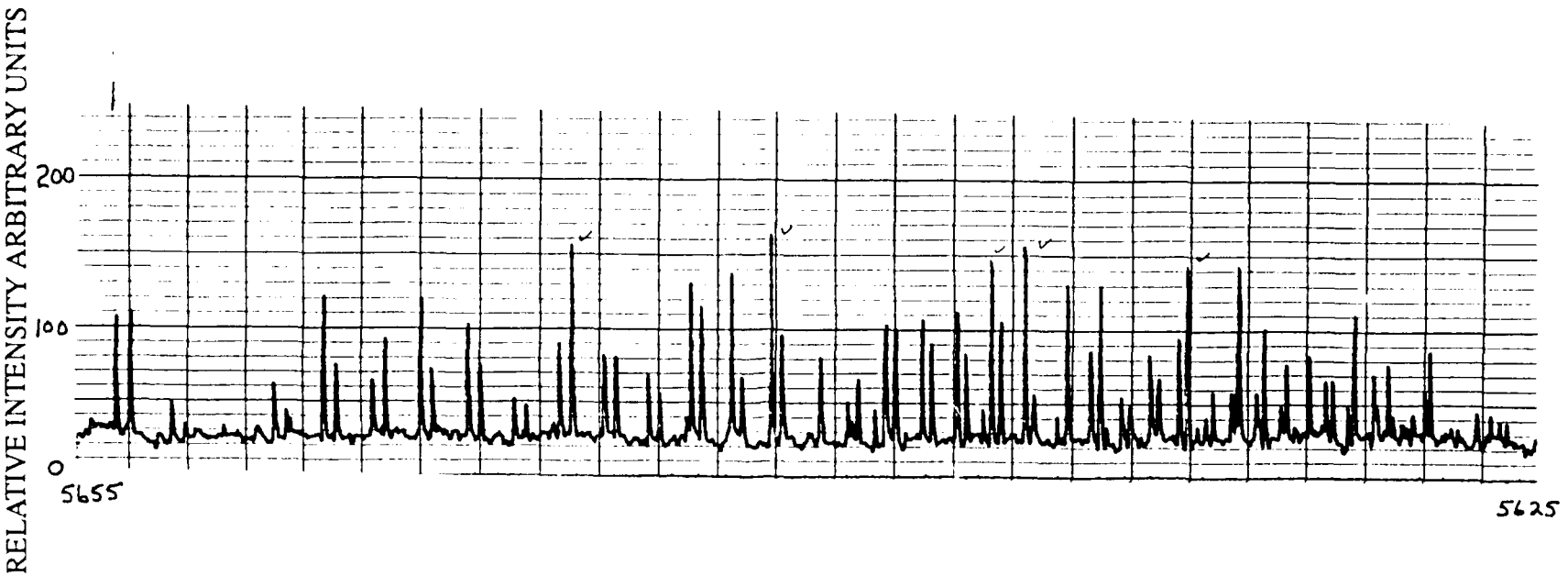

Figure 35. Stimulated Emission Spectra for Br_2 Pressure of 6.1 Torr

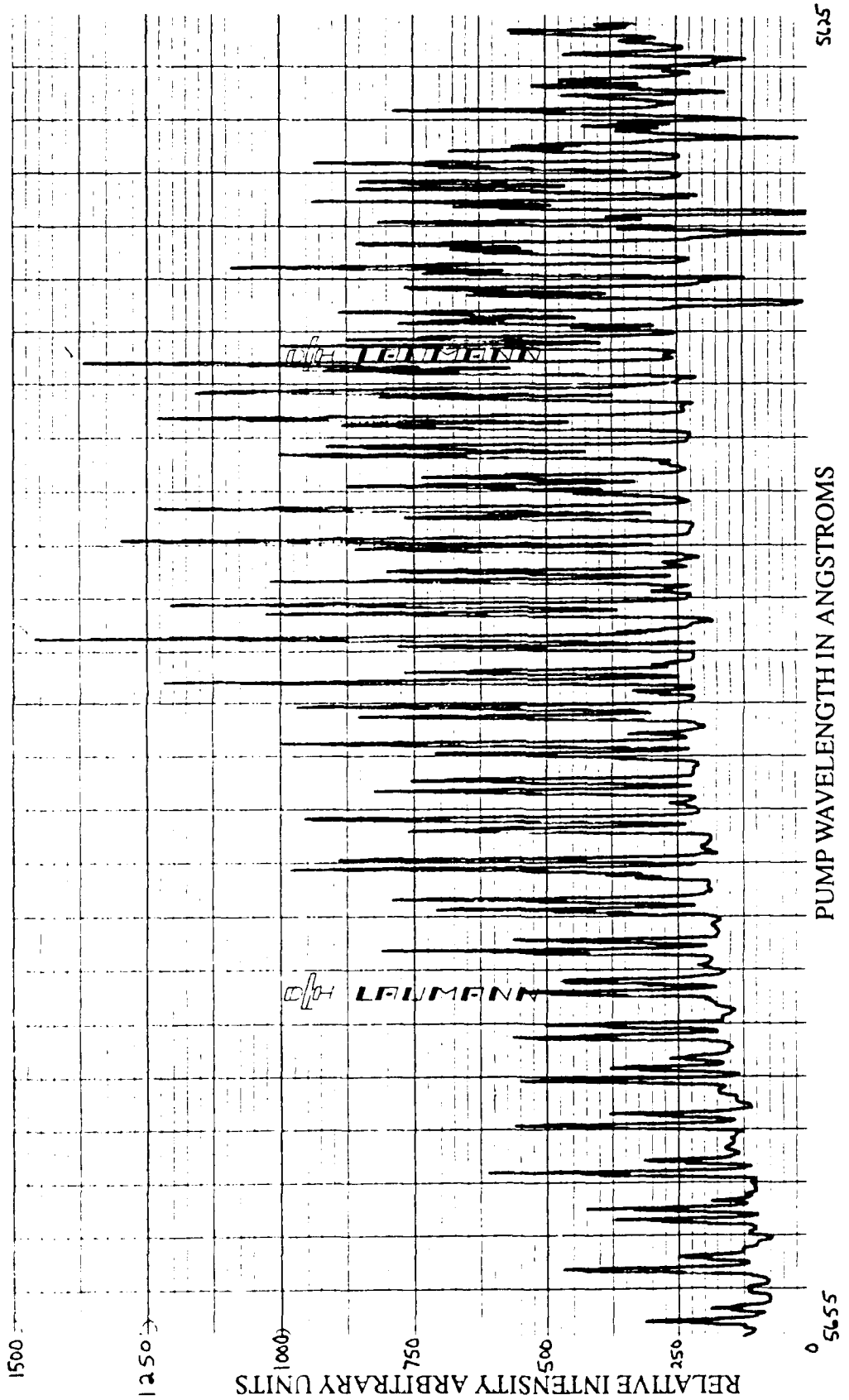

Figure 36. Stimulated Emission Spectra for Br2 Pressure of 10 Torr

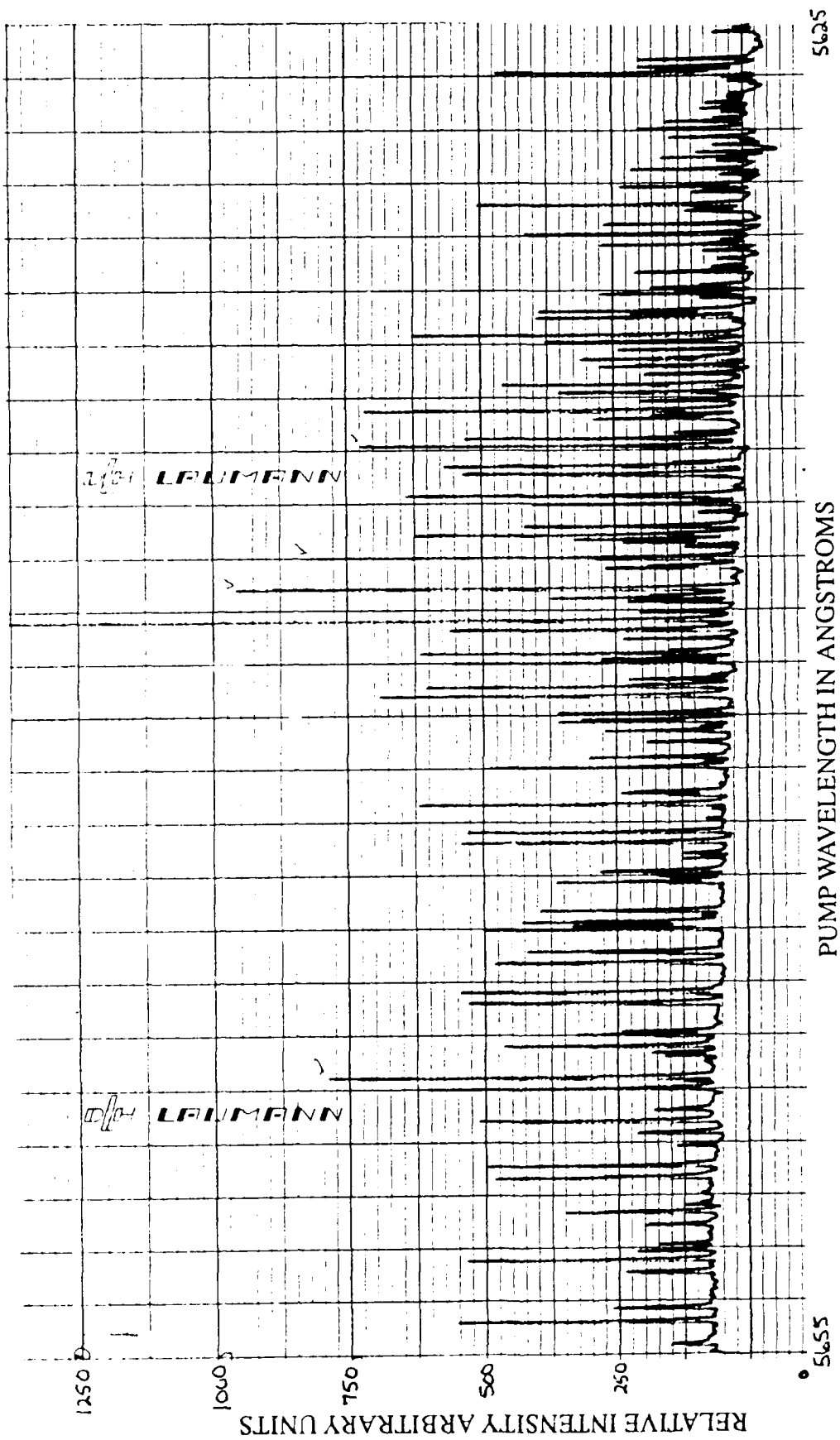

Figure 37. Stimulated Emission Spectra for Br_2 Pressure of 14 Torr

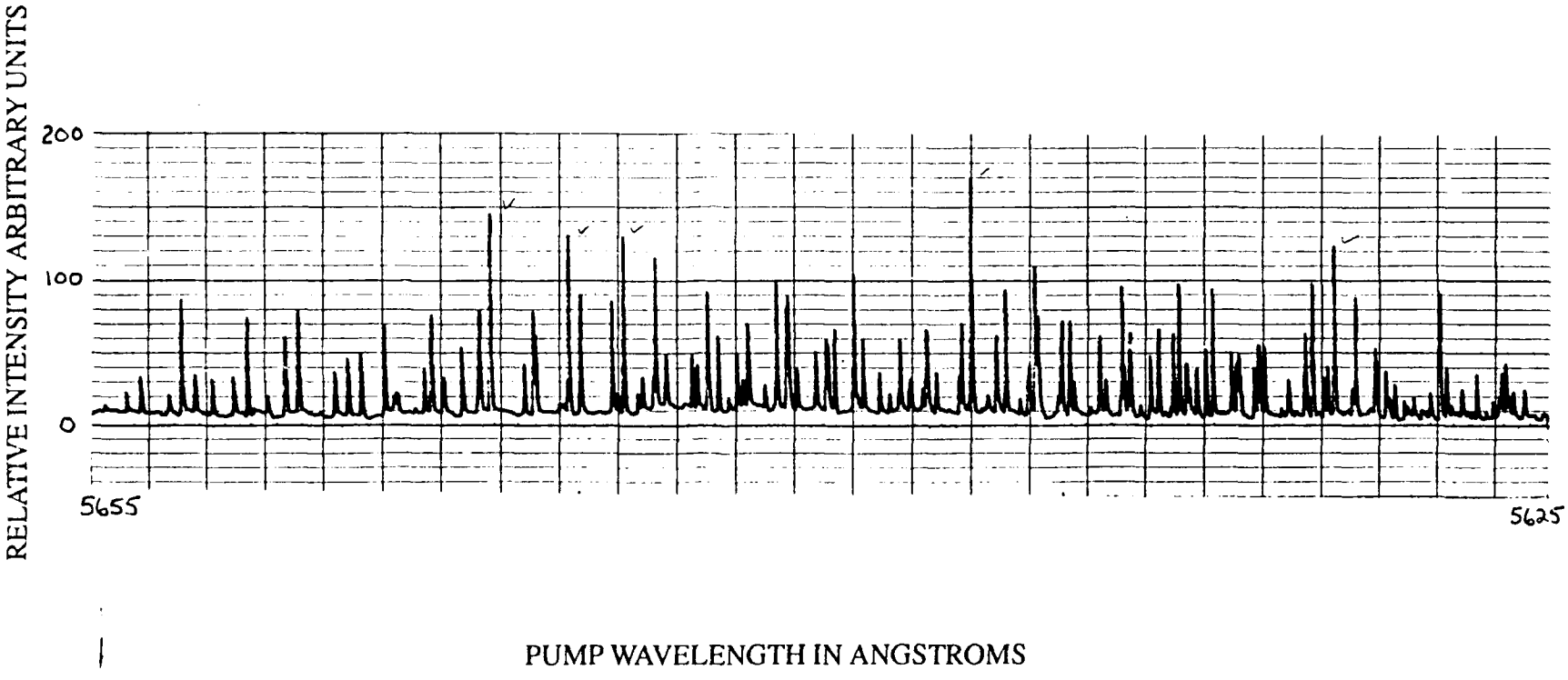

Figure 38. Stimulated Emission Spectra for Br_2 Pressure of 20.4 Torr

Appendix C

ASE Output vs Br_2 Pressure at Fixed Pumped Wavelength

Figures 39a through 42a show the ASE output dependence on Br_2 pressure for various pump wavelengths. The solid curves represent the appropriate total removal rates from the upper lasing level with time delays (t_D) of 12 (a), 14 (b) , and 16 (c) nanoseconds. Figures 39b through 42b plot ln (P/P_o) vs bromine pressure. The solid lines represent lines with a slope of $-kt_D$ for each data set. Figures 43 through 47 represent the raw data used to generate Figure 17 and Figures 39 through 42. This data was collected via method two which involved sitting at a fixed pump wavelength and varying the Br_2 pressure as described earlier.

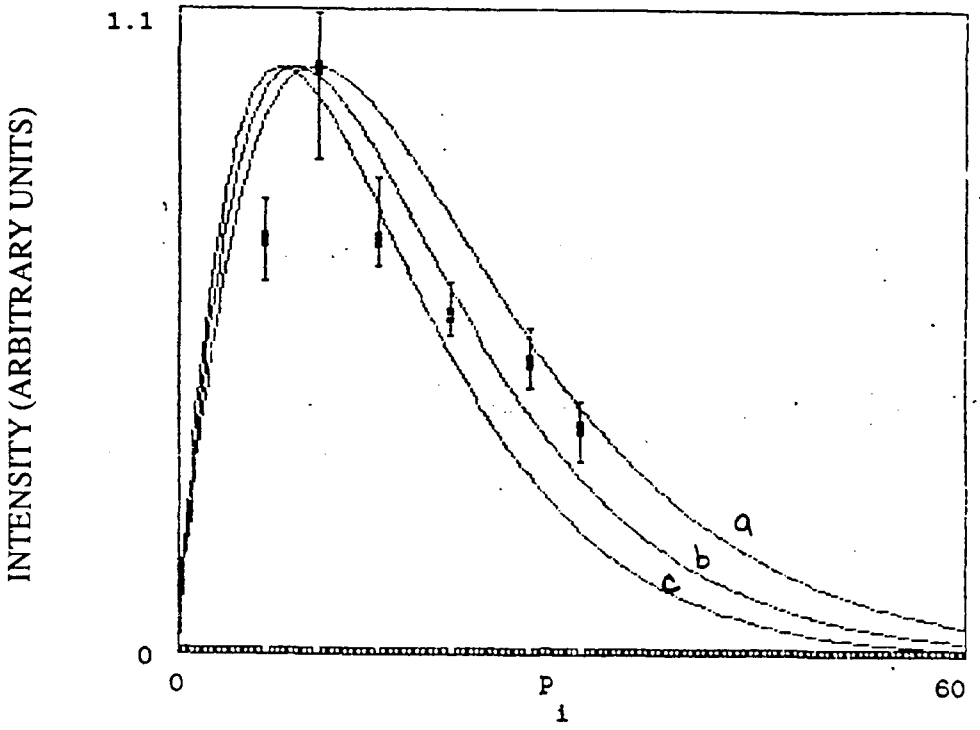

Figure 39a. The solid curves represent a total removal rate of 2.5×10^{-10} cm^3 $molecule^{-1}$ s^{-1} with a time delay (t_D) of 12 (a), 14 (b), and 16 (c) nanoseconds.

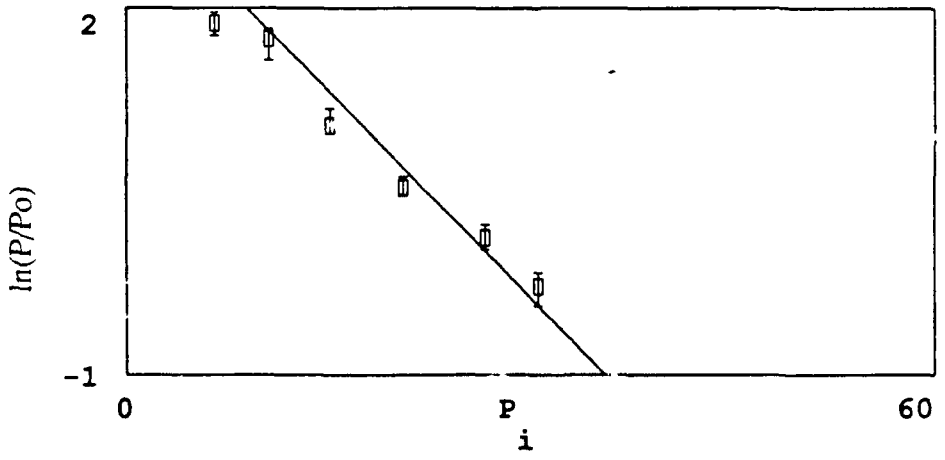

Figure 39b. $\ln(P/P_0)$ vs bromine pressure. The solid line represents a slope of $-kt_D$ with t_D = 14 ns and $k = 2.5 \times 10^{-10}$ cm^3 $molecule^{-1}$ s^{-1}.

Figure 39. ASE Output vs Br_2 Pressure at Fixed Pump Wavelength of 565.412 nm

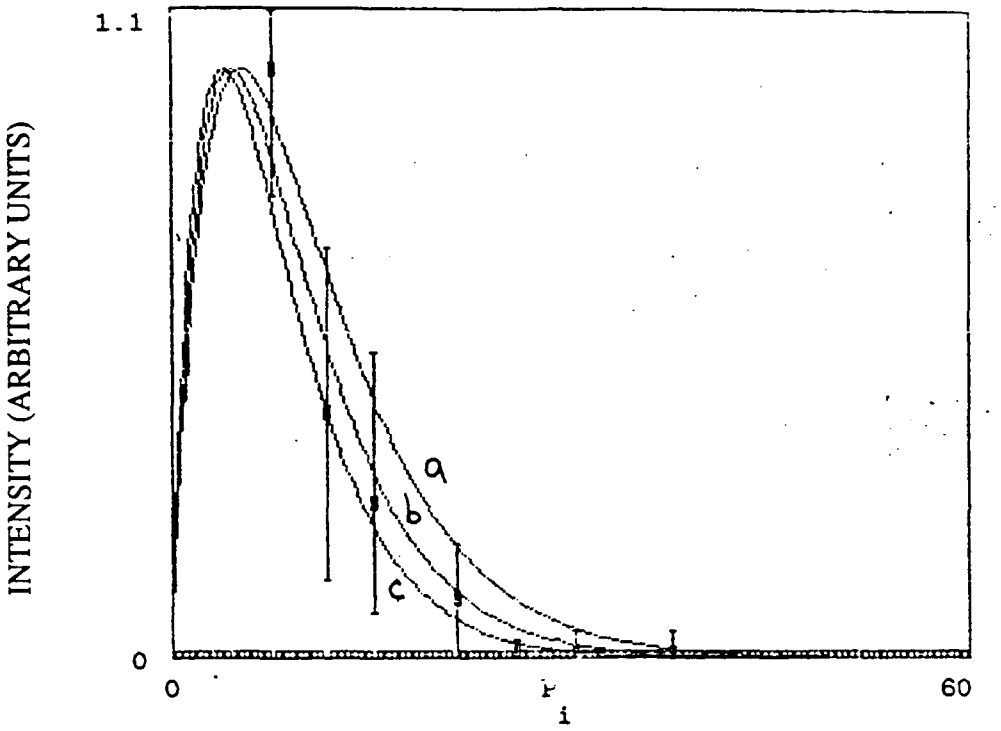

Figure 40a. The solid curves represent a total removal rate of 5.0×10^{-10} cm^3 $molecule^{-1}$ s^{-1} with a time delay (t_D) of 12 (a), 14 (b), and 16 (c) nanoseconds.

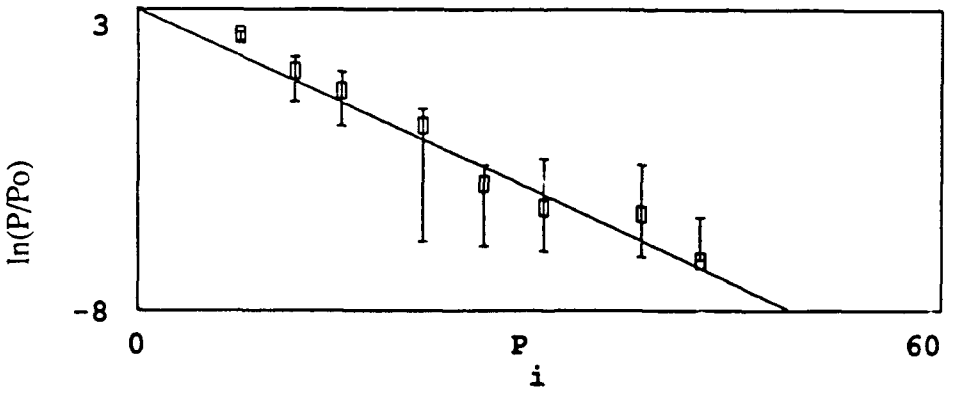

Figure 40b. $\ln(P/P_0)$ vs bromine pressure. The solid line represents a slope of $-kt_D$ with t_D = 14 ns and $k = 5.0 \times 10^{-10}$ cm^3 $molecule^{-1}$ s^{-1}.

Figure 40. ASE Output vs Br_2 Pressure at Fixed Pump Wavelength of 562.856 nm

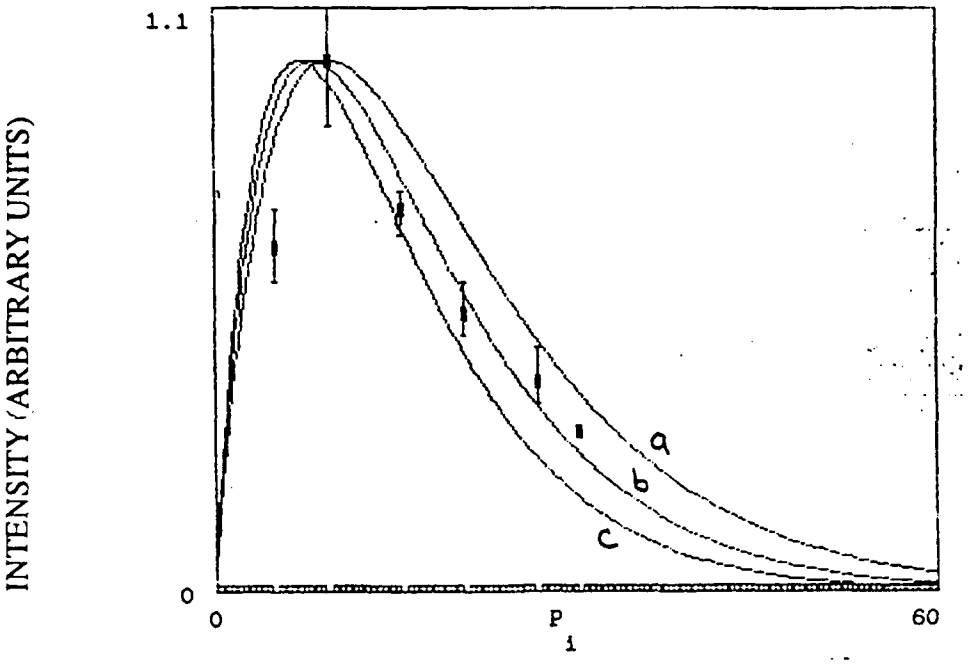

Figure 41a. The solid curves represent a total removal rate of 2.7×10^{-10} cm^3 $molecule^{-1}$ s^{-1} with a time delay (t_D) of 12 (a), 14 (b), and 16 (c) nanoseconds.

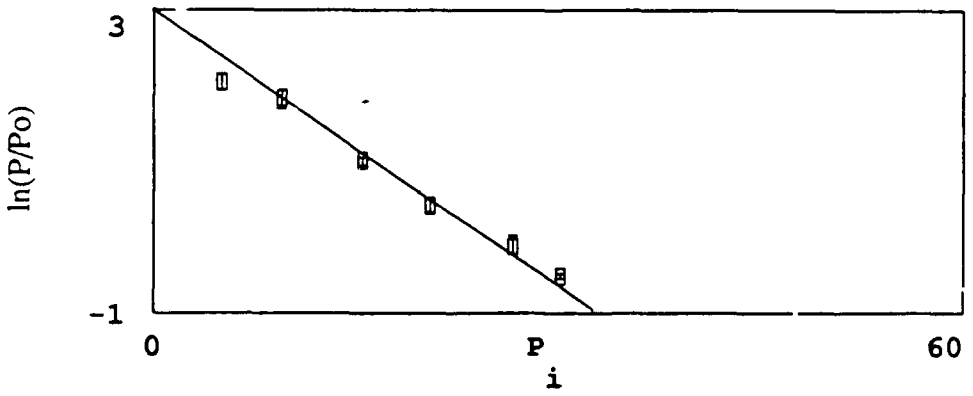

Figure 41b. $\ln(P/P_0)$ vs bromine pressure. The solid line represents a slope of $-kt_D$ with t_D = 14 ns and $k = 2.7 \times 10^{-10}$ cm^3 $molecule^{-1}$ s^{-1}.

Figure 41. ASE Output vs Br_2 Pressure at Fixed Pump Wavelength of 562.868 nm

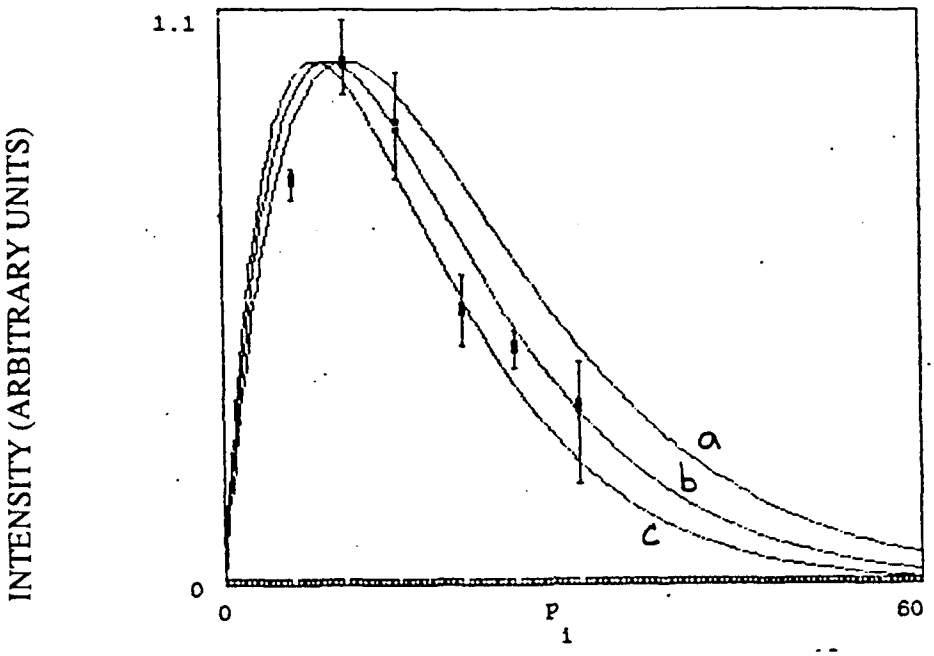

Figure 42a. The solid curves represent a total removal rate of 2.4×10^{-10} cm^3 molecule^{-1} s^{-1} with a time delay (t_D) of 12 (a), 14 (b), and 16 (c) nanoseconds.

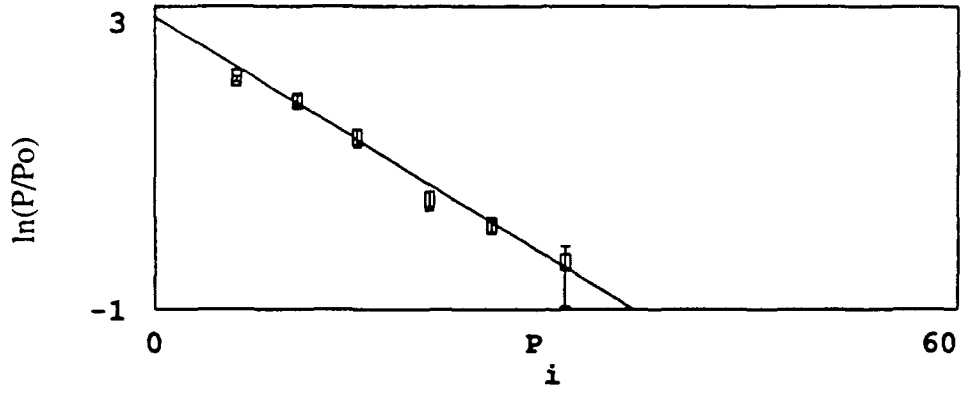

Figure 42b. $\ln(P/P_o)$ vs bromine pressure. The solid line represents a slope of $-kt_D$ with t_D = 14 ns and $k = 2.4 \times 10^{-10}$ cm^3 molecule^{-1} s^{-1}.

Figure 42. ASE Output vs Br_2 Pressure at Fixed Pump Wavelength of 565.420 nm

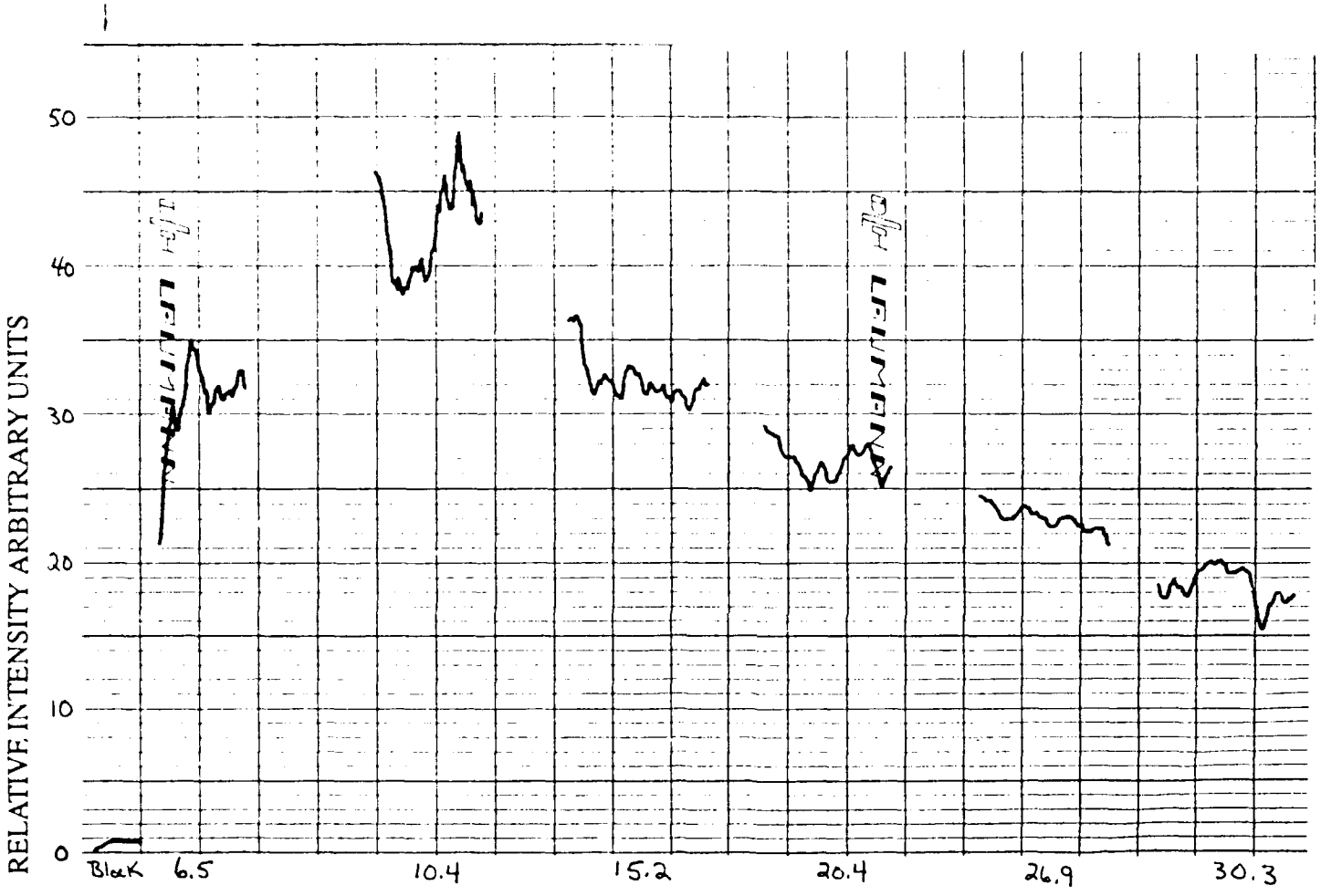

Figure 43. Raw ASE Output vs Br_2 Pressure:
Pump Wavelength of 565.412 nm

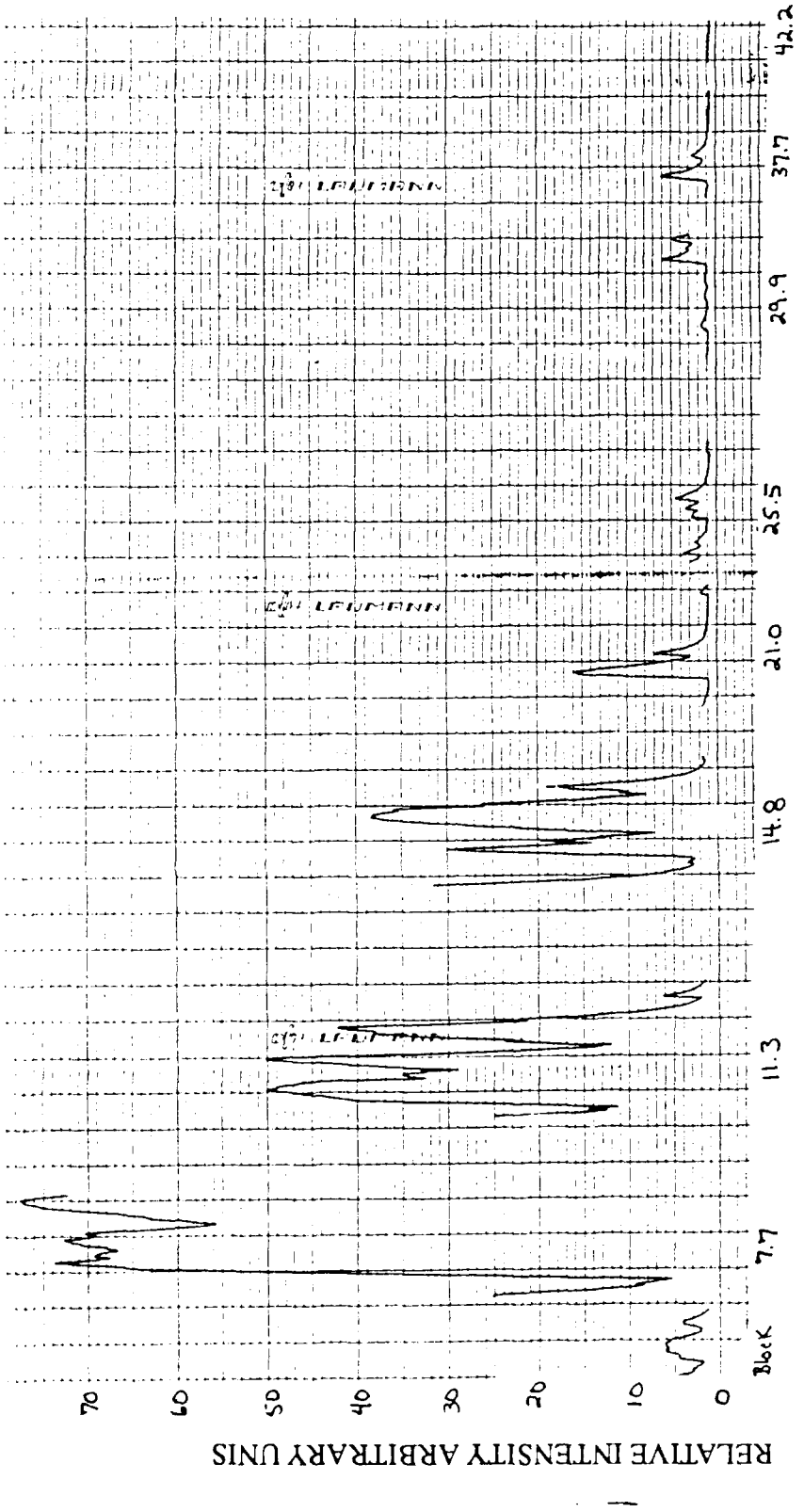

Figure 44. Raw ASE Output vs Br_2 Pressure: Pump Wavelength of 562.856 nm

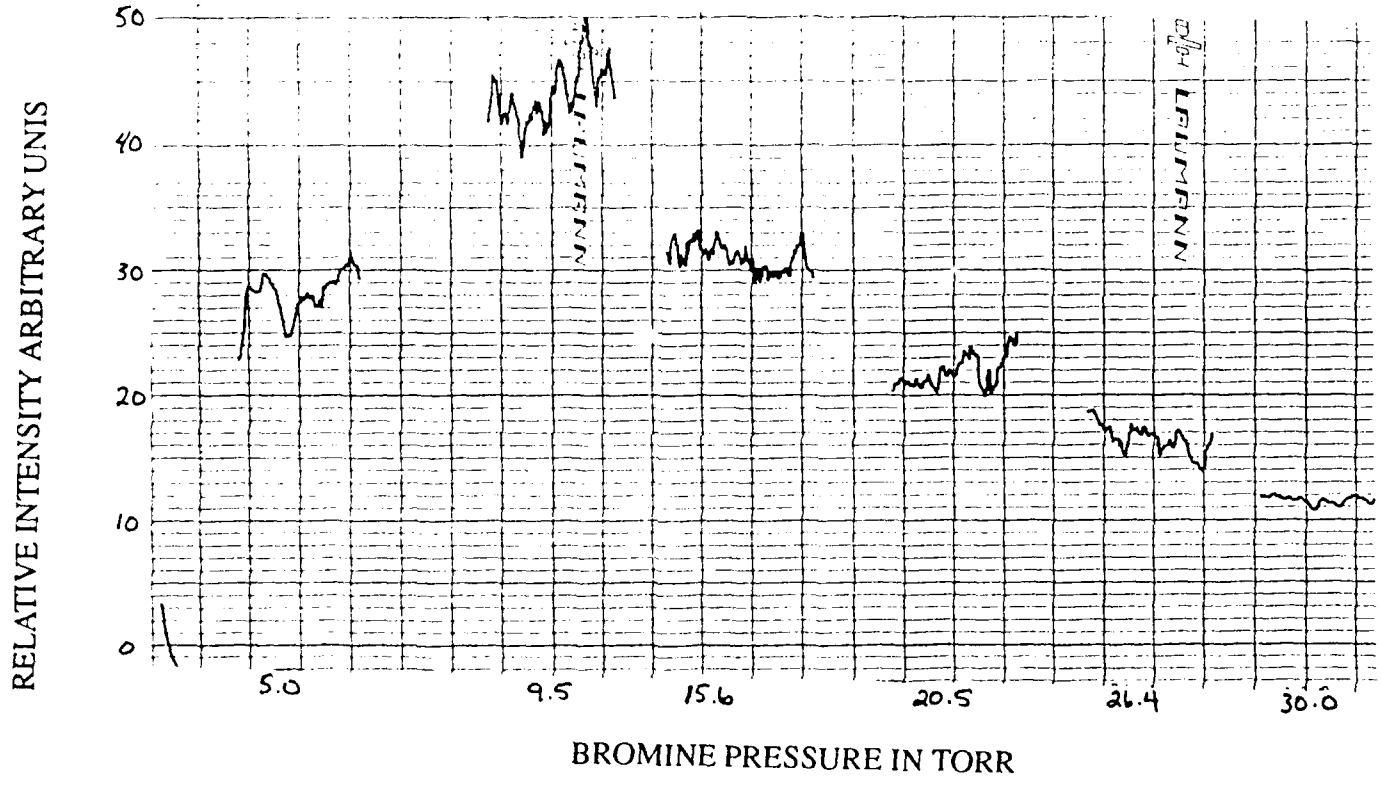

Figure 45. Raw ASE Output vs Br_2 Pressure:
Pump Wavelength of 562.868 nm

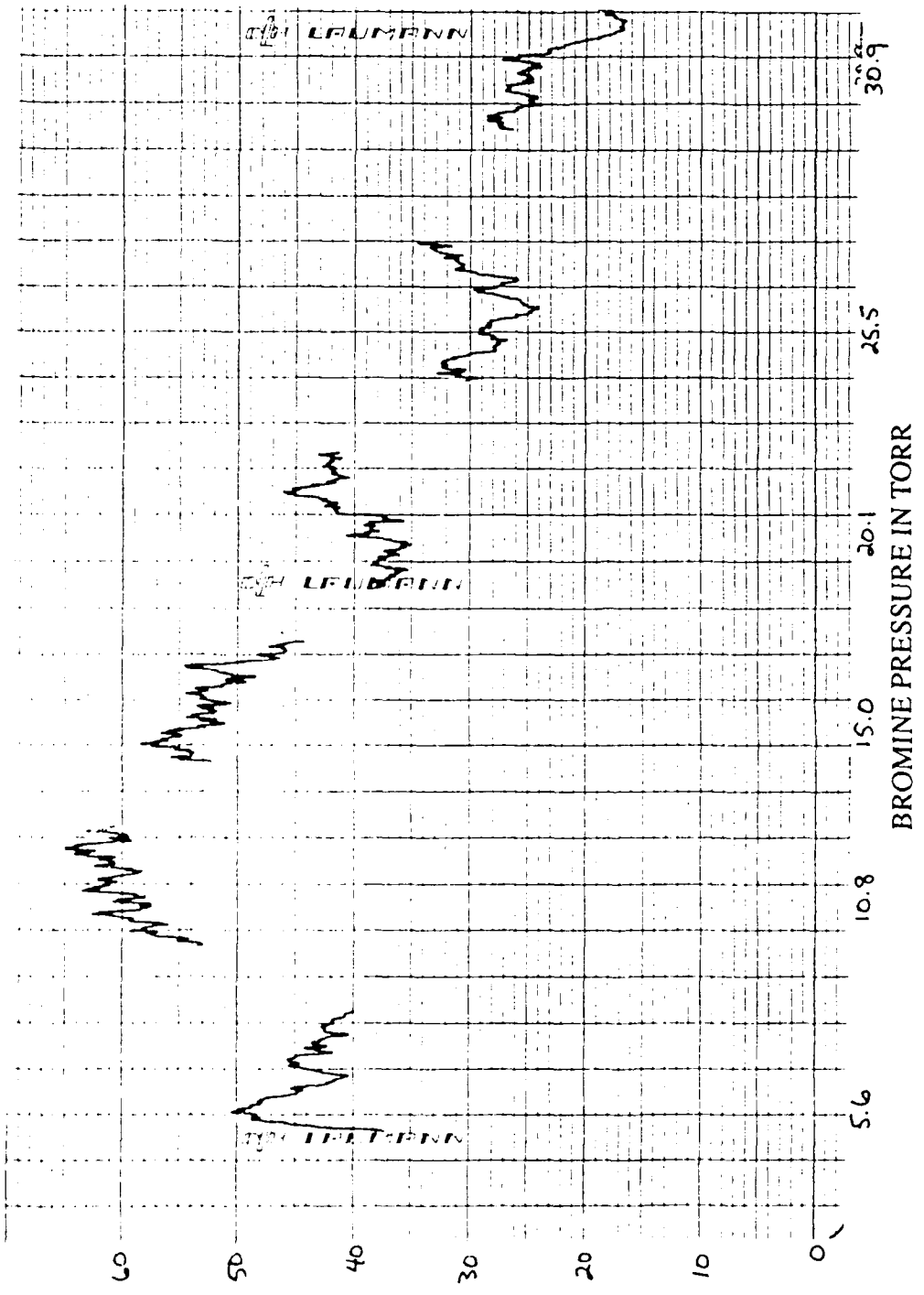

Figure 46. Raw ASE Output vs Br2 Pressure:
Pump Wavelength of 564.164 nm

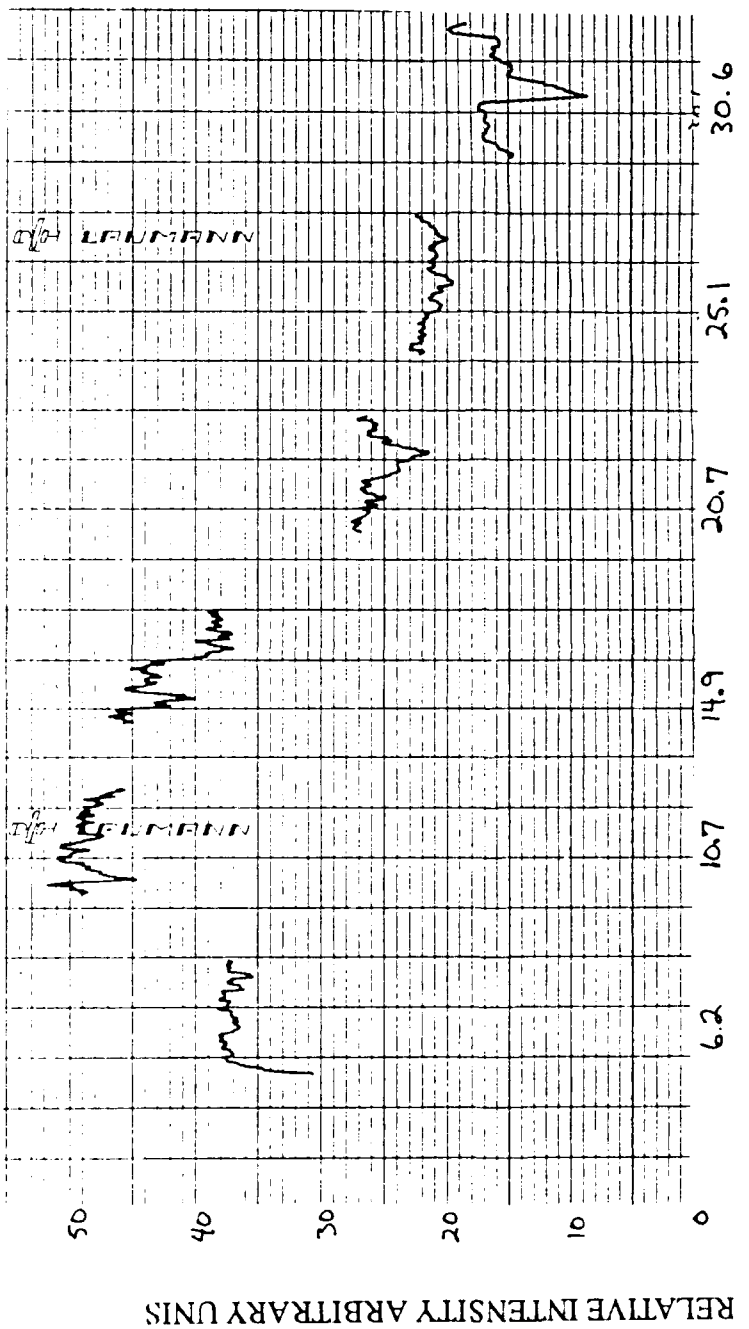

Figure 47. Raw ASE Output vs Br2 Pressure:
Pump Wavelength of 565.420 nm

Appendix D

Mathematical Model

This appendix details the mathematical model used to predict the amplitude of the dye pump beam at the detector location during side fluorescence measurements. The model, while not exactly duplicating the inverted side fluorescence spectra, shows the general trend of an inverted side fluorescence spectra encountered during early experimentation. The mathematical model consists of three parts: Part one is a data file containing the line positions (generated with the constants of Barrow *et al.*(3)) of the (14,0), (17,1), and (20,2) bands of bromine. Separate data files were used for each of the three bromine isotopes. Part two is a MATHCAD program which reads the data file and calculates the bromine absorption coefficients taking into account the pressure, appropriate spectroscopic constants, Franck-Condon factors, rotational population effects, and relative isotope distributions (the bromine isotopes $^{79}Br^{79}Br$ and $^{81}Br^{81}Br$ each have relative populations of approximately one half the $^{79}Br^{81}Br$ isotope population). Separate MATHCAD programs were used for each bromine isotope to generate three separate data files of absorption coefficients. Part three consisted of a MATHCAD program which read in the absorption coefficients, added them together, and applied a Doppler line shape to form and plot a spectrum based on $I_{out}/I_{in} = \exp(-\alpha l)$. Figure 48 shows a typical line position data file, Figure 49 depicts a sample absorption coefficient generation program for one isotope, and Figure 50 lists the program used to read the absorption coefficients, add linewidth, and plot a theoretical spectrum.

Wavelength	J	Band	Wavelength	J	Band	Wavelength	J	Band
5625.41	22	0	5626.88	26	1	5631.12	9	2
5625.86	23	0	5627.43	27	1	5631.35	10	2
5626.34	24	0	5628	28	1	5631.60	11	2
5626.83	25	0	5628.59	29	1	5631.87	12	2
5627.34	26	0	5629.19	30	1	5632.15	13	2
5627.87	27	0	5629.82	31	1	5632.46	14	2
5628.42	28	0	5630.46	32	1	5632.79	15	2
5628.99	29	0	5631.13	33	1	5633.14	16	2
5629.57	30	0	5631.81	34	1	5633.51	17	2
5630.18	31	0	5632.51	35	1	5633.90	18	2
5630.80	32	0	5633.23	36	1	5634.31	19	2
5631.44	33	0	5633.97	37	1	5634.74	20	2
5632.10	34	0	5634.74	38	1	5629.91	0	2
5632.78	35	0	5625.19	26	1	5629.90	1	2
5633.48	36	0	5625.67	27	1	5629.91	2	2
5634.19	37	0	5626.18	28	1	5629.94	3	2
5634.93	38	0	5626.70	29	1	5629.99	4	2
5625.15	25	0	5627.24	30	1	5630.06	5	2
5625.60	26	0	5627.80	31	1	5630.14	6	2
5626.06	27	0	5628.38	32	1	5630.25	7	2
5626.54	28	0	5628.98	33	1	5630.38	8	2
5627.04	29	0	5629.60	34	1	5630.53	9	2
5627.56	30	0	5630.24	35	1	5630.69	10	2
5628.10	31	0	5630.89	36	1	5630.88	11	2
5628.66	32	0	5631.57	37	1	5631.09	12	2
5629.23	33	0	5632.26	38	1	5631.32	13	2
5629.83	34	0	5632.98	39	1	5631.56	14	2
5630.44	35	0	5633.71	40	1	5631.83	15	2
5631.07	36	0	5634.47	41	1	5632.12	16	2
5631.72	37	0	5629.99	1	2	5632.42	17	2
5632.38	38	0	5630.07	2	2	5632.75	18	2
5633.07	39	0	5630.16	3	2	5633.10	19	2
5633.77	40	0	5630.27	4	2	5633.46	20	2
5634.50	41	0	5630.40	5	2	5633.85	21	2
5625.35	23	1	5630.55	6	2	5634.25	22	2
5625.85	24	1	5630.72	7	2	5634.68	23	2
5626.36	25	1	5630.91	8	2			

Figure 48. Model Part One: Sample Line Position Data File

```
Bromine lines -- Calculation of absorption coefficient
taking into account rotational and vibrational effects.
cmathcadthesisbrspec
i := 1 ..330                *** read in data ***
x  := READ(lines)
 i
i := 1.4 ..328
λ     := x                  *** Sort out wavelength
 i+2     i                  in air in Angstroms ***
 ---
  3
i := 2.5 ..329              *** Sort out J Number of line ***
J     := x
 i+1     i
 ---
  3
i := 3.6 ..330              *** Sort out band ***
B  := x                     0=(14,0) 1=(17,1) 2=(20,2)
 i     i
 -
 3
******  Constants  *******
                                                  -23
wel := 323.3069   cm^-1        k := 1.3807 10       Pa m^3 K^-1
weu := 166.5688   cm^-1        Torr := 133.32       Pa
Bvi := 0.081093   cm^-1        T := 300  deg K
q014 := 0.00056                P := 128  Torr
q117 := 0.00924                N2 := 0
q220 := 0.02477
     P Torr   molecules/cm^3
N := ------                          18
          6  N = 4.119881 10
     k T 10

*** Cross Sections (in cm^2)  *
                  -17                      -16                      -16
σse014 := 1.49 10     σse117 := 2.46 10     σse220 := 6.59 10
*** Vibrational ***
                          [     0.5 ]                    [     1.5 ]
Nv1014 := exp [-wel ------]     Nv1117 := exp [-wel ------]
                          [     208 ]                    [     208 ]
                          [     2.5 ]
Nv1220 := exp [-wel ------]          Nv1014 = 0.459701
                          [     208 ]      Nv1117 = 0.097146
                                           Nv1220 = 0.020529
```

Figure 49. Model Part Two:
Sample Absorption Coeff Generation Program

*** Rotational ***

NJ1=(hc/kT)Bv1(2J+1)exp[-Bv1J(J+1)(hc/kT)]

$i := 1 \,..110$

$$NJ1_i := \left(\frac{1}{208}\right) Bv1 \left(2 J_i + 1\right) \exp\left(-Bv1\, J_i \frac{J_i + 1}{208}\right)$$

Calculate absorption coefficient -α=ΣNσse=[N2-(g2/g1)N1]σse

********************************* g2=g1 N2=0

σse=(λ^2/(8π))A21g(v)

$i := 1 \,..110$

$Nt_i := 0 \qquad \alpha_i := 0$ Initialize

$i := 1 \,..110$

$$Nt_i := \mathrm{if}\left[\left(0 - B_i\right) \ne 0, Nt_i, Nv1014 \cdot NJ1_i \cdot N + Nt_i\right] \qquad (14,0)\ \text{band}$$

$$\alpha_i := \mathrm{if}\left[\left(0 - B_i\right) \ne 0, \alpha_i, \sigma se014 \cdot Nt_i + \alpha_i\right]$$

$i := 1 \,..110$

$$Nt_i := \mathrm{if}\left[\left(1 - B_i\right) \ne 0, Nt_i, Nv1117 \cdot NJ1_i \cdot N + Nt_i\right] \qquad (17,1)\ \text{band}$$

$$\alpha_i := \mathrm{if}\left[\left(1 - B_i\right) \ne 0, \alpha_i, \sigma se117 \cdot Nt_i + \alpha_i\right]$$

$i := 1 \,..110$

$$Nt_i := \mathrm{if}\left[\left(2 - B_i\right) \ne 0, Nt_i, Nv1220 \cdot NJ1_i \cdot N + Nt_i\right] \qquad (20,2)\ \text{band}$$

$$\alpha_i := \mathrm{if}\left[\left(2 - B_i\right) \ne 0, \alpha_i, \sigma se220 \cdot Nt_i + \alpha_i\right]$$

*** place absorption coeff by λ ***

$pt := 0 \,..1000 \qquad \alpha b_{pt} := 0$ initialize variables

$pt := 0 \,..1000$

$i := 1 \,..110$

$$\alpha b_{pt} := \mathrm{if}\left[\left[\left(5625 + \frac{pt}{100}\right) - \lambda_i\right] \ne 0.0, \alpha b_{pt}, \alpha_i\right]$$ fill in α where there are no lines.

$pt := 0 \,..1000$

$WRITE(brabco) := \alpha b_{pt}$ Write absorption coeff to data file

Figure 49. Model Part Two:
Sample Absorption Coeff Generation Program

Read data from brabco (absorb coef) Add linewidth to lines
and create spectrum   cmathcadthesispltbro

$l := 25$ cm

$k := 0 .. 1000$ *** read data ***   ** initialize **

$M_k := READ(brabco) + READ(abco79) + READ(abco81)$ $m_k := 0$

$k := 20 .. 980$ *** allow for line width 20 is 5625.2 A
980 is 5634.8 A ******************

$$\delta v := \frac{.1}{5630}\left(\frac{3\cdot 10^{8}}{5630\cdot 10^{-10}}\right)$$ line width based on data

$\delta v = 9.464648\cdot 10^{9}$

$c := 3\cdot 10^{8}$

$Cnt := -20, -19 .. 20$ +/- 0.2 Angstroms

$$v_{k+Cnt} := \frac{c}{\left(5625 + \frac{k + Cnt}{100}\right)10^{-10}} \qquad vo_k := \frac{c}{\left(5625 + \frac{k}{100}\right)10^{-10}}$$

*** calculate lineshape and form spectrum ***

$$m_{k-Cnt} := m_{k+Cnt} + M_k\left(\frac{4\ln(2)}{\pi}\right)^{.5}\frac{1}{\delta v}\exp\left[-4\ln(2)\left(\frac{v_{k+Cnt} - vo_k}{\delta v}\right)^{2}\right]$$

$pt := 0 .. 1000$

$m_{pt} := \exp(-m_{pt}\,l)$ $Iout/Iin = \exp(-\alpha l)$

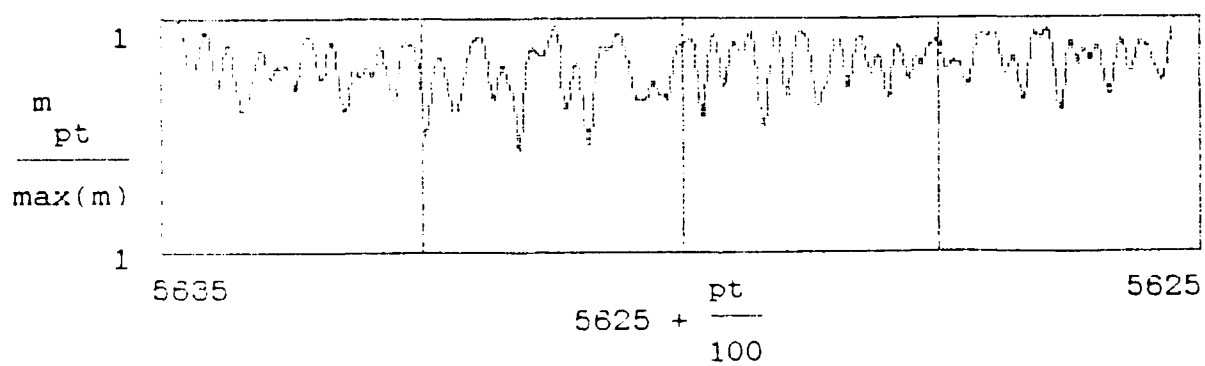

l=25 cm   P=128 Torr

Figure 50. Model Part Three:
Program to Add Linewidth and Plot Spectrum

Bibliography

1. Perram, Glenn P. "Visible Chemical Lasers," *Proceedings of the International Conference on Lasers '89.*

2. Davis, S. J. "Prospects for Visible Chemical Lasers," *Southwest Conference on Optics SPIE, 540*: 188-195 (1985).

3. Barrow, R. F. and others. "The $B^3\Pi O_u^+ - X^1\Sigma_g^+$ System of Br_2: Rotational Analysis, Franck-Condon Factors, and Long Range Potential in the $B^3\Pi O_u^+$ State," *Journal of Molecular Spectroscopy,51*: 428-449 (1974).

4. Coxon, J. A. "Low-lying Electronic States of Diatomic Halogen Molecules," *Molecular Spectroscopy*, Volume 1, London: The Chemical Society, 1973.

5. Glessner, Capt John W. *Amplified Spontaneous Emission of the Iodine B3Π(Ou+) - X1Σ(Og+) System.* PhD dissertation. School of Engineering, Air Force Institute of Technology (AU), Wright-Patterson AFB OH, April 1987.

6. Clyne, Michael A. A. and Michael C. Heaven. "Kinetics of Excited States of Br2 Using Laser Excitation Part 1," *Journal of the Chemical Society Faraday II, 74*: 1992-2013 (1978).

7. ----- and others. "Kinetics of Excited States of Br2 Using Laser Excitation Part 2," *Journal of the Chemical Society Faraday II, 76*: 405-419 (1980).

8. ----- and others. "Laser-Excitation Studies of Br2," *Journal of the Chemical Society Faraday II, 76*: 961-978 (1980).

9. Luypaert, R. and others. "Lifetimes and Collisional Quenching Cross Sections of Single Rotational States in Bromine," *Journal of Chemical Physics, 72 (11)*: 6283-6288 (1 June 1980).

10. Smedley, John E. and others. "Collision-Induced Dissociation of Laser-Excited Br_2[B3Π(Ou+);v',J']: Formation of $Br^*(^2P_{1/2}) + Br(^2P_{3/2})$ at Energies 1-5 kT Below Dissociation," *Journal of Chemical Physics, 86 (12)*: 6801-6812 (15 June 1987).

11. Wodarczyk, Francis J. and Howard R. Schlossberg. "An Optically Pumped Molecular Bromine Laser," *The Journal of Chemical Physics, 67 (10)*: 4476-4482, (15 November 1977).

12. Perram, G. P. and S. J. Davis. "Spectroscopic and Kinetic Studies of a Dye Laser Pumped Br_2 $B^3\Pi(O_u^+) - X^1\Sigma_g^+$ Laser," *The Journal of Chemical Physics, 84 (5)*: 2526-2533 (1 March 1986).

13. Van de Burgt, L. J. and M. C. Heaven. "Rate Constants for Collisional Deactivation of Br_2 $B^3\Pi(O_u^+)$ by $Br_2(X)$ and He," *Chemical Physics, 103*: 407-416 (1986).

14. Perram, Capt Glenn P. Associate Professor School of Engineering, Air Force Institute of Technology. Personal Interviews. Air Force Institute of Technology, Wright-Patterson AFB OH, April through September 1990.

15. Verdeyen, Joseph T. *Laser Electronics* (Second Edition). Englewood Cliffs NJ: Prentice Hall 1989.

16. Koffend, J. Brooke and others. "Pulsed and CW Optically Pumped Lasers for Novel Applications in Spectroscopy and Kinetics," *Journal of Applied Physics, 48*: 4468, (1977).

17. Davis, S. J. "Potential of Halogen Molecules as Visible Chemical Laser Systems," AFWL-TR-79-104: 167-189, Kirtland AFB NM.

Vita

Jon W. Morrison was born on 29 March 1959 in Salem, Ohio. He graduated third in his class from Salem High School in 1977 and attended Ohio University from which he received a Bachelor of Science degree in Electrical Engineering, with honors, in June 1981. Upon graduation, he began his civil service career at the Aerospace Guidance and Metrology Center at Newark Air Force Base. His initial assignment was with the Microwave and Laser Engineering Branch. He was responsible for many microwave calibration systems and was instrumental in the development of a new Instrument Landing System calibration standard. Next, he served briefly as the Branch Chief of the Mass and Dimensional Standards Laboratory. In 1986, he was promoted to a Supervisory Engineering position in the Systems Metrology Engineering Branch. This branch is responsible for on site calibration of Air Force automatic test equipment throughout the world. He entered the School of Engineering, Air Force Institute of Technology, in June 1989. Upon completion of his studies, he will return to Newark Air Force Base.

REPORT DOCUMENTATION PAGE

Form Approved
OMB No. 0704-0188

1. AGENCY USE ONLY (Leave blank)	2. REPORT DATE	3. REPORT TYPE AND DATES COVERED
	December 1990	Master's Thesis

4. TITLE AND SUBTITLE

AN OPTICALLY PUMPED
MOLECULAR BROMINE LASER

5. FUNDING NUMBERS

6. AUTHOR(S)

Jon W. Morrison

7. PERFORMING ORGANIZATION NAME(S) AND ADDRESS(ES)

Air Force Institute of Technology,
WPAFB OH 45433-6583

8. PERFORMING ORGANIZATION REPORT NUMBER

AFIT/GEO/ENP/90D-3

9. SPONSORING/MONITORING AGENCY NAME(S) AND ADDRESS(ES)

10. SPONSORING/MONITORING AGENCY REPORT NUMBER

11. SUPPLEMENTARY NOTES

12a. DISTRIBUTION/AVAILABILITY STATEMENT

Approved for public release;
distribution unlimited

12b. DISTRIBUTION CODE

13. ABSTRACT (Maximum 200 words)

An optically pumped molecular bromine laser was studied to investigate the quenching kinetics of the $B^3\Pi(O_u^+)$ state of Br_2. This included characterization of the pressure dependence of the laser output power. The approach was to excite molecular bromine in a sealed cell with a Nd:YAG pumped dye laser. Unresolved side fluorescence and amplified stimulated emission (ASE) spectra were recorded. ASE offered the advantage of a simpler optical system with no externally induced wavelength dependencies. Stimulated emission as a signal monitor offered greater resolution than side fluorescence spectra and facilitated spectroscopic assignment. The spectra obtained were attributed to the (14,0) band of the $^{79}Br^{81}Br$ isotope. The ASE output power peaked around Br_2 pressures from 8-12 Torr. A total removal rate, including all processes which remove population from the upper laser level, of 2.9×10^{-10} cm^3 $molecule^{-1}$ s^{-1} is proposed. This removal rate is consistent with the ASE output pressure dependence and the observed time delay between the dye pump beam and ASE pulses.

14. SUBJECT TERMS	15. NUMBER OF PAGES
Bromine, Optically Pumped Laser, Quenching, Amplified Spontaneous Emission (ASE), Fluorescence	98
	16. PRICE CODE

17. SECURITY CLASSIFICATION OF REPORT	18. SECURITY CLASSIFICATION OF THIS PAGE	19. SECURITY CLASSIFICATION OF ABSTRACT	20. LIMITATION OF ABSTRACT
Unclassified	Unclassified	Unclassified	UL

GENERAL INSTRUCTIONS FOR COMPLETING SF 298

The Report Documentation Page (RDP) is used in announcing and cataloging reports. It is important that this information be consistent with the rest of the report, particularly the cover and title page. Instructions for filling in each block of the form follow. It is important to **stay within the lines to meet optical scanning requirements.**

Block 1. Agency Use Only (Leave Blank)

Block 2. Report Date. Full publication date including day, month, and year, if available (e.g. 1 Jan 88). Must cite at least the year.

Block 3. Type of Report and Dates Covered. State whether report is interim, final, etc. If applicable, enter inclusive report dates (e.g. 10 Jun 87 - 30 Jun 88).

Block 4. Title and Subtitle. A title is taken from the part of the report that provides the most meaningful and complete information. When a report is prepared in more than one volume, repeat the primary title, add volume number, and include subtitle for the specific volume. On classified documents enter the title classification in parentheses.

Block 5. Funding Numbers. To include contract and grant numbers; may include program element number(s), project number(s), task number(s), and work unit number(s). Use the following labels:

C	- Contract	**PR**	- Project
G	- Grant	**TA**	- Task
PE	- Program Element	**WU**	- Work Unit Accession No.

Block 6. Author(s). Name(s) of person(s) responsible for writing the report, performing the research, or credited with the content of the report. If editor or compiler, this should follow the name(s).

Block 7. Performing Organization Name(s) and Address(es). Self-explanatory.

Block 8. Performing Organization Report Number. Enter the unique alphanumeric report number(s) assigned by the organization performing the report.

Block 9. Sponsoring/Monitoring Agency Names(s) and Address(es). Self-explanatory.

Block 10. Sponsoring/Monitoring Agency. Report Number. (If known)

Block 11. Supplementary Notes. Enter information not included elsewhere such as: Prepared in cooperation with...; Trans. of ..., To be published in .... When a report is revised, include a statement whether the new report supersedes or supplements the older report.

Block 12a. Distribution/Availablity Statement. Denote public availability or limitation. Cite any availability to the public. Enter additional limitations or special markings in all capitals (e.g. NOFORN, REL, ITAR)

DOD - See DoDD 5230.24, "Distribution Statements on Technical Documents."
DOE - See authorities
NASA - See Handbook NHB 2200.2.
NTIS - Leave blank.

Block 12b. Distribution Code.

DOD - DOD - Leave blank
DOE - DOE - Enter DOE distribution categories from the Standard Distribution for Unclassified Scientific and Technical Reports
NASA - NASA - Leave blank
NTIS - NTIS - Leave blank.

Block 13. Abstract. Include a brief (Maximum 200 words) factual summary of the most significant information contained in the report.

Block 14. Subject Terms. Keywords or phrases identifying major subjects in the report.

Block 15. Number of Pages. Enter the total number of pages.

Block 16. Price Code. Enter appropriate price code (NTIS only).

Blocks 17. - 19. Security Classifications. Self-explanatory. Enter U.S. Security Classification in accordance with U.S. Security Regulations (i.e., UNCLASSIFIED). If form contains classified information, stamp classification on the top and bottom of the page.

Block 20. Limitation of Abstract. This block must be completed to assign a limitation to the abstract. Enter either UL (unlimited) or SAR (same as report). An entry in this block is necessary if the abstract is to be limited. If blank, the abstract is assumed to be unlimited.